5-1988

Petrology of Passive Margin-Epeiric Sea Sediments: The Garden City Formation, North-Central Utah

Susan K. Morgan
Utah State University

PETROLOGY OF PASSIVE-MARGIN EPEIRIC SEA SEDIMENTS:

THE GARDEN CITY FORMATION, NORTH-CENTRAL UTAH

by

Susan K. Morgan

A thesis submitted in partial fulfillment
of the requirements for the degree

of

MASTER OF SCIENCE

in

Geology

Approved:

UTAH STATE UNIVERSITY
Logan, Utah

1988

ACKNOWLEDGEMENTS

I would like to express my appreciation and thanks to my major professor, Pete Kolesar, who suggested the thesis topic and provided assistance throughout the project. I would also like to thank Dave Liddell and Don Fiesinger for their suggestions and review of the thesis.

A very special thanks to my husband, Glenn Leonard, who provided financial and emotional support throughout the long process. A special thanks also to my mom who encouraged me to continue my education.

Funding for this project was in part provided by the J. Stewart Williams Fellowship and the President's Fellowship, Utah State University.

Sue Morgan

TABLE OF CONTENTS

LIST OF TABLES

LIST OF FIGURES

ABSTRACT

Petrology of Passive Margin-Epeiric Sea Sediments:
the Garden City Formation, North-central Utah

by

Susan K. Morgan, Master of Science

Utah State University, 1988

Major Professor: Dr. Peter T. Kolesar, Jr.
Department: Geology

The Lower Ordovician Garden City Formation is part of the thick sequence of Lower Paleozoic limestones, dolostones, and minor siliciclastic sedimentary rocks of the western United States. The carbonate rocks were formed predominantly by shallow water deposition in tropical, passive-margin epeiric seas.

The Garden City Formation is composed of nine lithotypes which represent the various environments. The formation is a storm-influenced transgressive sequence which may be divided into inner-shelf shallow subtidal and outer-shelf deep subtidal environments separated by a skeletal accumulation. The skeletal accumulation, formed by storm initiation, was a submerged topographic high, below normal wave base. The inner shelf includes the initial peritidal transgressive and shoreface material, which was extensively reworked by storm action, and a patchy distribution of shallow subtidal deposits. It is characterized by shoreward fossil banks and mud mounds, a restricted fauna, large amounts of terrigenous material and repeated occurrences of storm-created intraclastic layers within a nodular limestone.

The outer shelf sediments have a diverse fauna, are extensively burrowed and bioturbated, and have significant amounts of chert. Uncommon intraformational conglomerate layers signify deposition below mean storm-wave base.

The Garden City Limestone facies were deposited in broad, energy-related zones parallel to the ancient shoreline. These facies were compared to the model of epeiric sea deposition presented by Shaw (1964) and Irwin (1965). There was a lack of evidence within the Garden City sediments to support the existence of an extensive, shoreward, tideless low-energy zone as predicted by the model. The inner shallow subtidal environments remained near normal marine conditions, with water circulation provided by tidal action.

Early diagenetic features of the Garden City Formation include compaction, micritization, cementation and neomorphism. Chert formation preceded pressure solution and probably represents silicification of burrows.

Dolomitizing fluids moved along faults, unconformities, and bedding planes to selectively dolomitize the formation. Near-surface weathering resulted in dedolomitization and the oxidation of pyrite to hematite.

(168 pages)

CHAPTER I

INTRODUCTION

The Lower Ordovician Garden City Limestone is part of the thick sequence of Lower Paleozoic carbonate rocks of the western United States. The Paleozoic carbonate rocks were formed predominantly by shallow water deposition in tropical epeiric seas.

In Utah the Garden City Formation has long been recognized as a shallow water deposit, and it is unique in the large amounts of intraformational conglomerate and chert it contains. The fauna of the formation has been described in detail elsewhere, and many of the faunal zones have been correlated with other Ordovician limestones (Ross 1951). To date, however, there has not been a comprehensive study of the petrology of the formation, detailing the depositional environments and diagenetic changes recorded in the rocks.

The purpose of this paper is twofold. First, lithotypes are defined, depositional environments interpreted, and local paleogeography reconstructed. The sediments of the Garden City Formation were examined to provide a test of the broad applicability of epeiric sea deposition as defined by Shaw (1964) and Irwin (1965). The sediments were also analyzed to determine the importance of storm sedimentation on shallow water deposition. Second, the diagenetic events are outlined and a model of diagenesis for the Garden City Formation is proposed.

The information gained from this study will add to the general knowledge of epeiric sea deposition and the effects of storm sedimentation on passive continental margins.

CHAPTER II

DEPOSITIONAL ENVIRONMENTS OF A STORM-INFLUENCED PASSIVE MARGIN EPEIRIC SEA: THE LOWER ORDOVICIAN GARDEN CITY FORMATION, NORTH-CENTRAL UTAH

INTRODUCTION

The thick sequences of Lower Paleozoic carbonate rocks in the western United States represent predominantly shallow water deposition in tropical epeiric seas. In Utah the Lower Ordovician Garden City Formation was deposited as a transgressive sequence, following an upper Cambrian hiatus, when the sea flooded vast areas of the craton. The formation has large amounts of intraformational conglomerate and is unique as the first Paleozoic formation to contain considerable amounts of chert.

The purpose of this paper is to use the sediments of the Garden City Formation to test the model of epeiric sea deposition presented by Shaw (1964) and Irwin (1965). The Garden City limestone was chosen for study because its sediments were deposited in such a sea and to date no comprehensive study of the formation has been done.

Shaw's and Irwin's models describe three generalized energy zones within epeiric seas: a seaward, broad, low-energy zone; a middle narrow, high-energy zone; and a landward, broad, low-energy zone. They suggest that tide action was unlikely in the low-energy interior regions of epeiric seas. These interior regions should contain deposits characteristic of very-shallow restricted water environments including evaporites, mudcracks, syngenetic dolomite, numerous pellets, and fine-grained carbonate mud. There was a conspicuous lack of evidence within the Garden City sediments to support the existence of an extensive, shoreward, tideless low-energy zone. Instead, it was determined that tidal action was probable in the Ordovician sea, providing water circulation responsible for near normal marine conditions in the Garden City sediments.

The sediments were also analyzed to ascertain the importance of storm sedimentation on shallow water deposition. Storm sedimentation has a strong influence on the deposits of the Garden City Formation and was probably the primary source of the abundant intraformational conglomerates.

GEOLOGIC SETTING

The Garden City Formation is a Lower Ordovician limestone which crops out from north-central and western Utah to southeastern Idaho. Its equivalents, the House and Fillmore limestones of the Pogonip Group, crop out to the south and west in Utah and extend into eastern Nevada (Hintze 1951). The Garden City limestone terminates to the east at the western margin of the Green River Basin (Williams 1955). The termination is probably a result of non-deposition and signifies the location of the craton (Hintze 1951). In the study area of north-central Utah the formation lies disconformably on the Cambrian Saint Charles Formation (Taylor and Landing 1981) and has an abrupt upper contact with the Middle Ordovician Swan Peak Quartzite. It ranges in thickness from 322 meters in the east to 549 meters in in the west (Hanson 1949).

Sections of the Garden City Formation that were studied in detail are located in the Bear River Range and the Wellsville Mountains of north-central Utah (Fig. 1). This area lies on the western margin of the Idaho-Wyoming overthrust belt. The two mountain ranges trend north and are separated by the Cache Valley graben. They are made up of a thick sequence of Paleozoic miogeoclinal shallow-water limestones and dolostones with minor amounts of siliciclastic rocks. Strata of the Wellsville Mountains are folded in a northeast-dipping homocline, while those in the Bear River Range form the northeast-trending Logan Peak Syncline and Strawberry Valley Anticline. The mountains are part of the Cache allochthon (Crittenden 1972) which has been moved east 48 to 64 km by Cretaceous thrust faulting (Crittenden 1961).

PREVIOUS WORK

Previous studies of the Garden City Formation have concentrated both on the paleontology of the formation (Clark 1935; Ross 1951; Berry 1962) and on its part in the stratigraphic and structural evolution of the eastern Great Basin (Richardson 1913; Mansfield 1927; Williams 1948; Hanson 1949; Rigby 1958; Schaeffer 1960; Miller 1984). Ross (1951) noted the presence of intraformational conglomerate, channel scour-and-fill, and ripple marks as strong evidence for shallow-water deposition. Stratigraphic descriptions have subdivided the Garden City Formation into two informal lithologic members: a lower intraformational conglomerate member and an upper cherty member (Hanson 1949; Ross 1951; Rigby 1958; Schaeffer 1960).

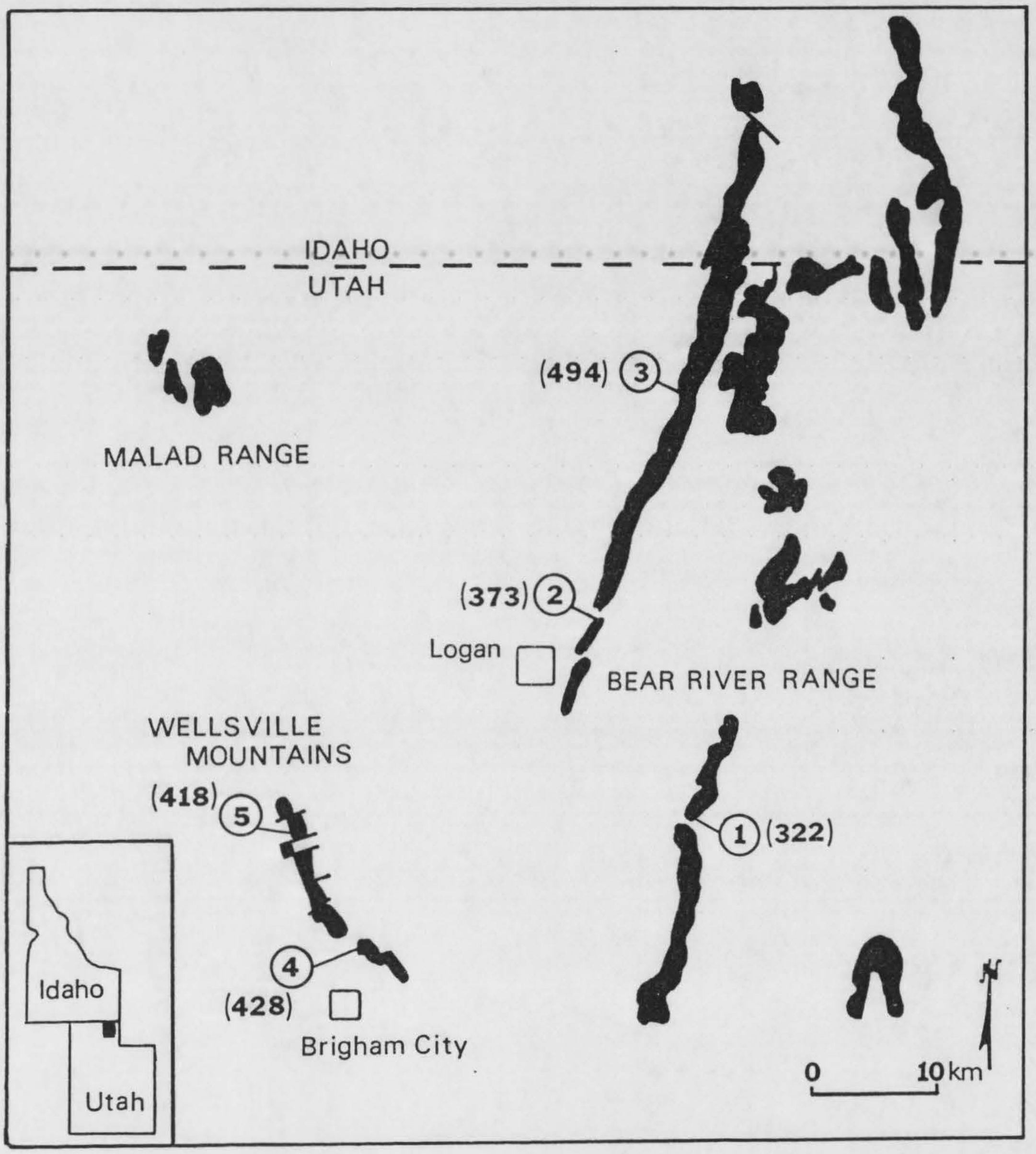

Fig. 1. Outcrop pattern of the Lower Ordovician Garden City Formation in north-central Utah. Circled numbers show locations of measured sections. Numbers in parentheses are thicknesses in meters (modified from Ross 1951).

The most recent work on the formation used paleomagnetism and conodont biostratigraphy to define the contact in north-central Utah between the Garden City Formation and the underlying Cambrian Saint Charles Formation (Taylor et al. 1981; Taylor, Landing, and Gillett 1981; Taylor and Landing 1981). The contact was found to be a diachronous disconformity, becoming younger towards the southeast.

METHODS

Five stratigraphic sections of the Garden City Formation (Fig. 1) were measured using a Brunton compass and Jacob-staff and described in detail. The sections ranged in thickness from 322 to 494 meters. Field information warranted the division of the sections into identifiable lithologic units. The units were then sampled at ten meter intervals using a stratified systematic sampling method (Krumbein and Graybill 1965). A total of 277 samples were collected. Polished slabs and acetate peels from all samples, plus 77 thin sections stained with alizarin red-S and potassium ferricyanide to aid in recognition of dolomite, iron-rich calcite, and iron-rich dolomite, were analyzed with petrographic and binocular microscopes for lithotype and environmental information. The thin sections were point counted, with a minimum of 300 points per slide. Ten acetate peels were point counted using a 10 square per inch grid. The remainder of the peels were estimated using comparison charts from Flugel (1982). X-ray diffraction of insoluble residues of all samples and detailed field relationships provided additional data.

LITHOTYPES

Nine lithotypes are identified in the Garden City Formation and were named using the classification of Dunham (1962). The lithotypes consist of nodular wackestone/mudstone with packstone lenses, intraclastic packstone/grainstone, green shale, laminated packstone/grainstone, cryptalgalaminite, fossiliferous packstone, boundstone, *Calathium*/sponge, and burrowed fossiliferous wackestone/packstone with chert. Variability exists within most lithotypes and is described where appropriate. The various lithotypes may have formed in more than one type of environment; therefore stratigraphic relationships were used in environmental interpretations.

Nodular Wackestone/Mudstone with Packstone Lenses

The nodular wackestone/mudstone lithotype consists of very silty limestone, sedimentary boudinage and nodular limestone punctuated with lenses of planar-laminated, hummocky cross-stratified, and uncommon ripple-laminated limestone. Minor amounts of whole and fragmented fossils, chiefly trilobites, pelmatozoans, sponge spicules, and rare lingulid brachiopods, and peloids occur as packstone lag deposits. Few fossils except sponge spicules occur in the mudstones, whereas clotted fabrics are common, possibly resulting from compaction of peloids. The predominantly horizontal and infrequent vertical burrows in the mudstones and wackestones are filled with pellets. Stylolites concentrate non-carbonate material, resulting in many wavy silty partings.

These limestones have a wide range of visible nodularity which depends on the amount of argillaceous material and burrowing/ bioturbation, and on the weathering aspect of the outcrop. They grade from very nodular (Fig. 2A) to sedimentary boudinage, alternating pinched layers of limestone and very silty limestone (Fig. 2B). The average insoluble residue is 25%, with kaolinite being the dominant clay mineral. The clay minerals are concentrated in the very silty limestone layers.

Sedimentary structures include horizontal and vertical trace fossils, ripple marks, hummocky cross-stratification, planar-laminations, load structures, and possible mudcracks. The trace fossils have variable diameters up to 2 mm and consist of burrow casts and trails. The horizontal trace fossils and ripple marks are seen in associated float and on the infrequently-exposed bedding surfaces. Rippled, hummocky cross-stratified and planar-laminated limestones generally occur in lenses, 1 to 30 cm thick, within otherwise nodular or layered limestones. Some of the ripple marks are draped by argillaceous material. Possible mudcracks are observed only in polished slabs, but never on bedding surfaces. Load structures occur at the contacts of coarse- and fine-grained limestones, with the coarse material protruding down into the underlying finer-grained material (Fig. 2B). The limestone lenses and sedimentary structures appear to be primary features unaffected by bioturbation (compare with Demicco 1983).

Nodular bedding has been interpreted by Wanless (1979) as a diagenetic imprint of pressure solution on bioturbated, originally layered argillaceous and calcareous material. There is much evidence for pressure solution in the nodular limestones. Stylolites are

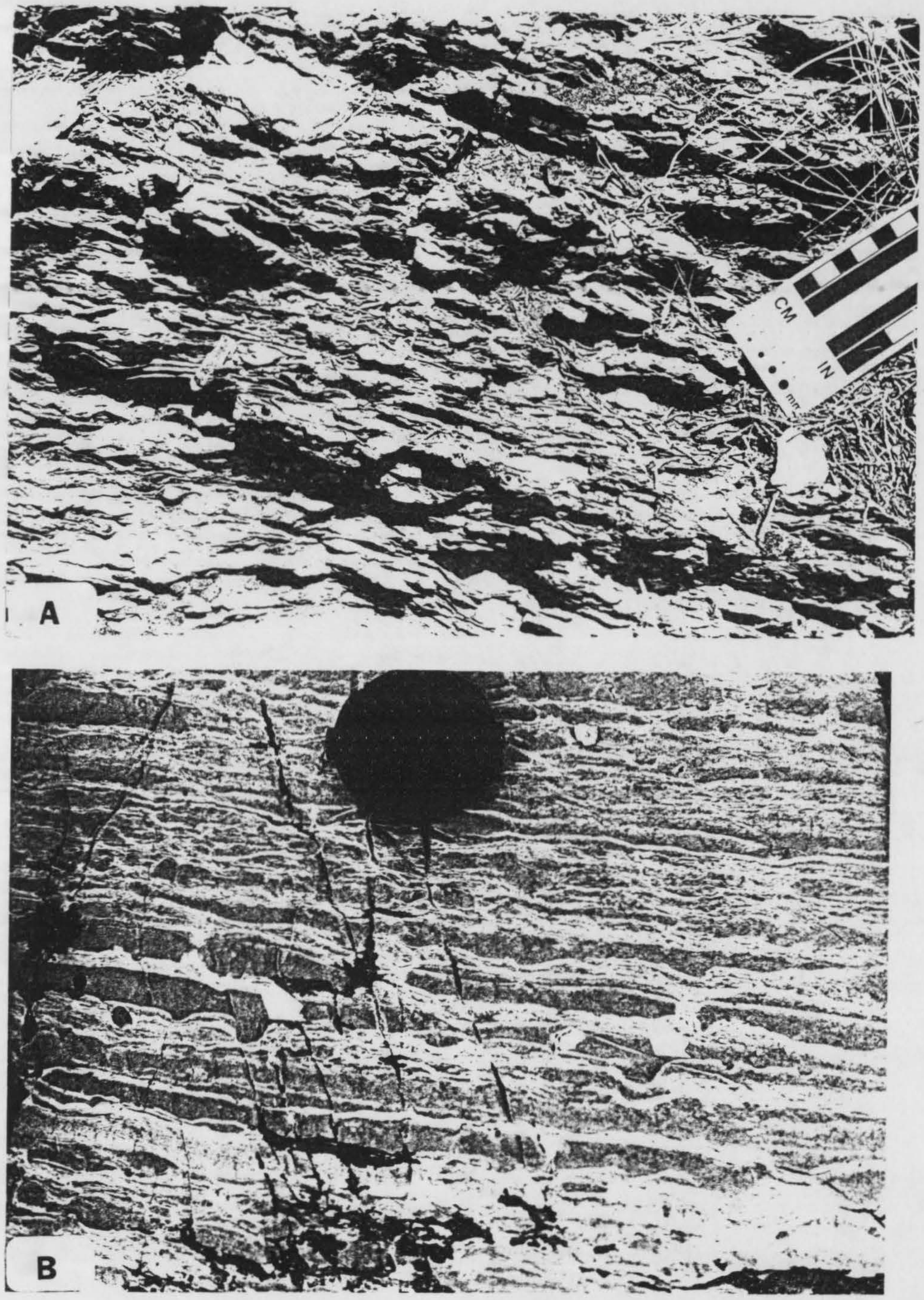

Fig. 2. Range of nodularity in nodular wackestone/mudstone. A) Well-developed nodular bedding B) Sedimentary boudinage, alternating pinched layers of limestone and very silty limestone. Arrows point to load structures. Diameter of lens cap is 5 cm.

common and form stylolaminations and wispy stylonodular features in these limestones.

Nodular limestones are the predominant lithotype of the lower informal member of the Garden City Formation. This lithotype resulted from retention of primary depositional features with some diagenetic reshaping. The dark, yellow-orange argillaceous material imparts an overall yellowish-gray color to the member. Nodular layers generally weather more readily to form slopes and incompetent outcrops.

Intraformational conglomerate layers and lenses between 8 cm and 3 m thick recur throughout the nodular wackestone/mudstone lithotype. The layers and lenses have abrupt upper and lower contacts.

Environment of Deposition.--A shallow subtidal, low-energy depositional environment has been postulated for the formation of sedimentary boudinage and silty nodular wackestone/mudstone (Wilson 1969; Cook and Taylor 1977; Aigner 1985). The stratigraphic associations with shoal water lithotypes of fragmented fossiliferous packstone and mud mounds strengthen the shallow subtidal interpretation. There is no evidence to suggest subaerial exposure of the sediment by tidal action. Packstone lenses of shell-lag and planar-laminated material probably resulted from storm-related currents.

The intraformational conglomerate layers and lenses signify a drastic change in the hydrologic regime. The lenses and layers are predominantly single-event storm deposits composed of a couplet of intraformational conglomerate topped by laminated fine-grained limestone. The pattern of the deposits and stratigraphic location, similar to those described by Bayer et al. (1985), suggest a distal environment which was affected by hurricane-velocity storms.

Intraclastic Packstone/Grainstone

Intraclasts are the dominant allochems in the intraclast packstone/grainstone lithofacies. The intraclasts are in a fossiliferous packstone to grainstone matrix composed of brachiopod, pelmatozoan, gastropod, unidentified mollusc shells, and trilobite debris, and uncommon Nuia and peloids. Nuia is a problematical codiacean alga restricted in occurrence to lower Ordovician rocks (Wray 1977). Many of the bioclasts have micrite rims. Sparite is neomorphic, and is in most cases clear, suggesting recrystallization of original cement.

Intraclasts show two time periods of burrowing/boring. Burrows and borings restricted to intraclasts occurred prior to transport, whereas faunal activity after transport is indicated by burrowing of both matrix and intraclasts.

Most clasts have rounded, smooth boundaries with truncated fossils. The rounding, due to transport, plus surface borings suggest extensive lithification of the sediment to firmgrounds or hardgrounds.

The intraclasts have the following compositions: micrite, with or without sponge spicules; fossiliferous quartz-laminated packstones; fossiliferous packstone/wackestones; and peloid-laminated packstones. They are bladed to blocky, well-rounded to subangular.

Bladed clasts may reflect thin hardground or firmground formation or be a result of algal mat binding. Since there is a paucity of evidence for either algal activity or subaerial exposure, break-up of lithified sea floor was probably the most important source of intraclasts.

Some of the smaller intraclasts are casts of fossils with little to no shell material retained, but with the fossil shape still recognizable. This may have been an important source of the small intraclasts. If the clasts were exhumed after the shell had been dissolved, they may have been reworked so any original organism shape is unrecognizable.

A small number of intraclasts, irrespective of composition, have synaeresis-type cracks (topside and bottomside) which are filled with clear sparite. The cracks do not extend past the clast boundary. Cracks may form from subaerial exposure. The cracks subsequently became filled by cementing material.

Environment of Deposition.--The intraclastic packstone/grainstone lithotype may have formed as: 1) storm sheet deposits, representing single events or an amalgamation of a series of events; 2) storm surge channel deposits; and/or 3) tidal channel deposits. Outcrop geometry of the intraformational conglomerate provides clues to its origin. The author used the criterion of consistent lateral extent over tens of meters to signify storm sheet deposits. Many of the conglomerate units contain erosion surfaces within, evidence of multiple storm deposits.

Conversely, channel deposits would probably pinch out laterally in distances of ten meters or less to produce an overall lens shape. Storm-surge channel deposits, as opposed to tidal channel deposits, would more likely be burrowed, with organisms returning after the current subsided. Storm-surge channel deposits would also be more likely to have fining-upwards sequences. Many channel deposits were identified and attributed to storm activity because they contained burrowed, fining-upwards sequences. Actual tidal channels were difficult to identify, particularly due to the paucity of intertidal evidence in associated lithotypes.

Storm sheet deposits show evidence for waning currents, with stacked Bouma-type sequences of hummocky cross-stratified to planar-laminated material followed by settled, previously-suspended fine material (Selley 1976). Many of the laterally extensive intraformational conglomerate units are topped by planar-laminated wackestone/mudstone material. Intraclasts, exhumed fossils, infiltration fabric, and conglomerate/wackestone couplets within the sheet deposits suggest a strong current followed by a waning current, typical of storms.

Some of the intraformational conglomerate beds had been lithified early on the sea floor as evidenced by erosional surfaces truncating clasts (Fig. 3). Osmond (1963) also found erosional surfaces on some intraclast layers in the Garden City Formation in the Stanbury Mountains. Lithification resulting in firmgrounds or hardgrounds may be due to slow sedimentation rates and submarine cementation in shallow subtidal environments (Sepkoski 1982). These are the same processes that are forming lithified sediments off the Florida coast today (Multer 1977).

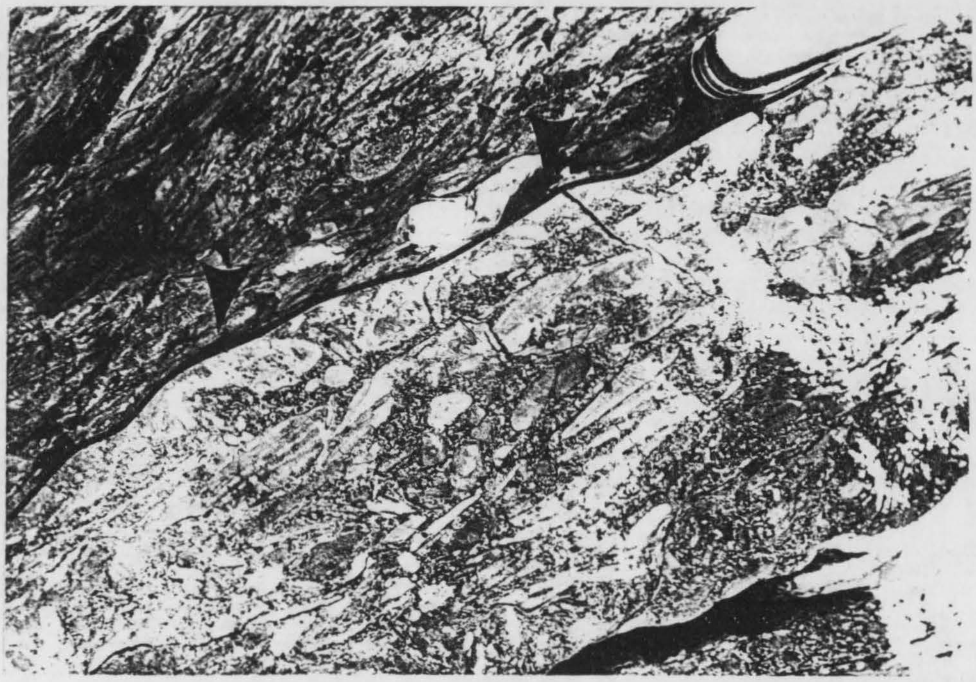

Fig. 3. Intraformational conglomerate with erosional surface (outlined in black) truncating clasts (arrows), evidence for early, sea-floor lithification.

Green Shale

Calcareous to clayey grayish olive-green shale is interbedded in layers from 1 to 30 cm thick within the nodular limestone lithotype in all locations. Kaolinite is the primary clay mineral in the shale facies. The shale increases in abundance to the south and southwest at sections four and five.

Environment of Deposition.--The presence of kaolinite indicates a terrigenous source and a near-coastal shallow-sea environment of deposition for the shale (Flugel 1982). The increase in abundance at sections four and five could have resulted from proximity to a fluvial source. The variability in the shale and silt content within sections and from section to section may have resulted from a shift in source area, seasonal changes in stream input, or storm pulses as noted by Ball (1983).

The shale has abrupt contacts with, and is frequently sandwiched between, intraformational conglomerate layers, an indication of a drastic change in water energy. Mount (1984) noted that rare-event input of sediments will result in abrupt, not gradational, contacts between siliciclastic and carbonate rocks. Therefore, the shale may represent event deposition.

Laminated Packstone/Grainstone

Well-sorted pelmatozoan fragments and peloids comprise the laminated packstone/grainstones. Variability in the amounts of these allochems creates a range in composition from primarily pelmatozoan fragments to a mixture of peloids and pelmatozoan fragments.

Scattered throughout are minor amounts of intraclasts and lingulid brachiopod and trilobite fragments. Many of the bioclasts have micrite rims. Some fossils are infilled with micritic material that is different than the surrounding matrix. This suggests exhumation and redeposition of the fossils (LaPorte 1967). The most likely source of currents strong enough to exhume fossils is storms (Kreisa 1981). Laminations result from increased quartz-silt and clay content and parallel alignment of the long axis of allochems.

The rocks are very-thin- to thin-bedded, planar-laminated to hummocky cross-stratified, and graded, and form either lenses within the nodular limestones or separate units which are found directly above nodular limestones or intraformational conglomerates (Fig. 4). Laminated limestones have been dolomitized in the lowermost 1 to 3 meters of the formation.

Environment of Deposition.--Sedimentary structures and laminations similar to those in the laminated packstone/grainstone have been related to deposition by waning storm currents by Kreisa (1981), Aigner (1985), and Duke (1985). The fine-grained material put in suspension by storm-wave turbulence is rapidly deposited during waning currents. The presence of the laminated packstone/grainstone units scattered within the nodular limestone and above some intraformational conglomerates argues for their intermittent-storm-generated origins.

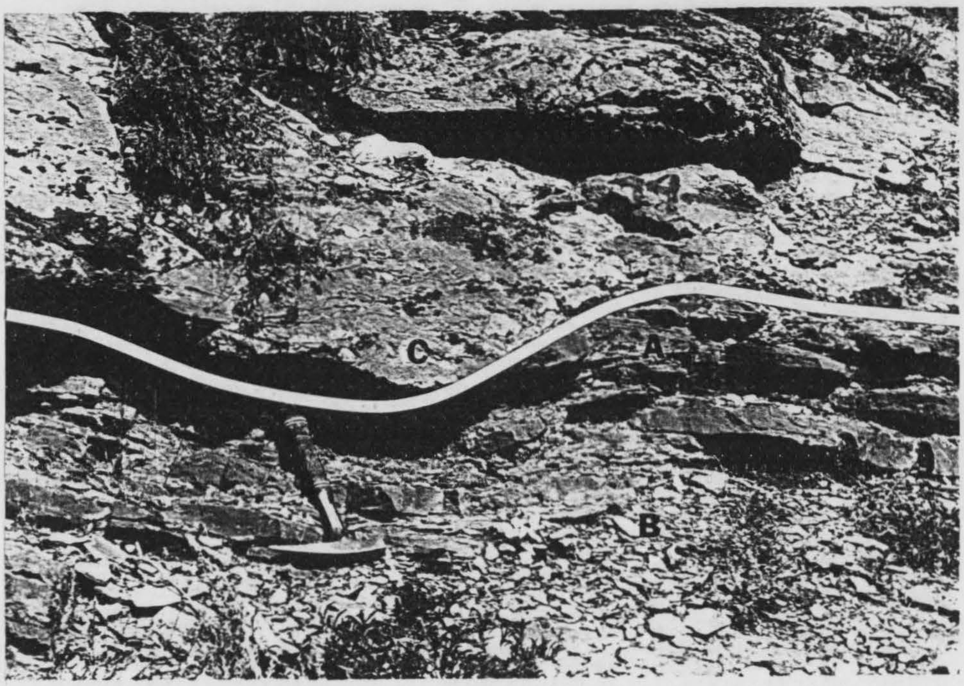

Fig. 4. Laminated packstone/grainstone (A) above nodular limestone (B). An intraformational conglomerate layer (C) was deposited directly on top. A small channel (outlined by white line) was eroded into the laminated packstone/grainstone.

Cryptalgalaminite

Cryptalgalaminites are a rare lithotype recognized in only one of the measured sections, within the nodular limestones. They form successive cryptalgally laminated layers, 2.5 to 16 cm thick, which have been diagenetically altered to chert. The cryptalgalaminites are interbedded with unaltered intraformational conglomerate, having a combined total thickness of 76 cm. Possible tepee structures and a clastic dyke cross-cut the thin-laminated units. In one layer, small digitate stromatolites, with maximum amplitude of 13 mm, underlie the sheet-like algal mat. Both the algal mat and stromatolites are dissected by vertical burrows.

Environment of Deposition.--Cryptalgalaminites form by the sediment-binding ability of algae and bacteria (Aitken 1967) and may have subtidal to intertidal origins (Scoffin 1987). Tepee structures in the algal mat and the mat's presence above digitate stromatolites indicate local shoaling to a tidally influenced environment.
A patchy distribution of intertidal sequences defined by the rare cryptalgalaminites and possible mudcracks is interspersed in the nodular lithotype. However, the cryptalgalaminites and mudcracks are not found together nor is there an order to their occurrence from one section to another. They may have formed as intertidal shoals within the subtidal zone in response to localized hydrodynamic regimes and increased carbonate production.

Fossiliferous Packstone

There are two major fossiliferous packstone deposits within the Garden City Limestone. In addition, lenses of fossiliferous packstone lag deposits are scattered throughout the lithotype. The biota of both types of fossiliferous packstones are similar, and include pelmatozoan, trilobite, the problematic alga Nuia, gastropod and other mollusc, brachiopod, rare lingulid brachiopod, and rare bryozoan fragments. Some bioclasts have micrite rims. Geopetal and infiltration fabrics are common. Many horizons of fossiliferous packstone are topped by fine material which probably represent a slackening of current.

Fragmented Fossiliferous Packstone.--These packstones are composed of fragmented skeletal material (fossil hash) and intraclasts and occur only in the lower part of the formation. The fragmented fossiliferous packstone outcrops are tinged orange-pink and are massive, with local planar laminations and hummocky cross-stratification. They recur vertically as layers and lenses from 0.3 to 3.5 meters thick interspersed with nodular wackestone/mudstone layers and mud mounds.

Environment of Deposition.--Fragmented fossiliferous packstones form small skeletal banks within a shallow subtidal environment. These represent local agitated shoal conditions on the shelf. Fossil accumulations may result from storm action moving skeletal debris onshore with subsequent winnowing and reworking by bottom turbulence from normal wave action (Aigner 1985). The accumulations are irregular, both in thickness and in the frequency of occurrence from section to section. The repeated occurrence signifies several shoaling or apparent regressive cycles.

Whole-fossil Fossiliferous Packstone.--Higher in the formation the packstones consist primarily of whole, unsorted fossils, uncommon intraclasts, some of which are shell molds, and peloids. The packstones form burrowed, thin-bedded outcrops. This lithotype is found in all sections and varies from 24 to 30 meters thick. Infrequent intraformational conglomerate lenses are scattered within the lithotype. There is a high concentration of brachiopods, pelmatozoan column fragments, and Nuia. Infiltration fabric and burrowing are common.

Environment of Deposition.--The whole-fossil fossiliferous packstone is interpreted as a skeletal build-up which created a submerged topographic high, below normal wave-base but still affected by storm wave-base. The skeletal accumulation separates the inner and outer shelves. Waning storm currents allowed deposition of suspended sediments which caused infiltration fabrics. Whole fossils and the amount of micrite argue for a below-normal-wave-base, less-agitated environment. The accumulation may have been initiated and subsequently perpetuated by storm accretion. The open-marine seaward side of the skeletal build-up would be a natural habitat for pelmatozoans and brachiopods. The accumulations did not form a continuous front but were dissected by channels, shown by lenses of intraformational conglomerate. The channels allowed storm effects landward of the accumulations. There is no evidence to suggest that these accumulations ever built up to a shoal environment.

Boundstone

Mud mounds and stromatolites make up the boundstones which recur vertically with varying thicknesses in each location. The mud mounds are domal to mushroom shaped, and are between 15 and 76 cm in diameter and between 13 and 71 cm high. Some mounds have coalesced to form sheets. Mud mounds generally are grouped along the same horizon. They are common in some sections while nearly absent in others.

The mounds are surrounded by two types of material. Nodular limestones pinch out against, and drape over, most of the mud mounds (Fig. 5A). The mud mounds may grow from a nodular limestone or an intraclastic substrate. A small proportion of mud mounds are surrounded by, and in some cases propagated from, the fragmented fossiliferous packstone. A layer composed of light-colored sheet-like mounds dissected by channels filled with the darker-colored fragmented fossiliferous packstone is present in each location (Fig. 5B). The channels have very sharp, but irregular boundaries with the mound rock indicating the mounds were somewhat consolidated prior to channel cutting (Toomey 1970). The channel cutting may have been initiated by shoaling.

Differential weathering in section three has exposed the three-dimensional nature of the mounds. The mounds are tubular shaped and extend into the outcrop (Fig. 5C). Church (1974) also found uniformly aligned "sausage-shaped" mounds in the correlative House Limestone of the Ibex Mountains. Mud mounds result from current activity and preferential bottom stabilization by organisms (Toomey 1970; Church 1974; Pratt and James 1982). Since the mounds appear

Fig. 5. Features of mud mounds found in the Garden City Formation. A) Mud mound of the boundstone lithotype outlined by dark line. Note that the nodular limestone pinches out against the mound (arrow) and drapes over the mound. Diameter of lens cap is 5 cm. B) Light-colored sheet-like mound horizon dissected by a channel (outlined by black lines) filled with darker-colored fragmented fossiliferous packstone. These represent an apparent regression into shoal conditions. C) Weathering reveals the three dimensional nature of mud mounds at section three. The mounds are tubular shaped and extend into the outcrop (arrow). Diameter of lens cap is 5 cm.

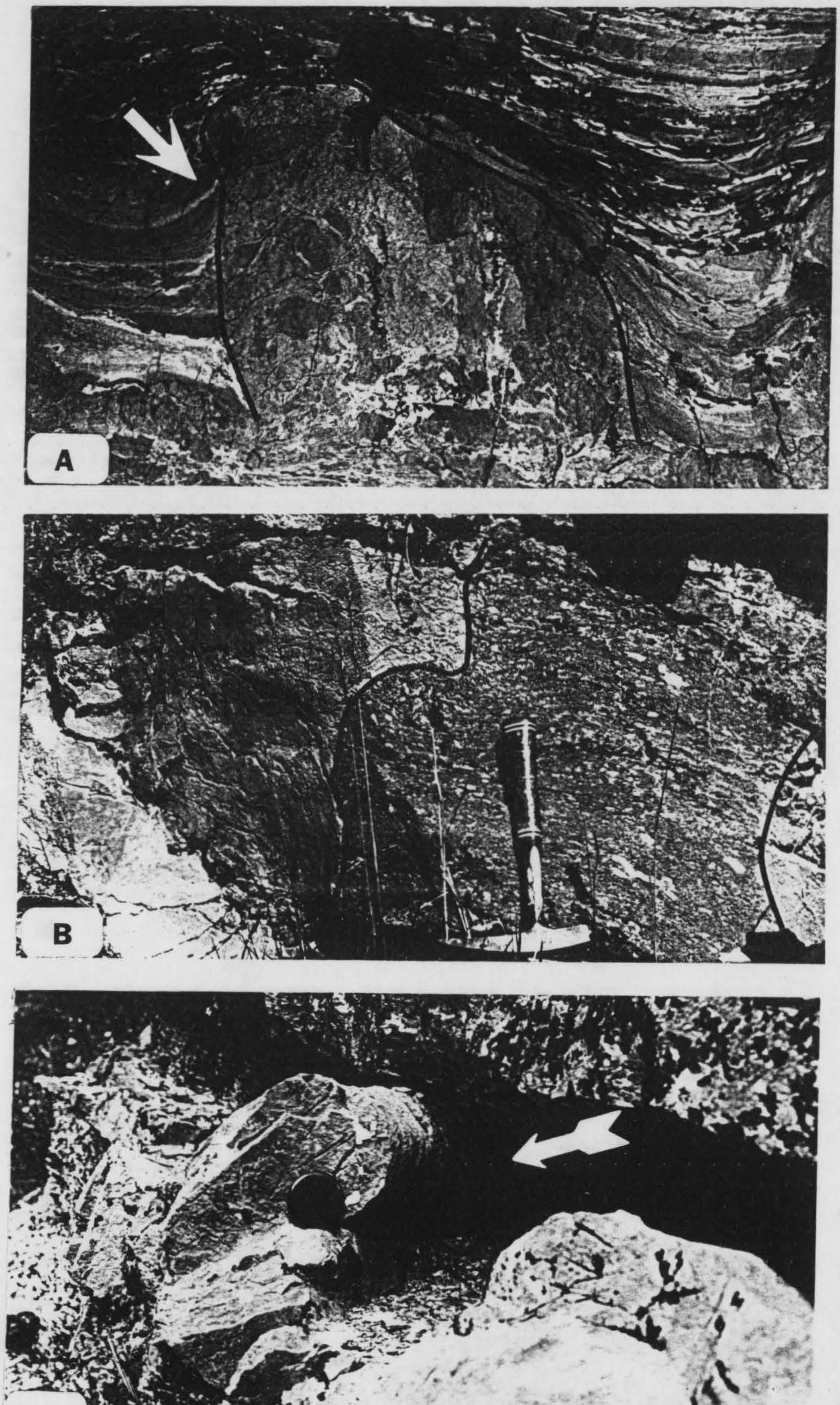
A
B
C

to parallel the shoreline in both section three and in the Ibex area studied by Church, the hydrodynamic processes must have been influenced by the ocean/land interface.

Float associated with the mud-mound zone contains rare, isolated stacked hemispheroidal stromatolites. The stromatolite morphology and the surrounding medium of fragmented fossiliferous packstone suggest that the stromatolites may have grown on top of the mounds and extended into shallower and more turbulent water. Stromatolites also occur at the base of the formation in section four and are associated with cryptalgalaminites in section three.

Internally the mud mounds reveal very few scattered fossils of Nuia, sponge spicules, and pelmatozoan fragments in a micrite matrix. A lower algal mat layer is evidenced by silt-floored, parallel fenestrae interspersed with quartz silt layers. This is similar to evidence used by Pratt (1982a) to determine algal mats. The algal mat is overlain by spongiform and clotted fabrics. This gives the appearance of a colonization sequence similar to that of equivalent Ordovician mounds elsewhere in Utah (Church 1974). However a more detailed analysis of the Garden City mud mounds is needed before such a sequence can be documented.

The mounds have a massive to rare, faintly-laminated fabric, but do not exhibit the mottled texture that characterizes thrombolites. According to Kennard and James's (1986) recent nomenclature, they are most accurately named spongiform microbial boundstones.

Environment of Deposition.--Mud mounds are associated with both the fragmented fossiliferous packstone banks and the nodular wackestone/mudstone lithotypes. They grew in shoal conditions within the shallow subtidal zone. Several of the mounds have channels eroded into them with subsequent infilling of fossil debris. The eroded channels may indicate a relative drop in sea level. Modern mud mounds have proven to be storm-wave-resistant; therefore storm currents probably had little deleterious effect on ancient mounds (Ball et al. 1967). Mounds are well developed and exposed in only three sections; in addition, they do not display much lateral continuity. Therefore a patchy distribution of the mounds, dependent on local conditions, is postulated. Orientations of tabular mounds indicate they formed parallel to the shoreline.

Calathium/Sponge

Calathium is a dasycladacean algae (Church 1974) and is associated with listhid sponges in the Garden City Formation. *Calathium* is rare, scattered randomly throughout the sections, and generally increases in abundance just below the chert zone in the upper part of the formation. At section three a prolific *Calathium*/sponge assemblage forms a prominent unit, 3.3 meters thick.

Environment of Deposition.--Because the fossils are whole and well-preserved in a wackestone/packstone (Fig. 6), and because these fossil types would probably not survive transport, this is interpreted as an autochthonous assemblage indicative of low energy in a deeper, below-normal-wave-base environment (Wray 1977). The unit's thickness and presence in all sections also indicates autochthonous origins. Stratigraphic location of the *Calathium*/sponge lithotype directly

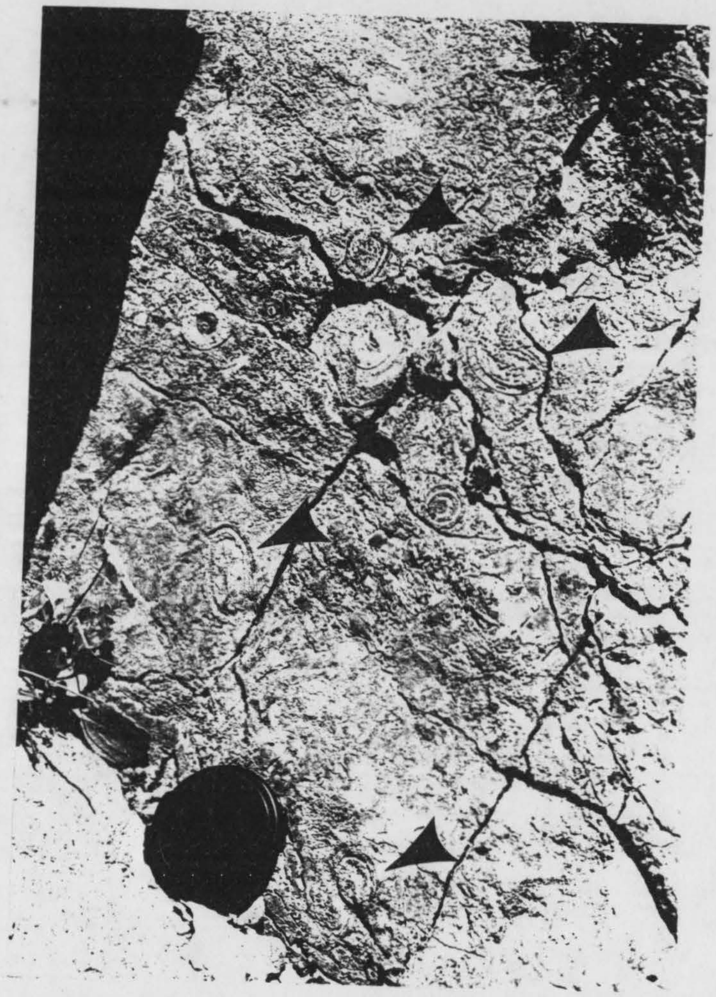

Fig. 6. Calathium (arrows) forming a prominent unit at section three, just below the chert zone. Sponges are associated with the Calathium. Diameter of lens cap is 5 cm.

above the whole fossiliferous packstone skeletal accumulation suggests they may have enjoyed a position seaward of the skeletal accumulation.

Due to poor outcrop exposure the lateral extent and configuration were not determined. However, since the concentration is limited locally it may represent a patch reef community that developed in association with the skeletal bank.

Burrowed Fossiliferous Wackestone/Packstone With Chert

This lithotype is characterized by whole and fragmented fossils, rare intraclasts, and peloids disseminated throughout a stylolitic wackestone by bioturbation and burrowing. Clotted fabric and synaeresis-type cracks filled with clear sparite are most prevalent in this lithotype, whereas very few intraformational conglomerate lenses or layers are present. The lithotype also contains fossiliferous packstone lag deposits. The fossil assemblage exhibits high variability but low abundance of types. Fossils include sponge spicules, trilobites, brachiopods, gastropods, unidentified molluscs, pelmatozoans, *Nuia*, conodonts, and ostracods. Ostracods are limited to this lithotype.

Sections two, four, and five exhibit a unique feature. The uppermost 33 to 45 meters of the three sections are dolostone and have recurring horizontal bands and irregular blebs of sparite (Fig. 7). These may be stromatactis structures (Bathurst 1980). Stromatactis form in subtidal environments but so far have only been described in association with bioherms (Ross et al. 1975; Bathurst 1980). However, dolomitization has obscurred most of the petro-

Fig. 7. Horizontal bands (possible stromatactis?) (arrows) in dolomitized burrowed fossiliferous wackestone/packstone.

graphic information.

This lithotype comprises all of the uppermost informal cherty member previously mentioned. Its most stunning aspect is the gradual increase in black, gray, and white chert to a maximum of 40 to 50% of the rock and then a similar gradual decline to no chert. The gradational changes are apparent at all locations, but the thickness of the chert unit between localities varies from 33 to 55 meters.

The chert's habit is nodular, banded, and anastomosing and appears to follow burrows or areas of bioturbation. The white color is probably a weathering rind since it extends 10 mm or less below the surface. Numerous relict sponge spicules are apparent within the chert. The limestone within the chert zone is similar to that above and below; however there is a marked increase in monaxon and rare triaxon sponge spicules in the limestone. This suggests a biogenic source for the chert.

Dolomite formation has been related to chert formation (Knauth 1979). Secondary dolostone is present in the chert zone. Dolostone also is prominent below the contact with the Swan Peak Formation. It has an irregular lateral contact with the limestone which suggests a diagenetic origin.

There is a dramatic increase in angular to subangular quartz-silt and fine sand content in the uppermost 1.5 meters of the facies.

<u>Environment of Deposition</u>--The peloids, prolific burrowing and bioturbation, variety of fossils, and lack of wave-generated sedimentary structures indicate a deeper subtidal environment, below

normal-wave and most storm-wave bases. The limited occurrences of intraformational conglomerate layers may represent rare megastorms or storm surge channels. Pockets of coarse fossiliferous material and erosional surfaces may reflect storm-induced oscillatory currents (Kreisa 1981). Insoluble residue and visual appearance indicate only minor amounts of silt and clay minerals were deposited in the open marine deep subtidal environment. Pyrite is found in slightly higher amounts indicating local reducing conditions.

DISCUSSION

Storm Sedimentation

Storm (event) sedimentation dominated the Garden City Formation, particularly the lower informal member (Table 1). Storms are responsible for onshore and some offshore movement of material (Fig. 8). Coastal water set-up, a result of wind, barometric effects, and wave action move material landward (Aigner 1985). This water returns offshore by bottom gradient currents, forming storm-surge channels which move material seaward. Offshore material is deposited as laminated, graded storm layers (Aigner 1985). Lag deposits and erosional surfaces are common. Mean wave-base is greatly increased during storms to a storm wave-base estimated at 40-80 meters deep (Flugel 1982). Kreisa (1981) noted oscillatory currents created by storm waves occurring at depths to 200 meters. Therefore much of an epeiric sea bottom would be influenced by storm sedimentation. Study of modern storm deposits indicates the rock record may be biased in favor of sporadic catastrophic depositional events overprinting

Table 1. Storm-generated features and their observed occurrences in the Garden City Formation (see Kreisia 1981 for references to most features).

Sedimentary Feature	Common	Uncommon
Interbedded coarse (storm deposits) and fine (normal deposits)	X	
Sharp erosional contacts between and within layers	X	
Gutter casts		X
Lag deposits	X	
Lag - suspension couplets	X	
Exhumed bioclasts	X	
Infiltration fabrics	X	
Reworked intraclasts (intraclast composed of intraclasts)	X	
Intraformational conglomerates	X	
Escape burrows		X
Hummocky cross-stratification	X	
Laminated beds - usually graded	X	
Reworked skeletal accumulations	X	

STORM PROCESSES AND MATERIAL TRANSPORT

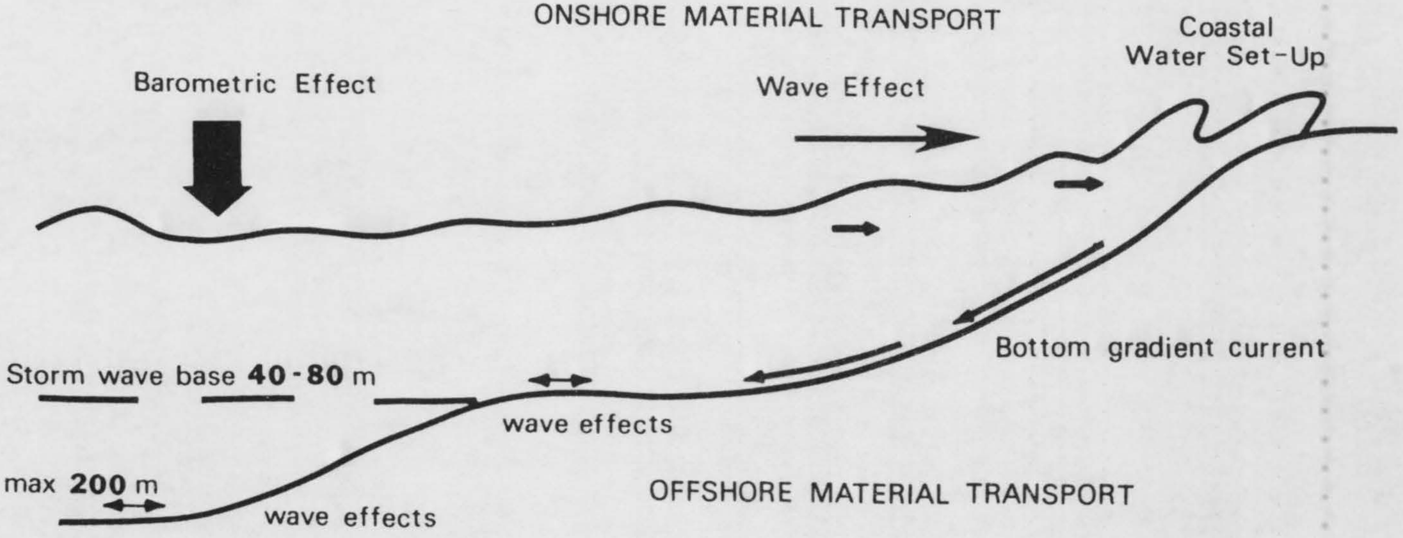

Fig. 8. Onshore transport of material is a result of barometric and wind effects moving water shoreward. Offshore transport results from water returning in bottom gradient currents. Oscillatory bottom currents are from storm wave effects (modified from Aigner 1985).

normal deposition (Hayes 1967). Normal intermittent deposits are reworked by storms numerous times, with only the strongest event recognizable (Seilacher 1982).

Depositional Environments

The deposits of the Garden City Formation can be divided into inner-shelf peritidal and outer-shelf subtidal environments. The inner-shelf peritidal deposits include reworked material and shallow subtidal nodular limestones interspersed with mud mounds and shoals of fossil banks and rare cryptalgalaminites. The outer shelf is a deeper subtidal environment composed of one basic lithotype, the fossiliferous wackestone/packstone. These two facies were separated by a submerged, muddy, predominantly whole-body skeletal accumulation. Figure 9 is a schematic diagram using lithotypes and facies relationships to reconstruct the Ordovician shelf environments. The environments were responses to bathymetric and associated water-energy positions in an epeiric sea which had minor bottom irregularities and small slope breaks.

The initial transgression, a shallow water encroachment on the craton, is represented by reworked material of the following variety of lithotypes: laminated packstone/grainstone, intraclastic packstone/grainstone and nodular wackestone/mudstone. In association with these lithotypes are dolomitized sediments and rare stromatolites. The lithotypes do not appear to have a specific sequence of relationships to each other nor are they developed extensively. The sequence of relationships may have resulted from reworking which is typical of nearshore transgressive deposits. Iden and Moore (1983)

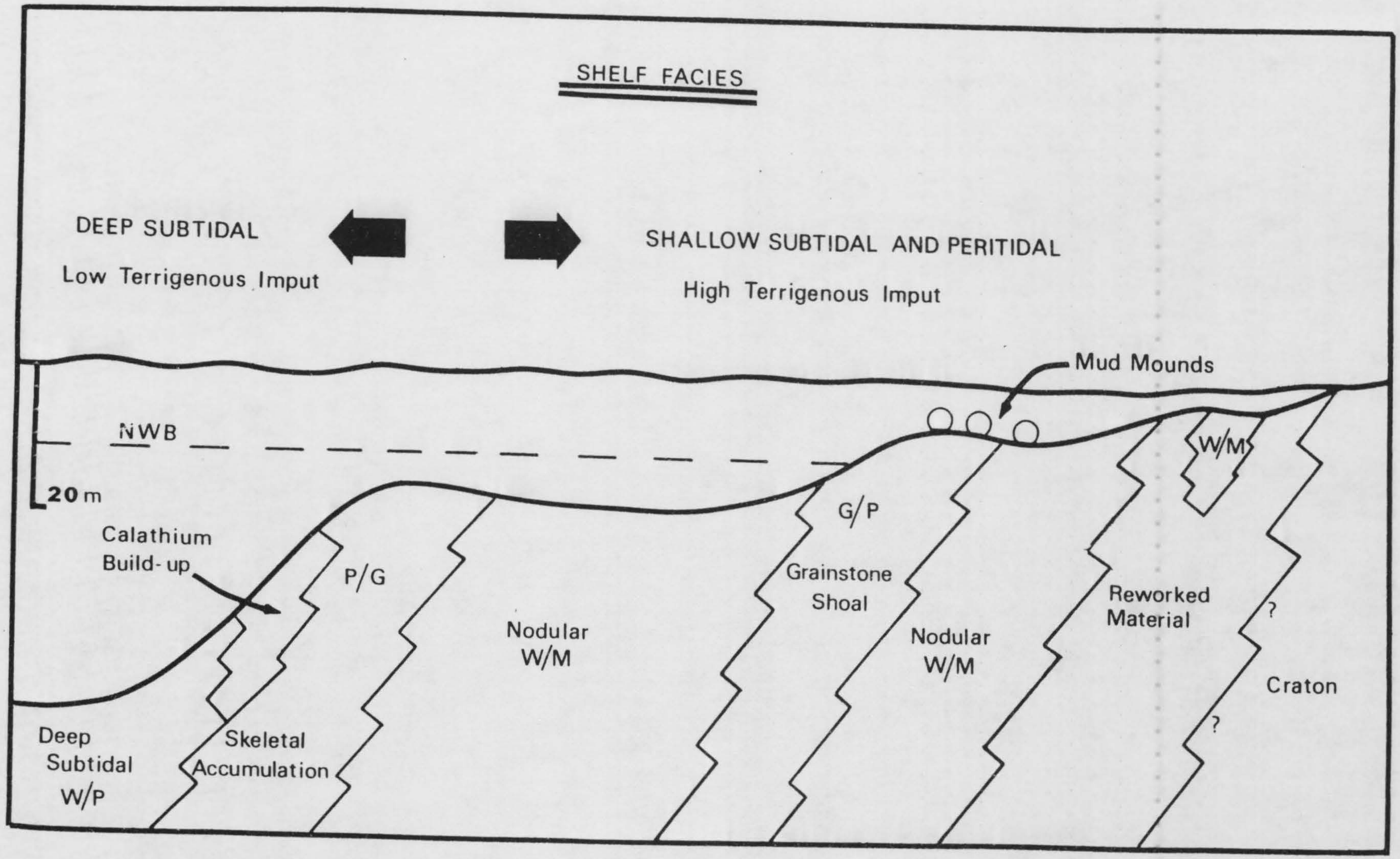
SHELF FACIES
DEEP SUBTIDAL
Low Terrigenous Imput
SHALLOW SUBTIDAL AND PERITIDAL
High Terrigenous Imput
Mud Mounds
NWB
20 m
W/M
G/P
Calathium
Build-up
P/G
Grainstone
Shoal
Reworked
Material
?
Nodular
W/M
Nodular
W/M
Craton
?
Deep
Subtidal
W/P
Skeletal
Accumulation

and Einsele (1985) noted that strandline deposits in transgressive sequences are reworked by wave and storm erosional events to produce fossil lag and amalgamated intraclast deposits with relict thin-laminated carbonate sands. A modern analogy, the Holocene transgression in Biscayne Bay, Florida, produced extensive eroded, reworked and redistributed material (Wanless 1969). Kreisa (1981) has also demonstrated that thick amalgamated storm layers are a product of shallow water.

The base of the Garden City Formation is characterized by numerous erosional surfaces within thick, large-bladed intraclastic layers and lenses. The intraclastic layers are interbedded with planar-laminated lenses and layers and rare stromatolites. Lingulid brachiopods are most common in this facies. The intermixed nodular limestones indicate that shallow subtidal conditions and/or quiet water lagoonal pockets were adjacent to the reworked intertidal material with the environments shifting in varying responses to storms and water depth changes.

On the leading edge of a transgression, in accordance with Walther's Law (Wilson 1975), one would expect coevolving supratidal, shoreline, and intertidal deposits. However, there is a conspicuous lack of evidence for these environments in the Garden City Formation. A relatively rapid transgression and reworking of material may have obliterated these characteristic deposits. A mud-flat shoreline with low amplitude tidal influence also could account for the lack of supratidal and intertidal deposits.

The epeiric sea depositional models of Irwin (1965) and Shaw (1964) call for low depositional slopes, < 0.3 meters per mile, which dictate that facies be deposited in broad, energy-related zones parallel to the ancient shoreline (Irwin 1965). The stratigraphic evidence confirms that the Garden City facies were indeed deposited this way. Figure 10 represents a north-south cross section of the Garden City facies. It illustrates the broad, parallel deposition of the facies to the locally southern shoreline.

Shaw's and Irwin's model of epeiric sea deposition also requires that there was no tidal influence over extensive, landward, low-energy deposits. With no tidal influence there would have been no means for promoting water circulation. Shaw (1964) has argued that storms, rivers, and precipitation could not provide sufficient input to maintain consistent normal-marine conditions; these could only be maintained by tidal action. The result of no tidal circulation would have been restricted marine environments of high salinity and associated evaporite deposition (Shaw 1964). In the study area no such deposits developed. This may have been a function of a steeper depositional slope than required in the Shaw-Irwin model.

The inner shallow subtidal environment probably remained near normal-marine conditions. Evidence includes occurrences of trace fossils, brachiopods and crinoids within fossil banks, Nuia, and scattered whole Calathium fossils, essentially a normal-marine biota. Although faunal variability appears restricted, trilobites are ubiquitous. Ross (1951) has identified up to 17 species within one faunal zone of the facies. There is also a complete lack of direct or indirect evidence for any evaporite formation. If the subtidal was normal marine, then there must have been tidal effects. Many workers (see Klein and Ryer 1978) have also found evidence for tidal

Fig. 10. Generalized north-south cross-section of the Garden City Limestone in the study area. Sections one, two, and three were used.

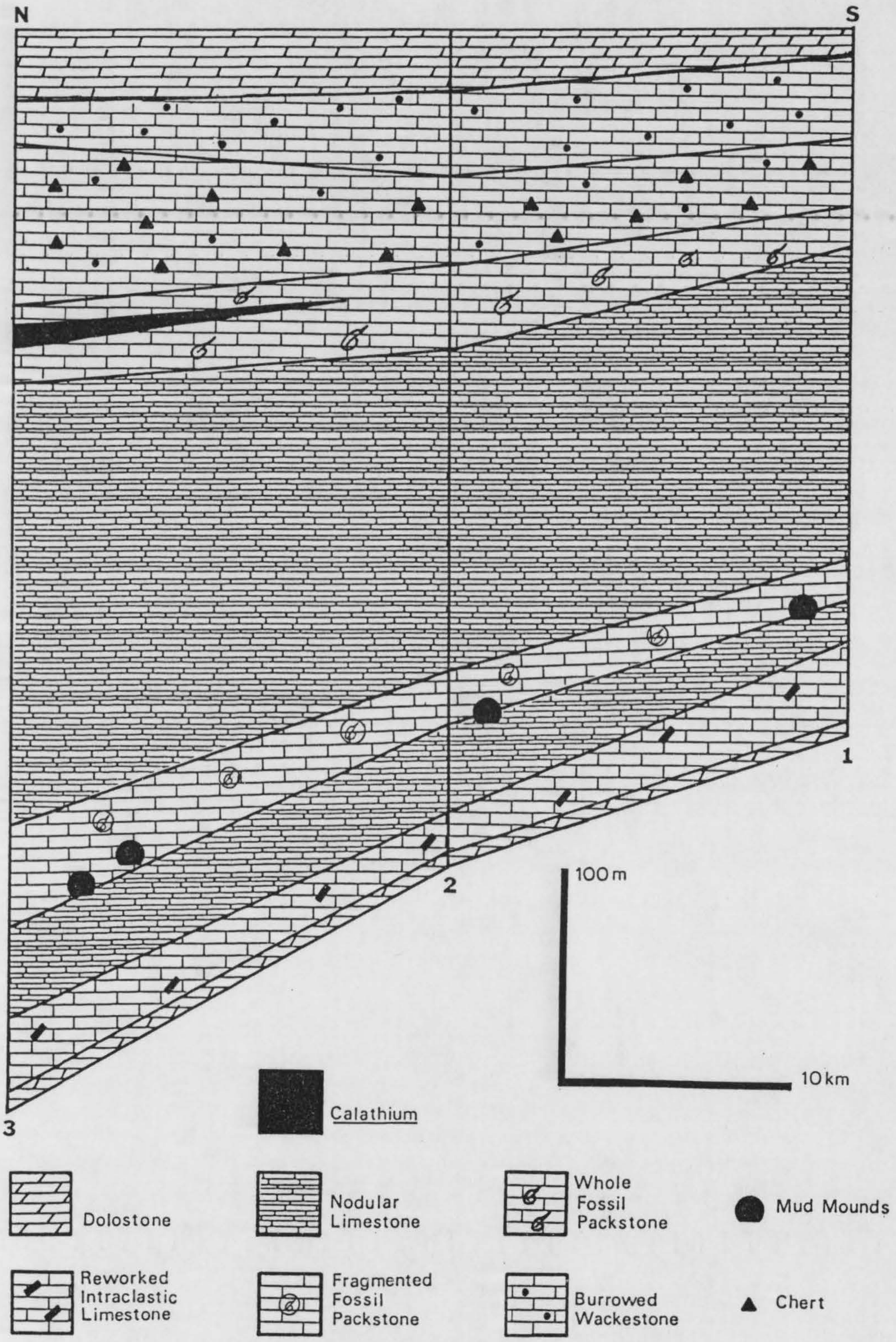
N
S
1
2
3
100 m
10 km
Calathium
Dolostone
Nodular Limestone
Whole Fossil Packstone
Mud Mounds
Reworked Intraclastic Limestone
Fragmented Fossil Packstone
Burrowed Wackestone
Chert

action within epeiric seas.

The shallow subtidal zone was influenced by tides, had lower faunal diversity and production, and had considerable terrigenous input of quartz silt- and clay-sized particles. The outer deeper subtidal zone had higher faunal diversity and production, with very little terrigenous material. The environmental differences are attributed to the terrigenous material and its damping effect on faunal grain production (La Porte 1969).

The rare intertidal deposits within the subtidal environment are interpreted as shoal islands formed by increased carbonate production, perhaps similar to, but not as well developed as, those described in the Ordovician St. George Group by Pratt and James (1986) and the Lower Devonian Manilus Formation described by LaPorte (1967). These irregular shoals may have been analogous to the anastomosing mud banks of Florida Bay (Multer 1977, p. 64).

The upper contact of the Garden City with the Swan Peak Formation throughout the study area is abrupt. This may represent a disconformity. A more detailed analysis of this contact, specifically noting the fossil content, would be helpful in answering questions about its nature.

PALEOGEOGRAPHY

Deposition of the Garden City Formation started in the Tremadocian Age and continued through the Arenigian Age of the Early Ordovician Period, a span of 27 million years. During that time North America was part of the Laurentia paleocontinent which rotated counterclockwise to the south (Scotese et al. 1979). The equator was located within 10-15^{o} of north-central Utah which produced a tropical, humid climate (Scotese et al. 1979; Taylor et al. 1981).

The Early Ordovician was a time of tectonic quiescence and cratonic subsidence, which resulted in widespread epeiric seas (Sloss 1964). The rocks of the Garden City Formation were deposited in the Cordilleran miogeocline (Stewart and Poole 1974) by an easterly transgression of a broad, shallow sea over the stable craton. The shelf/slope transition to deep water was in central Nevada (Cook and Taylor 1977). At maximum transgression, the shallow shelf extended into Utah (Fig. 11).

The Garden City Formation represents a long-term transgressive sequence of an open-marine shallow-shelf epeiric sea extending west as much as 500 km from the exposed craton at maximum transgression (Stewart and Poole 1974). The sedimentary environments are storm-influenced and are oriented parallel to the shoreline. The lower disconformable contact is marked by a thin, basal, very silty limestone layer above the massive, dolomitic upper Saint Charles Formation.

Utah was divided into two depositional basins by the emergent Tooele Arch, the Northern Utah Basin to the north and the Ibex Basin to the south (Hintze 1973). Figure 12 shows the thicknesses of the Garden City Formation and the equivalent Pogonip Group which define the paleotopographic high. The formation also thins to the north into Idaho; its deposition probably was influenced by the submerged Arco Arch (Oaks et al. 1977). In the study area the formation thins to the southeast. Such thinning suggests that the shoreline was to the south and east, in agreement with regional data.

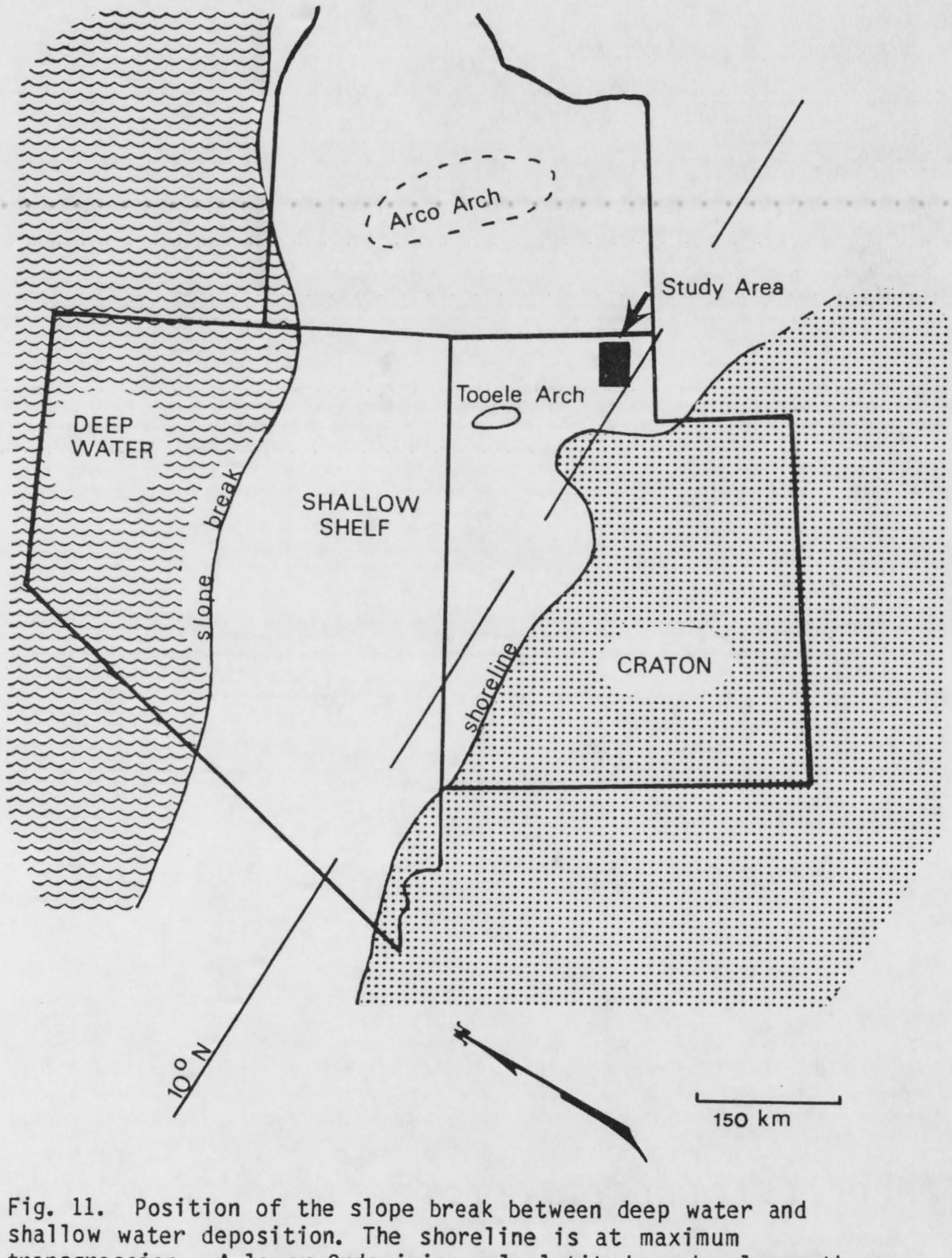

Fig. 11. Position of the slope break between deep water and shallow water deposition. The shoreline is at maximum transgression. A lower Ordovician paleolatitude and paleonorth are indicated (adapted from Eardly 1964; Hintze 1973; Scotese et al. 1979).

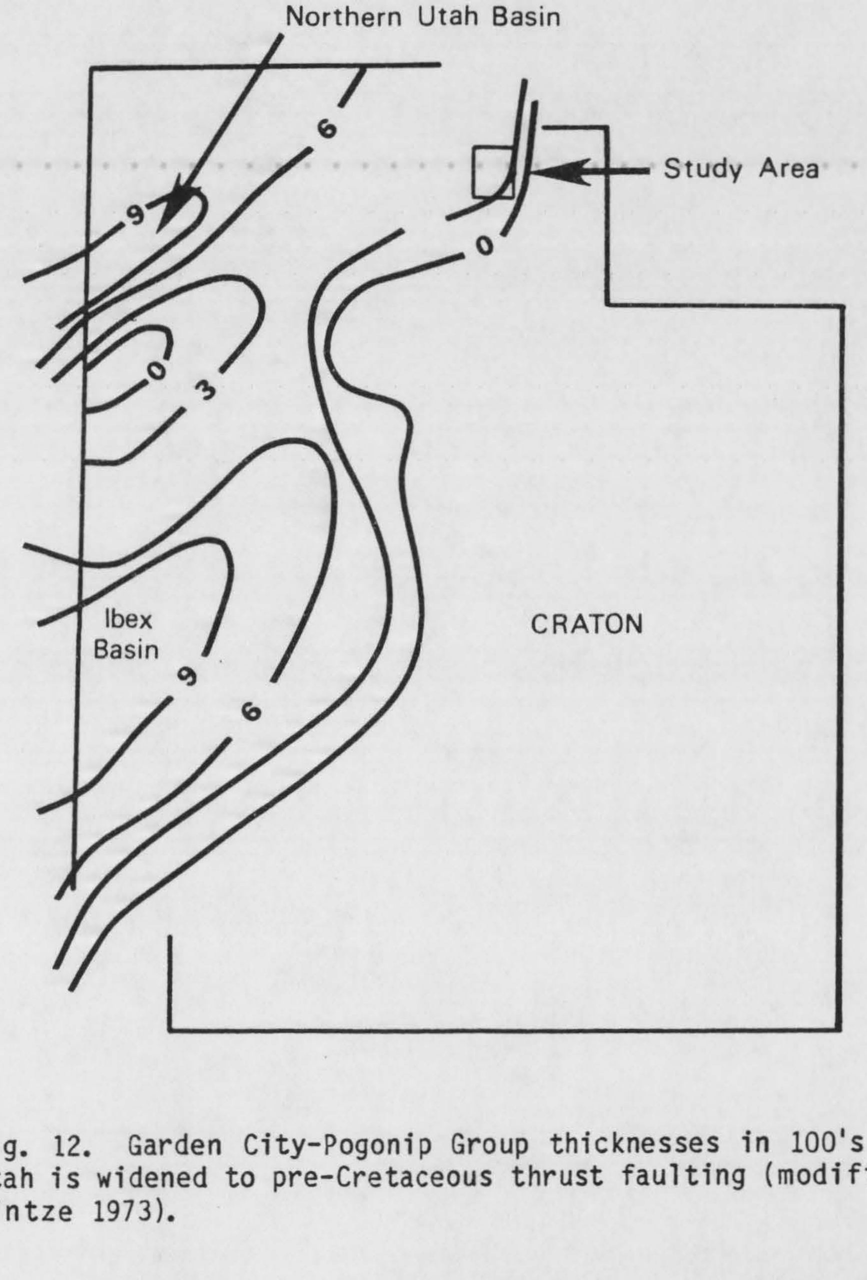

Fig. 12. Garden City-Pogonip Group thicknesses in 100's of meters. Utah is widened to pre-Cretaceous thrust faulting (modified from Hintze 1973).

Although part of the Tooele Arch was emergent, the epeiric sea had no topographic barriers to restrict circulation. It was not a sea surrounded by land, but was instead a vast expanse of open shallow water. Depocenters were controlled by gradually subsiding basins and gently uplifting arches.

The exposed barren craton to the east and the Tooele Arch to the south were sources of the silt- and clay-sized terrigenous material. Since there was no soil-stabilizing vegetation in the Ordovician, any weathering products would be highly susceptible to erosion by water and wind. The ubiquitous nature and the silt and clay size of the terrigenous material in the Garden City Formation suggest it may have been transported to the west by prevailing easterly trade winds and deposited in the sea (Dalrymple et al. 1985). Field observations show an increase in the amount of siliciclastic material in sections four and five, which implies a more localized origin and is possible evidence for placing a fluvial source nearby. The field observations are substantiated by insoluble residue data from samples of the silty nodular limestone. Sections one, two, and three had average insoluble residues of 13, 11 and 12% respectively while sections four and five had 22 and 16%. The averages were calculated using samples within the same lithologic boundaries. No chert was present in any of the samples. Current influence may have effectively prevented deposition of the terrigenous material in the other sections. However, the rocks may not have retained their original spatial relationships, since Oviatt (1985) has inferred a north-moving thrust fault under the Wellsville Mountains.

SUMMARY AND CONCLUSIONS

The Garden City Formation represents a storm-dominated transgressive sequence deposited in a broad epeiric sea. The formation is composed of nine lithotypes which represent various sedimentary environments. The transgression extended from the west covering the previously exposed and eroded Upper Cambrian Saint Charles Formation. The initial transgressive and shoreface material was extensively reworked by storm action and is characterized by erosional channels and thick intraformational conglomerate layers and lenses.

The shelf was subdivided into two distinct environments, a shallow-subtidal inner shelf and a deeper-subtidal outer shelf (Fig. 9). The shallow inner shelf was characterized by shoreward fossil banks and mud mounds, a restricted fauna, large amounts of terrigenous material, and repeated occurrences of intraformational conglomerate layers. Excessive sediment production resulted in the formation of irregularly distributed shoal islands.

The deeper outer-shelf sediments include a diverse fauna and are characterized by burrowing and bioturbation. They have a significant amount of black, white, and gray chert. The inner and outer shelf were separated by a submerged, storm-initiated skeletal accumulation.

The restricted fauna of the shallow inner shelf resulted from terrigenous input creating an unfavorable habitat. The Garden City sediments do not contain interior regions of extensive, tideless low-energy deposits as predicted by Shaw's (1964) and Irwin's (1965) models. Instead tides were an important aspect of the hydrodynamic regime of the Ordovician epeiric sea and provided water circulation to maintain near normal marine conditions.

Throughout the time of deposition of the Garden City Formation, Utah was located within 10-15^{o} of the equator, which produced a humid, tropical climate. Deposition was controlled by the gradually subsiding Northern Utah Basin and Ibex Basin and the gently uplifting Tooele Arch. There were no topographic barriers to restrict circulation in the vast expanse of the Ordovician sea. The transition to deep water was in central Nevada (Fig. 11).

CHAPTER III

DIAGENESIS OF THE LOWER ORDOVICIAN GARDEN CITY LIMESTONE: PETROGRAPHIC EVIDENCE

INTRODUCTION

The Lower Ordovician Garden City Formation, located in north-central to western Utah and southeastern Idaho, is part of a thick sequence of Lower Paleozoic shallow-water carbonate rocks that crop out in the western United States. In the study area of north-central Utah (Fig. 13) the Garden City Formation lies in diachronous disconformity on the Cambrian Saint Charles Formation (Taylor and Landing 1981) and has an abrupt to gradational upper contact with the Middle Ordovician Swan Peak Quartzite. The formation thins to the south and east (322 m) and thickens to the north and west (549 m) (Hanson 1949). It is predominantly limestone with minor amounts of siliciclastic rocks; however, portions of the base and top are dolostone. Banded, nodular, and anastomosing chert dominate the upper portion.

Previous work by Ross (1951) on the paleontology of the formation also included comments, based on outcrop data, on the diagenetic formation of the dolomite and chert. The purpose of this paper is to re-evaluate and expound upon the diagenetic events, using petrographic analysis and cathodoluminescence, and to define a model of diagenesis for the Garden City Formation.

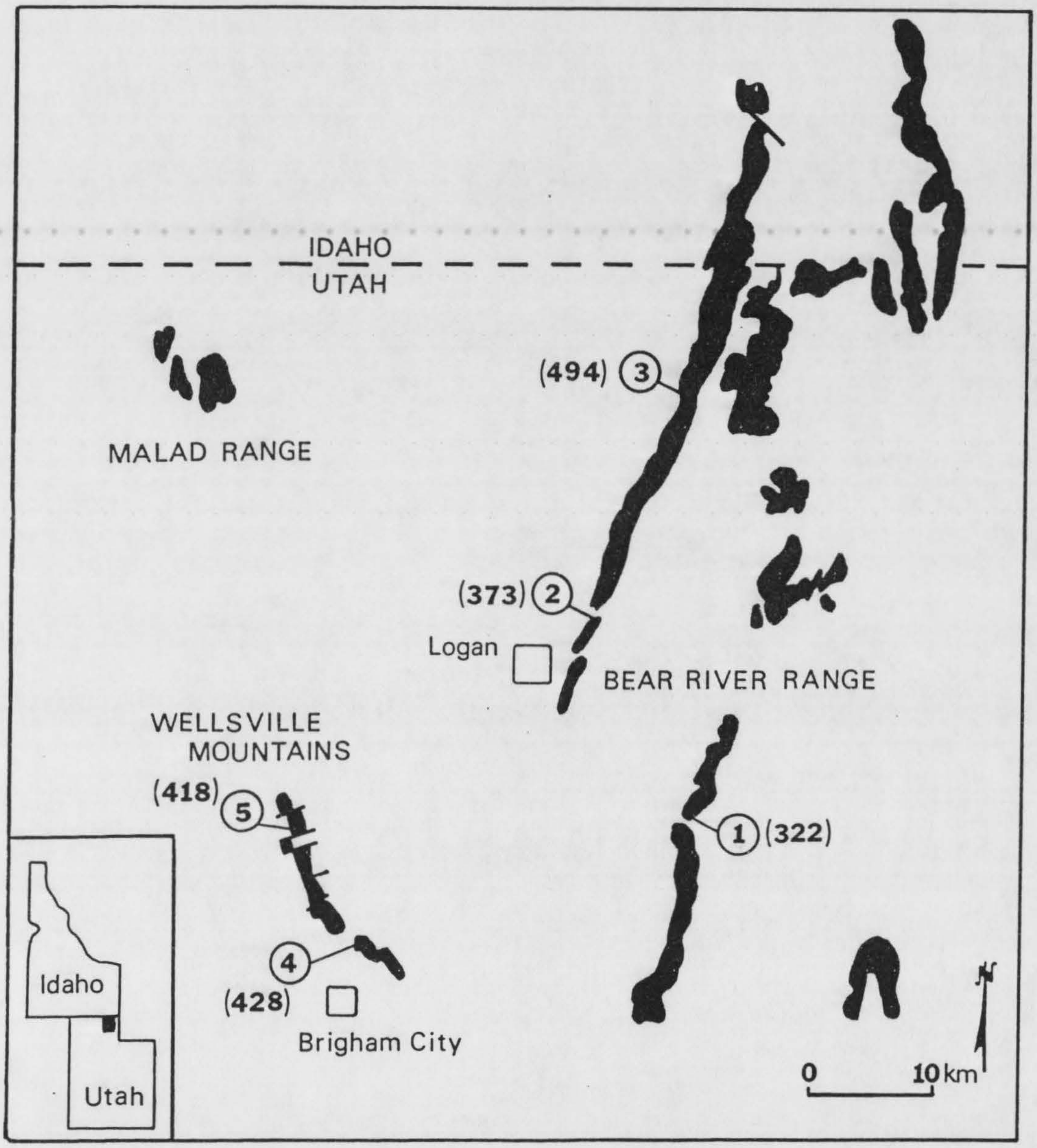

Fig. 13. Outcrop pattern of the Lower Ordovician Garden City Formation in north-central Utah. Circled numbers show locations of measured sections. Numbers in parentheses are thicknesses in meters (Modified from Ross 1951).

LITHOTYPES AND ENVIRONMENTS

The Garden City Formation is a storm-dominated transgressive sequence deposited within an epeiric sea under humid tropical conditions. Nine lithotypes compose the peritidal through deeper subtidal deposits. Peritidal environments consist of reworked transgressive and shoreface material. Adjacent shallow subtidal deposits include fossil banks, mud mounds, thin shales, and nodular limestones with interbedded storm layers and lenses of intraclast packstone/grainstones. A skeletal accumulation of fossiliferous packstone formed seaward of the shallow subtidal deposits at a slope break within the shelf and separated the shallow subtidal from deeper, bioturbated subtidal material.

METHODS

Samples from five stratigraphic sections (Fig. 13) which were used for lithotype and environment analyses were also used to determine diagenetic events. Acetate peels from 277 samples and 77 thin sections were analyzed with petrographic and binocular microscopes. The thin sections were stained with alizarin red-S and potassium ferricyanide to aid in dolomite, iron-rich calcite, and iron-rich dolomite identification. Cathodoluminescence was used on selected thin sections.

DIAGENETIC EVENTS

Diagenesis encompasses all changes, physical and chemical, that occur after sediment is deposited. These changes are affected by the original sediment and the pressure, temperature, and type of interstitial fluid to which the sediment is subjected. The effects in turn may be related to relative times of formation: early, intermediate, or late, and the specific depth of burial: surface, moderate, or deep. Diagenetic effects present in the Garden City Formation include compaction, neomorphism, cementation, micritization, the formation of minor amounts of pyrite and hematite, dolomitization, dedolomitization, the formation of chert, and fracture-fill.

Compaction

Compaction includes all processes, mechanical and chemical, that reduce the bulk volume, and hence porosity, of rocks (Flugel 1982). These processes can be influenced by grain type, grain size, and amount and timing of cementation. Mechanical compaction generally occurs during early burial diagenesis while chemical compaction takes place in the later stages of the diagenetic process.

Mechanical compaction effects of dewatering, grain realignment, and grain breakage result from compressive stress exerted by the weight of the overlying sediment. Initial mechanical compaction can be overprinted by later pressure solution features (Shinn et al. 1977; Pratt 1982b; Demicco 1983). Mechanical compaction can account for one third to one half of porosity reduction in mud-supported sediments (Scholle and Halley 1985).

Evidence indicating that the Garden City sediment was mechanically compacted is abundant. Many of the long, thin, phosphatic lingulid brachiopod fragments are broken in situ (Fig. 14A), whereas more resistant brachiopod and trilobite fragments are rarely broken. Shinn et al. (1977) have shown that substantial amounts of compaction can occur and result in only minimal shell breakage. Additional evidence for compaction are the possible realignment of the long axis of skeletal fragments, lenticular squashed burrows, interpenetration of intraclasts, and clotted fabrics.

Burrow preservation with no appreciable deformation argues for early cementation of the burrows. In compaction experiments on modern carbonate sediments, Shinn and Robbin (1983) noted aligned grains, little shell breakage, and pellets and burrows that were obliterated or deformed. They suggested that only 100 meters of overburden are needed to produce these compaction features.

The degree of preservation of peloids may be linked to the extent of early lithification. Good preservation of peloids indicates resistance to compaction due to early cementation, whereas poor preservation, resulting in clotted fabrics, indicates little to no early cementation. Clotted fabrics are common in sediments deposited in the subtidal environments of the Garden City Formation.

The most obvious and pervasive evidence of compaction is the presence of solution features. These form in response to stress due to compaction or deformation and are a combination of pressure-dissolution and shear fractures (Scoffin 1987). They can be of

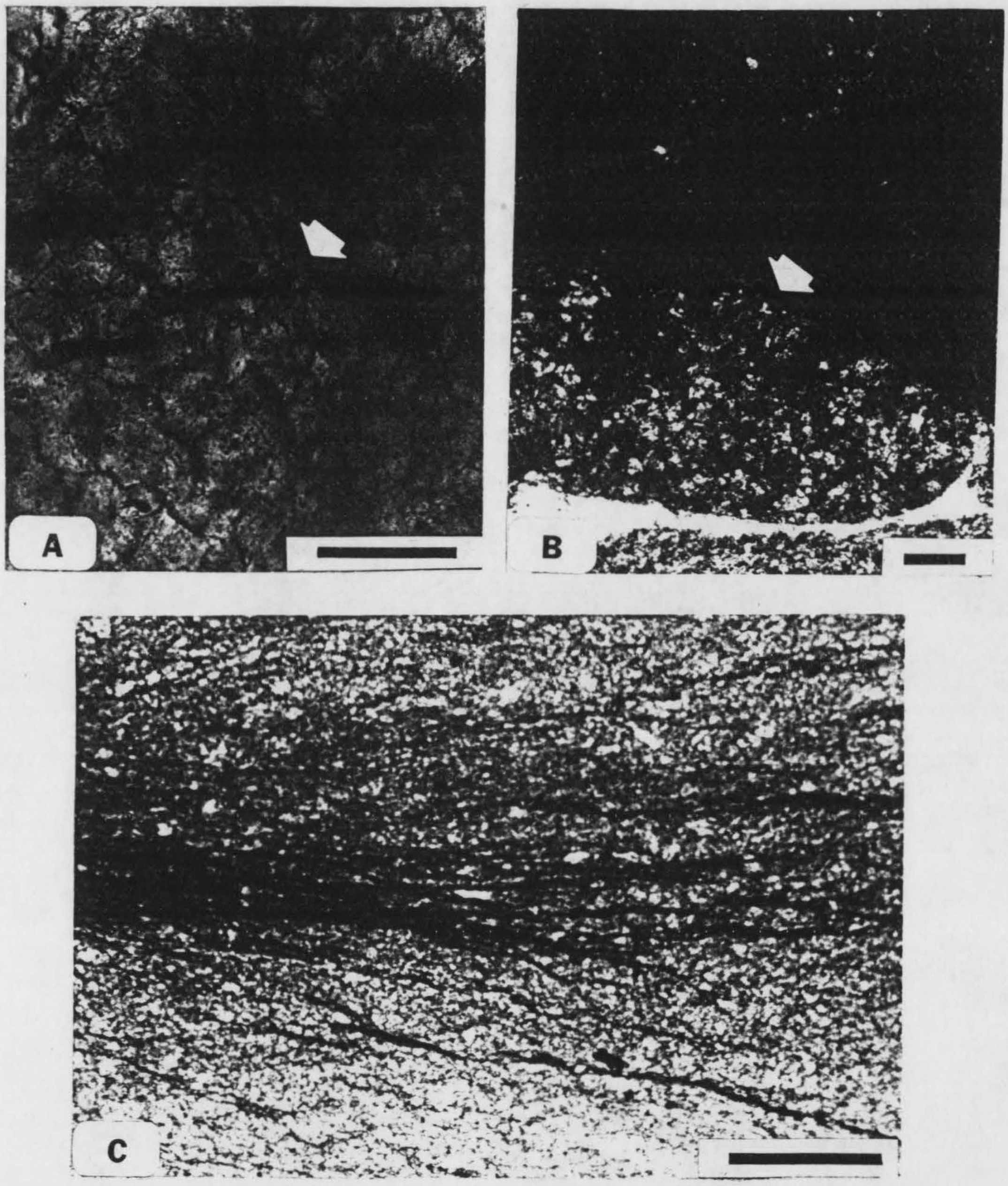

Fig. 14. Photomicrographs of evidence for mechanical and chemical compaction in the Garden City Formation. A) Arrow points to broken _in situ_ lingulid brachiopod fragment. Scale bar is 200 µm. B) Inter-granular solution between intraclasts (arrow). Scale bar is 200 µm. C) Stylolamination swarms (dark lines) in mudstone. Scale bar is 200 µm. All photomicrographs are plane-polarized light.

early, but are generally of late, diagenetic origin. Solution features are classified by Scholle and Halley (1985) into three types: inter-granular solution, solution seams, and stylolites. Inter-granular solution occurs at contacts between grains where stress is concentrated. It is common in grainstones and forms early in the solution process. Solution seams form in fine-grained clay-rich carbonate rocks and are associated with nodular limestones. The term "stylolite" is restricted to low- to high-amplitude sutured-seam solution features. The higher amplitude and larger stylolites generally form late in the solution process in wackestones to grainstones and at lithologic boundaries.

Inter-granular solution, seam solution, including stylolamination and wispy silt accumulations, and stylolites are common throughout the Garden City Formation. Stylolaminations and wispy silt accumulations dominate the wackestone/mudstone lithotype (Fig. 14B) while inter-granular solution (Fig. 14C) and stylolites are most common in the grainstone/packstone lithotypes. The microstylolites in the clay-rich zones create stylonodular fabrics. Stylolites almost always form between abrupt changes in lithotypes, an effect noted by Buxton and Sibley (1981). Nearly all stylolites formed parallel to bedding. The few that are perpendicular to bedding are of late diagenetic origin and may represent stresses applied during Late Cretaceous and Tertiary faulting.

One of the most prominent facies of the formation is the nodular wackestone/mudstone which is interspersed with primary depositional layers and lenses of ripple-marked, planar-laminated and hummocky cross-stratified limestone. The limestone nodules and lenses in the nodular wakestone/mudstone are nearly pure and are surrounded by, and in some cases draped by, quartz silt and clay minerals. The primary depositional features have been altered by some burrowing and diagenetic pressure dissolution (compare with Demicco 1983) which further enhances non-carbonate material concentrations (Wanless 1979).

Burial depths needed to produce pressure dissolution vary from over 300 meters to 4,000 meters (Scholle and Halley 1985). Deep burial appears to be the most important condition for pressure solution. Using the conodont alteration index (CAI) from conodonts found in the lower Garden City Formation, a minimum burial depth of 5700 meters can be calculated for the formation (Gillett and Taylor 1985). Such a significant burial depth could easily account for the pressure solution features.

Mechanical compaction thus played an important role in altering the finer-grained Garden City sediments, with later pressure solution affecting all the sediments.

Neomorphism and Cementation

Neomorphism as defined by Folk (1965) encompasses all transformations between one mineral and itself or its polymorphs. The abundance of microspar and sparite suggests that much of the Garden City Formation has been affected by neomorphism. Size and shape (equigranular) of the grains were the criteria used to identify the neomorphic transformation of micrite (<5 μm) to microspar (5-30 µm) (Folk 1965). To recognize the neomorphic origin of coarse sparite material the criteria were expanded to include the presence of: 1) large crystal diameters, up to 100 µm together with an irregular distribution of sizes; 2) floating patches of residual micrite in clear sparite; 3) embayments of sparite altering allochems; and (4) the low occurrence of enfacial junctions (Bathurst 1975).

Neomorphism is common in the packstone/grainstone lithotypes. In some cases clayey, non-carbonate material was "pushed" in front of the aggrading sparite and appears squeezed between sparite crystals.

It is postulated that two different types of original material underwent neomorphism. Dirty sparite and squeezed clay indicate replacement of a fine-grained micrite/clayey matrix. In some cases, however, no dirty residue is present, but other neomorphic evidence remains. This indicates that neomorphism of original cement may have occurred.

Three stages of cementation have taken place, an early rim cement, a later blocky, pore-space-filling cement, and a still later fracture-filling cement. Evidence for cementation in the Garden City Formation includes: skeletal grains with equant to bladed rim cements, and altered shells with unaltered micrite rims (Fig. 15). This is similar evidence for cementation used by Bathurst 1975.

Some skeletal grains, particularly trilobite and mollusc fragments, have fringes of bladed to equant rim sparite as evidence for early cementation. Gillett (1983) noted the same feature in the equivalent Ordovician Goodwin Limestone in Nevada and attributed it

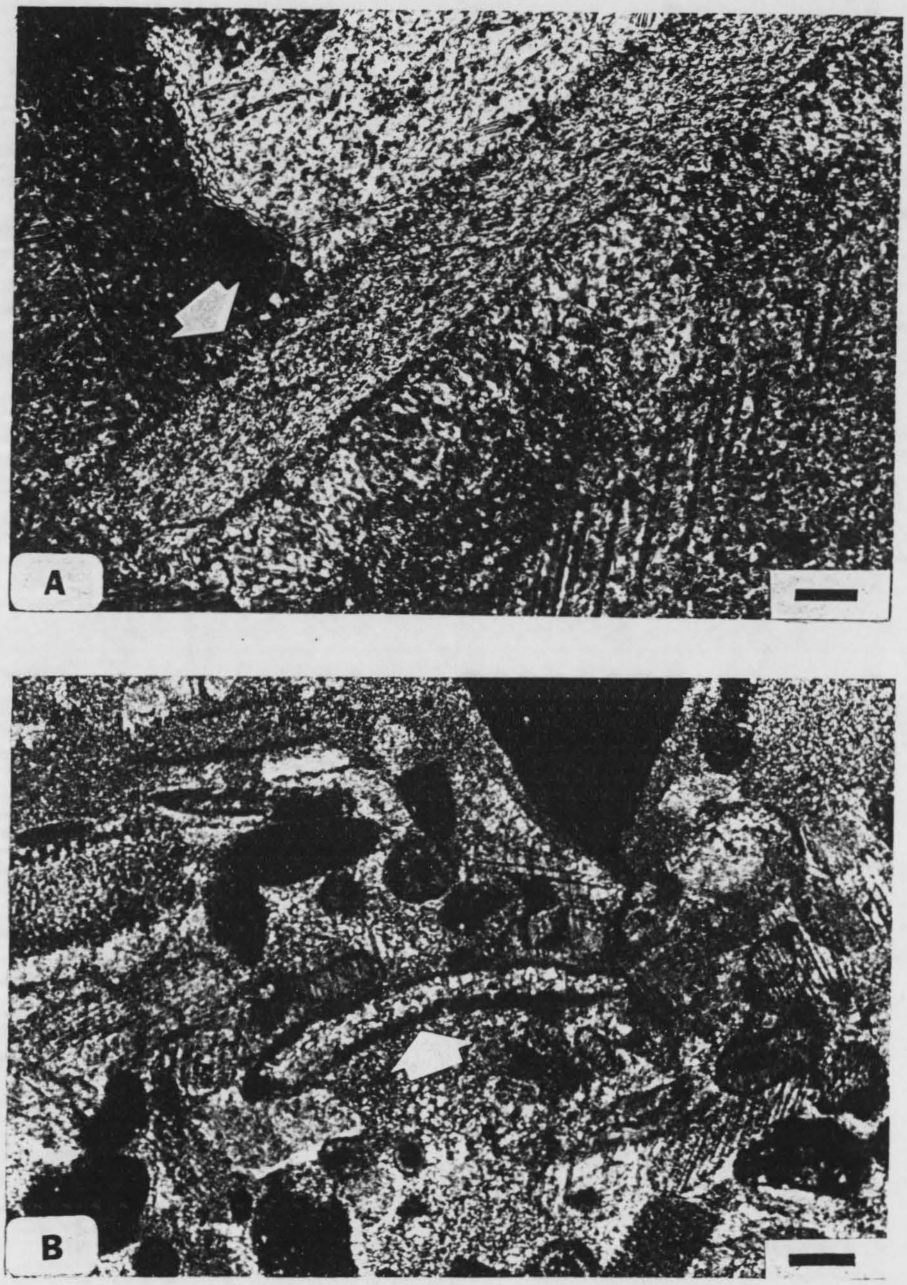

Fig. 15. Photomicrographs of evidence for cementation in the Garden City Formation. A) Fringes of bladed to equant early rim cement (arrow) on a skeletal fragment. Scale bar is 100 µm. B) Arrow points to altered bioclast with unaltered micrite rim. Scale bar is 200 µm. All photomicrographs are plane-polarized light.

to the recrystallization of acicular marine cements.

Syntaxial rims along with the preservation of uncompacted peloids and blocky sparite burrow infillings also may be the result of early cemention (Longman 1980). Syntaxial calcite rims are prevalent on pelmatozoan debris. They are less common on peloids and trilobite and mollusc fragments. The rims were formed as either early cement or neomorphic sparite and are most common in the coarse-grained packstone/grainstones. Pelmatozoan and other bioclast fragments found in the fine-grained wackestone/mudstones generally do not have syntaxial rims.

In the deep subtidal wackestone lithotype some of the bioclasts were totally altered to a sparry calcite mosaic within a micrite envelope. The shapes of the bioclasts indicate that they were originally molluscan shell fragments.

The early cementing material was provided by marine phreatic waters while the later cementing material was most likely provided by pressure solution as suggested by Scholle and Halley (1985).

Micritization

Many bioclasts possess micrite rims as evidence for micritization, a process accomplished through the work of boring algae (Bathurst 1975). Bathurst (1975) also noted that complete micritization of skeletal fragments was important in the origin of peloids in modern carbonate environments. The problematic codiacean alga Nuia commonly has been micritized in the Garden City Formation and may have been the source of some of the peloids (Fig. 16).

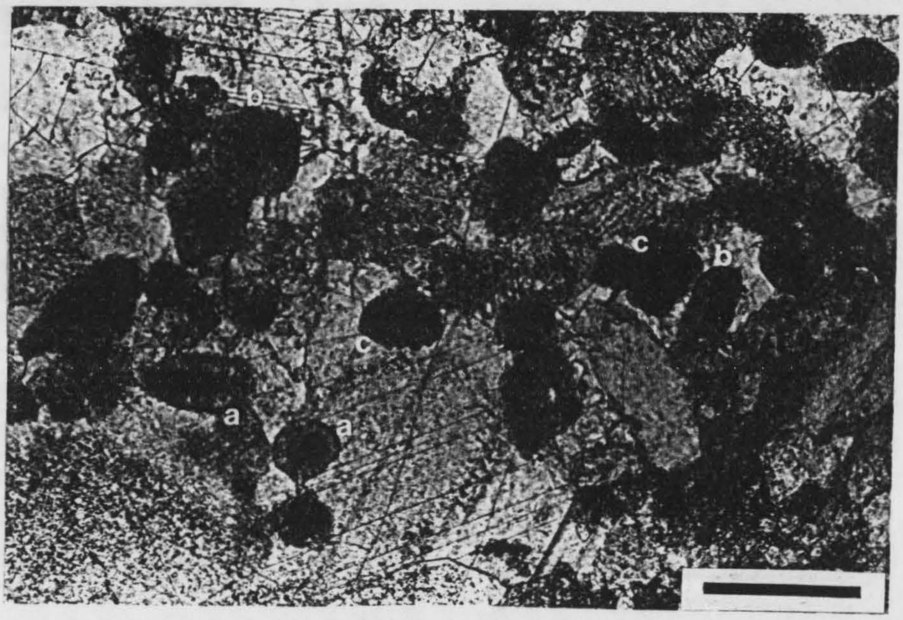

Fig. 16. Micritization of Nuia may have been the source of some of the peloids in the Garden City Formation. Photomicrograph of unaltered Nuia (a), partially altered Nuia (b), and Nuia completley altered to peloids (c). Scale bar is 200 µm. Plane-polarized light.

Dolomitization

The Garden City Formation contains minor amounts of dolostone in all sections, mainly in variable thicknesses within the uppermost 50 meters and also at the lower contact with the Saint Charles Formation. Additional scattered occurrences of dolostone are found throughout some sections. None of the dolostone appears to be facies controlled, as the contacts with limestone are irregular, irrespective of rock type. The major dolostone units are composed of xenotopic, fine- to medium-crystalline dolomite (Fig. 17). The original depositional textures, including intraclasts and bioclasts, and depositional structures are retained as ghost features.

A number of hypotheses have been suggested for dolomite formation (see discussion in Hardie 1987). Some of the dolostone found in the Garden City Formation may be attributed to migration of dolomitizing fluids along faults. In stratigraphic sections two, three, and five, scattered fault-controlled dolostone is recognized by field relationships of the dolostone to faults. The dolomite formed in zones that parallel the faults regardless of lithotype. Faulting, however, does not explain the persistent occurrence from section to section of both the lowermost and the upper dolostones.

Dolostone occurs at the contact with the underlying dolomitized Saint Charles Formation. However Taylor and Landing (1981) attributed the dolomitization of the Saint Charles Formation to an unconformity and accompanying subaerial exposure of the Saint Charles before Garden City deposition. Thus a different mechanism, unrelated to the dolomitizing event of the Saint Charles Formation, must have

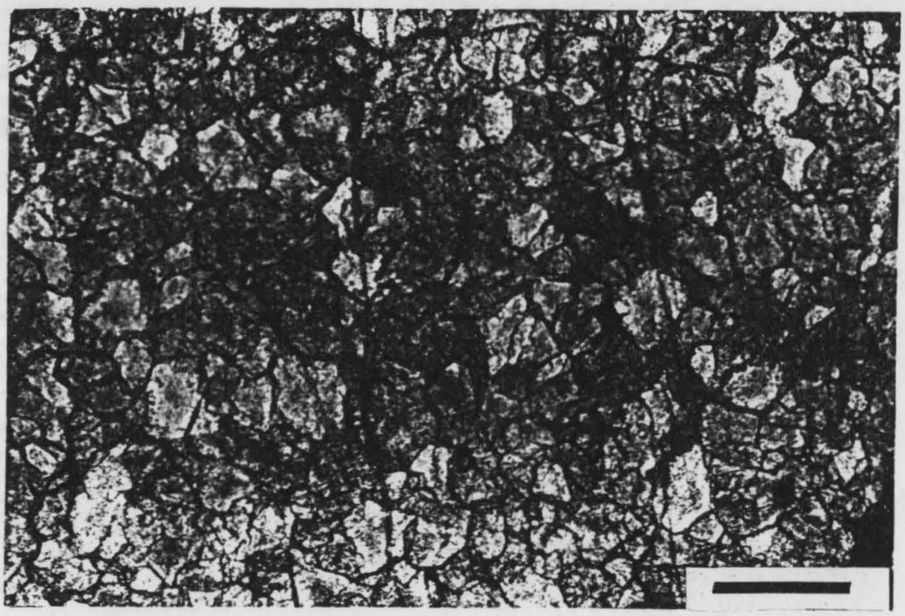

Fig. 17. Photomicrograph of the xenotopic texture of dolomite in the Garden City Formation. Scale bar is 200 µm. Plane-polarized light.

formed the dolomite in the lower part of the Garden City. In section two, the lowermost dolomite may be related to faulting as Landing (1981) identified a shear zone in the upper Saint Charles and lower Garden City.

Dunham and Olson (1980) surveyed the distribution of limestone-dolostone in lower and middle Paleozoic rocks of the Cordilleran miogeocline in Nevada and western Utah and found that the deeper water carbonate rocks to the west are primarily limestone, whereas the shallow water sediments of the east are preferentially dolomitized. They suggested the dolostone formed from mixing of freshwater and seawater and that the freshwater lens and recharge to the system was controlled by paleogeography. In this way they accounted for shifts in the limestone-dolostone boundary with time.

It is possible that the dolostone of the Garden City Formation resulted in response to mixing of fresh and marine water. However, dolomite formed as a result of mixing of waters is predominantly clear and euhedral, with plane crystal faces (Folk and Land 1975). That is not the type of dolomite found in the Garden City.

It is postulated instead that the dolostone of the Garden City Formation may have formed from deep-burial dolomitization processes. The evidence for deep-burial dolomitization includes: 1) xenotopic texture; 2) scattered zoned dolomite rhombs with dirty cores and clear rims; 3) ghost textures of original depositional environments preserved in crystalline dolomite; and 4) no boundaries of crystals evident with cathodoluminescence. Similar evidence was used by Lee and Friedman (1987) to prove deep-burial dolomitization in the

Ordovician Ellenburger Group carbonates. Gregg and Sibley (1986), however, attribute the xenotopic character of most dolomite to epigenetic conditions with temperature above 50°C.

Hardie (1987) claimed that burial dolomite can potentially form from any heated groundwater; therefore water composition is not as significant as is the fluid's ability to move at depth. According to Hardie (1987), burial dolostone will form at temperatures of 100° C, with fluid migration concentrating dolomite formation at basin edges, at unconformities, and at basement highs. He further stated that at passive margins the dolomitizing fluid system can be driven updip via thermal anomolies.

The lower dolostone may be related to dolomitizing fluids driven along the unconformity with the Saint Charles Formation, whereas the upper dolostone may somehow be related to fluids moving along the contact with the lowermost shale member in the Swan Peak Formation.

Porphyrotopic dolomite also occurs as scattered euhedral rhombs in burrows, in clay-rich seams, and under some intraclasts (Fig. 18A-C). Under cathodoluminescence the rhombs luminesce a darker orange than the background material, which indicates different modes of formation for the rhombs and the massive crystalline dolomite. The rhombs are generally associated with the finer-fraction clayey material and solution seams. The clays may contribute to the dolomitization by acting as membranes which impede ion migration, or as centers for nucleation of crystals (Kahle 1965). Fluids may have been able to migrate through the finer grained materials because they were not initially cemented as readily as the coarser fractions.

Fig. 18. Photomicrographs of dolomite rhombs in the Garden City Formation. A) Scattered euhedral dolomite rhombs in burrows. Scale bar is 200 µm. B) Clay-rich limestone with euhedral rhombs. Scale bar is 200 µm. C) Rhombs (arrow) formed under an intraclast. Scale bar is 200µm. D) Zoned dolomite rhombs, (a) iron-rich dolomite with limonite zones. and (b) non-iron-rich dolomite with limonite centers and rims. Scale bar is 200 µm. All photomicrographs are plane-polarized light.

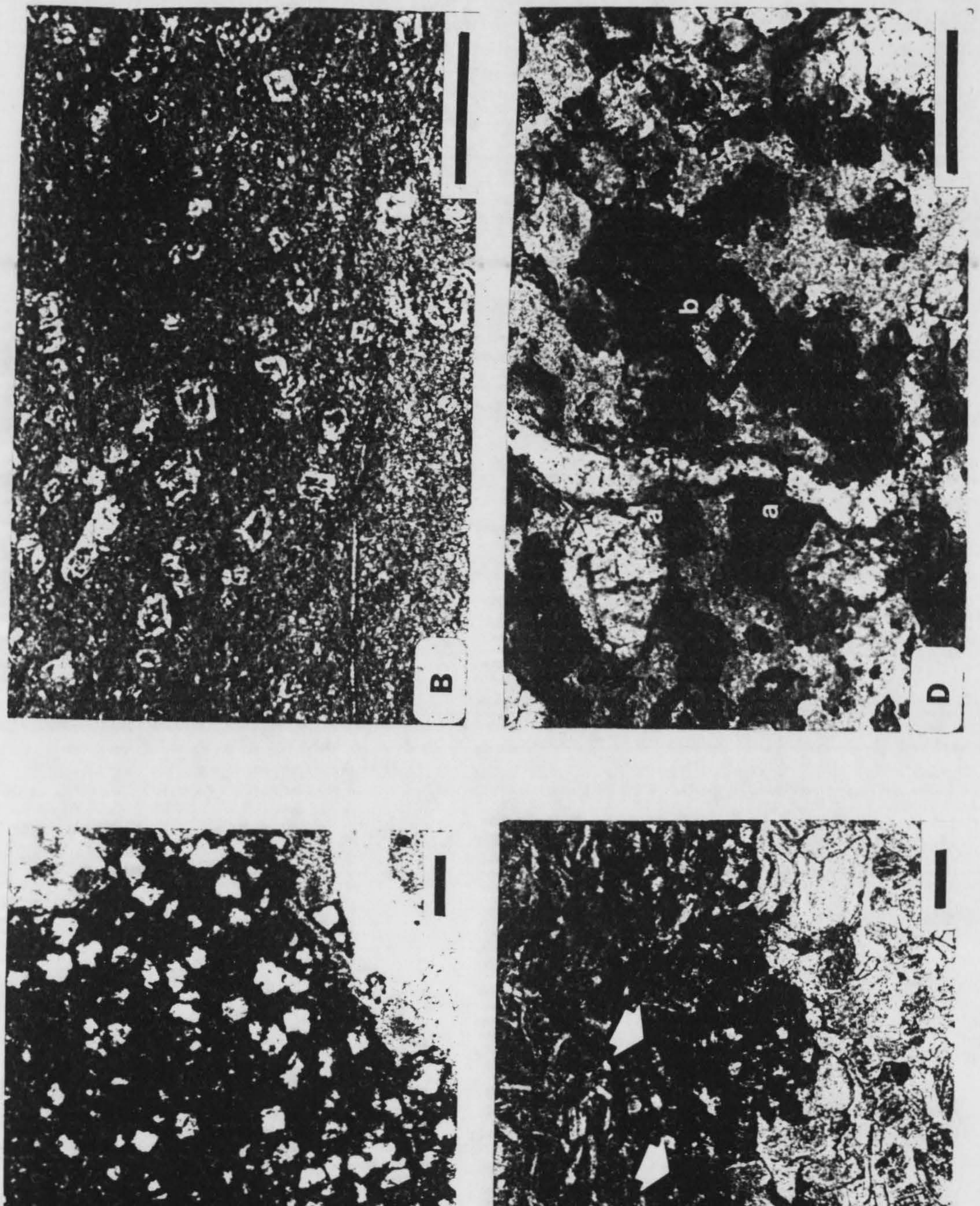
A
B
C
D
a
a
b

Staining revealed that some of the dolomite rhombs are zoned ferroan-dolomite and dolomite (Fig. 18D). This indicates a change in fluid composition as the crystals formed. Many rhombs have limonite rims, whereas some are completely altered to limonite or are zoned with limonite centers. Limonite is an alteration product of ferroan-rich dolomite (Gillett 1983). Iron-rich fluids may originate from the alteration of associated clay minerals providing a source for the iron (Bathurst 1975; Flugel 1982). The cause of the fluid composition changes required for rhomb zonation is unclear.

Timing of the dolomitization derived from thin section information indicates that the dolomite formed after the chert and most stylolites. This implies a time of formation after pressure solution had begun. Euhedral dolomite rhombs, identified by cathodoluminescence, floating in xenotopic crystalline dolomite represent a second dolomitizing event. Since minor stylolites occur in the dolostone, some pressure solution of the already dolomitized material may have been the source of fluids for the later dolomite rhomb formation.

In several thin sections rhombohedral-shaped pores resulting from dissolution of dolomite rhombs are common. Some pores have remnant dolomite within; therefore dedolomitization replacement with calcite did not occur. The pores and remnant rhombs are limonite-lined indicating that the original dolomite had an iron-rich composition. Dissolution of the dolomite could have been accomplished by migrating fluids which had been depleted with respect to magnesium.

Dedolomitization

Many thin sections have evidence of dedolomitization, the process of calcitization of dolomite. Evamy's (1967) description of the process requires that original dolomite rhombs be replaced by equicrystalline, high-magnesium calcite. Friedman and Sanders' (1967) evidence for dedolomitization includes: 1) dolomite remnants within calcite crystals; 2) pseudomorphs of calcite after dolomite; and 3) ghost dolomite rhombs in ferric oxide zones. The evidence for dedolomitization within the Garden City Formation is primarily restricted to calcite pseudomorphs of dolomite rhombs concentrated in ferric oxide zones. Figure 19 shows limonite-rimmed calcite pseudomorphs after dolomite. Limonite-rimmed calcite and dolomite rhombs occur within the same thin section in iron-rich zones under intraclasts. No dolomite remnants were observed nor did any of the replaced calcite appear to be equicrystalline. However, the presence of zoned rhombs composed of calcite and outlined with limonite was interpreted as a result of dedolomitization.

Friedman and Sanders (1967) noted that the dedolomitization process occurs in association with sulfate ions. Magnesium from dolomite combines with sulfate ions to form $MgSO_4$ and calcite. Sulfate ions can be supplied by the oxidation of pyrite (Evamy 1967; Friedman and Saunders 1967). There is ample evidence of the oxidation of pyrite to hematite in the Garden City Formation, which could provide a source for the sulfate ions.

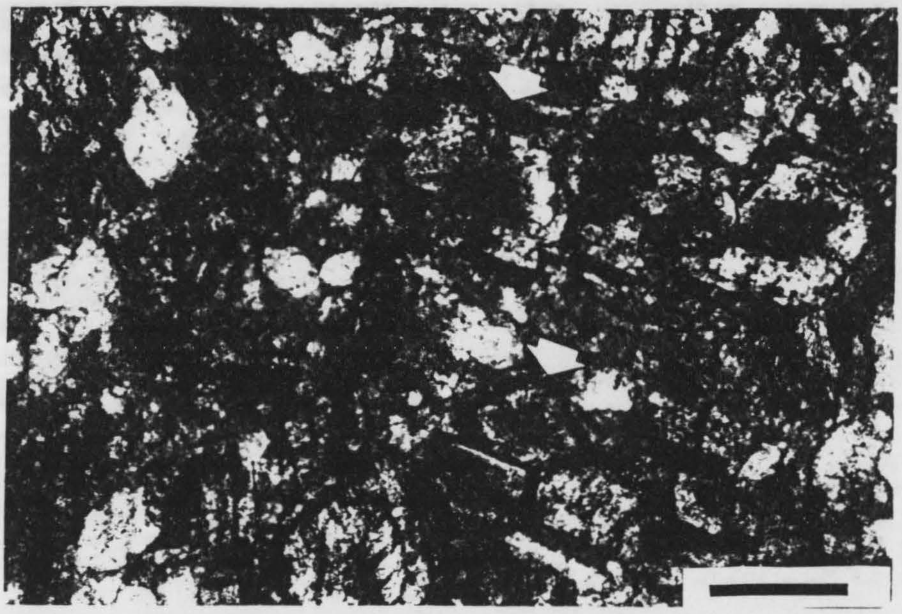

Fig. 19. Evidence for dedolomitization, limonite-rimmed calcite pseudomorphs after dolomite (arrows). Pseudomorphs stain red with alizarin red-S. Calcite pseudomorphs and dolomite rhombs occur within the same thin section in iron-rich zones under intraclasts. Scale bar is 200 um. Plane-polarized light.

Pyrite and Hematite

Scattered throughout the formation are small blebs of hematite pseudomorphs after pyrite, and rare pyrite. These occur as singular or clustered euhedral crystals and are associated with burrows or bioclasts and in some cases micritic intraclasts. There is more pyrite and hematite in the fauna-rich deeper subtidal lithotypes. More organics probably accumulated in these sediments because the less agitated, deeper environment resulted in less oxidation of organics. Berner (1984) found that pyrite is an early diagenentic alteration of metastable iron monosulfides produced by bacterial action on organic matter. Hematite is a late diagenetic alteration of the pyrite. No pyrite was observed on surface exposures, however, some was revealed in cut samples.

Chert

Chert is scattered throughout most of the formation as stringers, blebs, and nodules, with a notable concentration in the upper part of the formation. This upper chert zone varies in thickness from section to section, but all share the characteristic of a gradual increase of banded, anastomosing, and nodular chert until chert comprises up to 50% of the rock. Above this increased chert zone there is a corresponding gradual decrease in chert until none is present.

The chert color is variable in shades of grey and pink, and black and white. Pink is limited to the bottom of the formation, and white is found in the upper chert zone in only one section.

Colors are probably associated with trace elements and organic matter. The white may be a weathering rind as it is less than 10 mm thick. The chert consists of megaquartz, microquartz, and rare length-fast chalcedony. The chalcedony has a brown hue, possibly from included organic matter. The chert selectively replaced bioclasts, especially pelmatozoan, trilobite, and brachiopod fragments.

The chert in sections outside the chert zone replaced original material, leaving relict structures of fossils and intraclasts and in some cases lenses of intraformational conglomerate. No sponge spicules were observed within this chert; however the ubiquitious presence of sponge spicules in the sediment suggests that they could have been the source. In the chert zone of the upper member, the chert has abundant relict sponge spicules (Fig. 20). The limestone associated with the chert usually has high amounts of calcite-replaced monaxon and uncommon triaxon sponge spicules and numerous peloids. The originally siliceous spicules probably provided a biogenic source for the silica. The anastomosing habit of some of the chert in the highly burrowed and bioturbated deeper subtidal facies suggests that fluid migration followed burrows. Such fluid migration is a result of the increased permeability and organic content of burrow-fill sediment (Eckdale and Bromley 1986). Banded cherts may be caused by clayey layers that stop or impede migration of fluids along bedding.

Chert formation has been linked by Knauth (1979) to the mixing model for dolomitization. There is some dolostone associated with

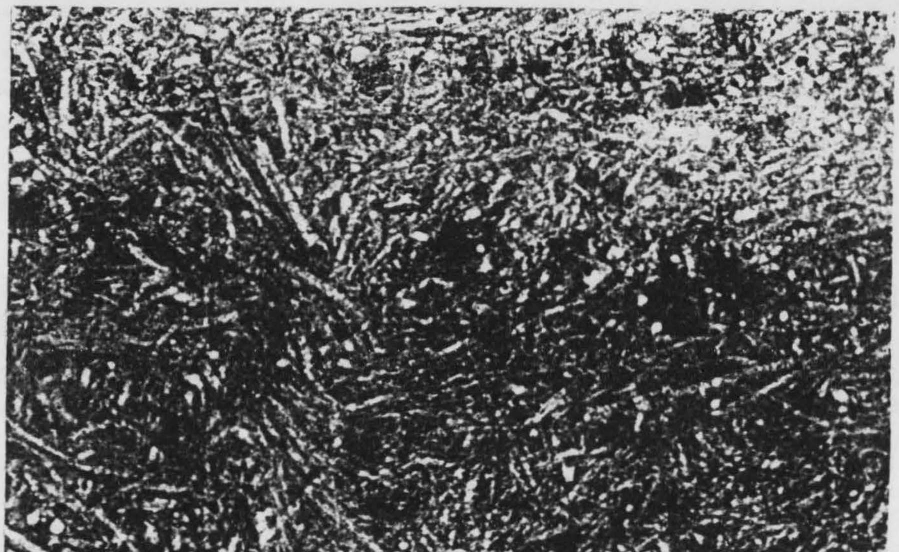

Fig. 20. Photomicrograph of abundant relict sponge spicules in chert in the upper chert-rich zone of the Garden City Formation. Scale bar is 200 µm. Plane-polarized light.

Fractures

Nearly vertical calcite-filled fractures are very common throughout the Garden City Formation but tend to increase in the chert zone. The fractures cut all other features and are a late diagenetic event, probably related to late Cretaceous and early Tertiary faulting. At least two events exist as evidenced by the cross-cutting relationships of the fractures.

DIAGENETIC MODEL

The Garden City Formation was deposited during a slow and steady transgression, with storm influence and sea level fluctuations adding complexity to diagenetic events. From the features observed the following generalized model of diagenetic events of the Garden City Formation can be postulated.

An early diagenetic feature formed at the sediment/water interface was the micritization of bioclasts by boring algae. A later diagenetic feature below the sediment/water interface, was the formation of pyrite. Reducing conditions, caused by abundant organic matter incorporated within the sediments, led to the pyrite formation.

The numerous intraclasts attest to the fact that early lithification of the sea floor was common. Equant to bladed rim cement was precipitated on bioclasts, and is still preserved on some trilobite and mulluscan shell fragments. Early cement filled some burrows and surrounded peloids, preventing their obliteration by contemporaneous compaction.

Neomorphism occurred after early cementation as both micrite and original cement were altered. A blocky pore-filling cement probably formed in the mid- to late-eogenetic system. The chert also formed at this time since it was in place before much pressure solution took place.

Continued addition of overburden initiated pressure solution which undoubtably continued from early- through late-stage mesogenetic diagenesis. If in fact there was burial dolomitization it would have occurred within the mesogenetic system.

Late Cretaceous thrust faulting and early Tertiary normal faulting probably caused the fractures in the Garden City Formation. These fractures are filled with a late-stage calcite cement. The faults were zones of weakness in the rock allowing migration of fluids that dolomitized the surrounding rock. Two stages of dolomitization occurred, the first replacing extensive portions of the rock and the second forming scattered euhedral rhombs within massive crystalline dolomite.

Oxidation of pyrite to hematite and the formation of limonite are the last of the diagenetic processes and occurred near the surface as a result of weathering.

SUMMARY AND CONCLUSIONS

The diagenetic events present in the Garden City Formation include compaction, neomorphism, cementation, micritization, dolomitization, dedolomitization, formation of chert, and fracture-fill.

Mechanical compaction includes grain breakage, grain realignment, squashed burrows, interpenetration of intraclasts, and clotted fabrics, all of which are early diagenetic features. Pressure solution, pervasive evidence for chemical compaction, occurs later in the diagenetic history.

Three stages of cementation occurred: an early stage, a later blocky pore-filling cementation, and the last event, late fracture-fill cementation. Neomorphism affected micrite and the early stage cement, altering them to microspar and sparite respectively. Chert formation occurred before much pressure solution and was probably a late eogenetic process. Dolomitizing fluids moved along faults, unconformities, and bedding planes to selectively dolomitize the Garden City rocks. The dolostone in the formation does not appear to be facies controlled. Dedolomitization and the oxidation of pyrite to hematite were late diagenetic events resulting from near-surface weathering.

CHAPTER IV

SUMMARY

The Garden City Formation represents a storm-dominated transgressive sequence deposited in an epeiric sea. The formation is composed of nine lithotypes which represent various depositional environments. The lithotypes consist of nodular wackestone/mudstone with packstone lenses, intraclastic packstone/grainstone, green shale, laminated packstone/grainstone, cryptalgalaminite, fossiliferous packstone, boundstone, Calathium/sponge, and burrowed fossiliferous wackestone/packstone with chert. Storm action extensively reworked the initial transgressive and shoreface materials which are characterized by erosional channels and intraformational conglomerate layers and lenses.

The broad shelf of the epeiric sea may be subdivided into two distinct environments, a shallow subtidal inner shelf and a deeper subtidal outer shelf. The shallow inner shelf was characterized by shoreward fossil banks and mud mounds, a restricted fauna, large amounts of terrigenous material, and repeated occurrences of intraformational conglomerate layers. Irregularly distributed shoal islands were formed as a result of excessive sediment production.

The deeper outer shelf sediments include a diverse fauna and are characterized by bioturbation and burrowing. These sediments have a significant amount of banded and anastomosing black, white, and grey chert. A storm-initiated skeletal accumulation separated the inner and outer shelves.

Terrigenous input created an unfavorable habitat within the shallow inner shelf which resulted in a restricted fauna. Tides provided water circulation to maintain near normal marine conditions in the shallow water, landward belt of the Ordovician epeiric sea.

The Garden City facies were compared to the model of epeiric sea deposition presented by Shaw (1964) and Irwin (1965). They describe three generalized energy zones and suggest that tide action was unlikely in the low-energy interior regions of epeiric seas. There was a lack of evidence within the Garden City sediments to support the existence of an extensive, tideless low-energy zone.

A tropical, humid climate prevailed throughout the time of deposition of the Garden City Formation. Deposition was influenced by the subsiding Northern Utah and Ibex Basins and the uplifting Tooele Arch. The transition to deeper water was in central Nevada.

The diagenetic events present in the Garden City Formation include compaction, neomorphism, cementation, micritization, dolomitization, dedolomitization, formation of chert, and fracture-fill.

Early diagenetic features of mechanical compaction include grain breakage, grain realignment, squashed burrows, interpenetration of intraclasts, and clotted fabrics. Numerous stylolites, stylo-laminations, and inter-granular solution are evidence for later chemical compaction.

Three stages of cementation occurred. Early rim cements were followed by blocky pore-filling cements and later fracture-fill cements. Neomorphism was common, affecting micrite and the early rim cement, altering them to microspar and sparite. Chert formation occurred before much pressure solution and probably represents silicified burrow fillings.

Dolomite in the Garden City Formation does not appear to be facies controlled. Dolomitizing fluids moved along faults, unconformities, and bedding planes to selectively dolomitize the formation. Late diagenetic near-surface weathering resulted in dedolomitization and the oxidation of pyrite to hematite.

REFERENCES

AIGNER, T., 1985, Storm depositional systems, in Friedman, G. M., Neugebauer, H. J., and Seilacher, A., eds., Lecture Notes in Earth Science No. 3: New York, Springer-Verlag, 174 p.

AITKEN, J. D., 1967, Classification and environmental significance of cryptalgal limestones and dolomites, with illustrations from the Cambrian and Ordovician of southwestern Alberta: Jour. Sed. Petrology, v. 37, p. 1163-1178.

BALL, M. M., SHINN, E. A., and STOCKMAN, K. W., 1967, The geologic effects of Hurricane Donna in south Florida: Jour. of Geology, v. 75, p. 583-597.

BALL, S. M., 1983, Significance of limestone-shale rock-stratigraphic contacts--the connecting links between areas of contemporaneous carbonate and terrigenous detritus sedimentation: Am. Assoc. Petroleum Geologists Bull., v. 67, p. 417-418.

BATHURST, R. G. C., 1975, Carbonate Sediments and Their Diagenesis (2nd ed.): New York, Elsevier, 658 p.

______, 1980, Stromatactis--origin related to submarine-cemented crusts in Paleozoic mud mounds: Geology, v. 8, p. 131-134.

BAYER, U., ALTHEIMER, E., and DEUTSCHLE, W., 1985, Environmental evolution in shallow epicontinental seas: sedimentary cycles and bed formation, in Bayer, U., and Seilacher, A., eds., Sedimentary and Evolutionary Cycles, Lecture Notes in Earth Science No. 1: New York, Springer-Verlag, p. 68-97.

BERNER, R. A., 1984, Sedimentary pyrite formation: an update: Geochem. Cosmochim. Acta, v. 48, p. 605-615.

BERRY, W. B. N., 1962, Comparison of some Ordovician limestones: Am. Assoc. Petroleum Geologists Bull., v. 46, p. 1701-1720.

BUXTON, T. M., and SIBLEY, D. F., 1981, Pressure solution features in shallow buried limestone: Jour. Sed. Petrology, v. 51, p. 19-26.

CHURCH, S. B., 1974, Lower Ordovician patch reefs in western Utah: Brigham Young University Geology Studies, v. 21, pt. 3, p. 41-62.

CLARK, T. H., 1935, A new Ordovician graptolite locality in Utah: Jour. of Paleontology, v. 9, p. 239-246.

COOK, H. E., and TAYLOR, M. E., 1977, Comparison of continental slope and shelf environments in the Upper Cambrian and lowest Ordovician of Nevada, in Cook, H. E., and Enos, P., eds., Deep-water Carbonate Environments: Soc. Econ. Paleontologists Mineralogists Spec. Pub. No. 25, p. 51-81.

CRITTENDEN, M. D., Jr., 1961, Magnitude of thrust faulting in northern Utah: U.S. Geol. Survey Prof. Paper 424-D, p. D128-D131.

______, 1972, Willard thrust and the Cache allochthon, Utah: Geol. Soc. America Bull., v. 83, p. 2871-2880.

DALRYMPLE, R. W., NARBONNE, G. M., and SMITH, L., 1985, Eolian action and the distribution of Cambrian shales in North America: Geology, v. 13, p. 607-610.

DEMICCO, R. V., 1983, Wavy and lenticular-bedded carbonate ribbon rocks of the Upper Cambrian Conococheague Limestone, central Appalachians: Jour. Sed. Petrology, v. 53, p. 1121-1132.

DUKE, W. L., 1985, Hummocky cross-stratification, tropical hurricanes, and intense winter storms: Sedimentology, v. 32, p. 167-194.

DUNHAM, R. J., 1962, Classification of carbonate rocks according to depositional texture, in Ham, W. E., ed., Classification of Carbonate Rocks: Am. Assoc. Petroleum Geologists Memoir 1, p. 108-121.

DUNHAM, J. B., and OLSON, E. R., 1980, Shallow subsurface dolomitization of subtidally deposited carbonate sediments in the Hanson Creek Formation (Ordovician-Silurian) of central Nevada, in Zenger, D. H., and Dunham, J. B., eds., Concepts and Models of Dolomitization: Soc. Econ. Paleontologists Mineralogists Spec. Pub. No. 28, p. 139-161.

EARDLEY, A. J., 1964, General College Geology: New York, Harper and Row Publishers, 499 p.

ECKDALE, A. A., and BROMLEY, R. G., 1986, Ichnologic controls of chertification in marine limestones: 12th International Sedimentological Congress, Canberra, Australia, Abstracts, p. 93.

EINSELE, G. 1985, Response of sediments to sea-level changes in differing subsiding storm-dominated marginal and epeiric basins, in Bayer, U., and Seilacher, A., eds., Sedimentary and Evolutionary Cycles, Lecture Notes in Earth Science No. 1: New York, Springer-Verlag, p. 68-97.

EVAMY, B. D., 1967, Dedolomitization and the development of rhombohedral pores in limestones: Jour. Sed. Petrology, v. 37, p. 1204-1215.

FLUGEL, E., 1982, Microfacies Analysis of Limestones: New York, Springer-Verlag, 418 p.

FOLK, R. L., 1965, Some aspects of recrystallization in ancient limestones, in Pray, L. C., and Murray, R. C., eds., Dolomitization and Limestone Diagenesis: Soc. Econ. Paleontologists Mineralogists Spec. Pub. No. 13, p. 14-48.

FOLK, R. L., and LAND, L. S., 1975, Mg/Ca ratio and salinity: two controls over crystallization of dolomite: Am. Assoc. Petroleum Geologists Bull., v. 59, p. 60-68.

FRIEDMAN, G. M., and SANDERS, J. E., 1967, Origin and occurrence of dolostones, in Chilingar, G. V., Bissell, H. J., and Fairbridge, R. W., eds., Carbonate Rocks, Developments in Sedimentology 9 A: New York, Elsevier, p. 267-348.

GILLETT, S. L., 1983, Major, through-going stylolites in the Lower Ordovician Goodwin Limestone, southern Nevada: petrography with dating from paleomagnetism: Jour. Sed. Petrology, v. 53, p. 209-219.

GILLETT, S. L., AND TAYLOR, M. E., 1985, Triassic remagnetization of lower Paleozoic rocks, Bear River Range, Utah-Idaho: a possible constraint on thermal history, in Kerns, G. J., and Kerns, R. L., Jr., eds., Orogenic patterns and stratigraphy of north-central Utah and southeastern Idaho: Utah Geological Assoc. Pub. 14, p. 249-260.

GREGG, J. M., and SIBLEY, D. F., 1986, Epigenetic dolomitization and the origin of dolomite texture, reply: Jour. Sed. Petrology, v. 56, p. 735-736.

HANSON, A. M., 1949, Geology of the southern Malad Range and vicinity in northern Utah (Unpub. Ph.D. dissert.): Madison, University of Wisconsin, 128 p.

HARDIE, L. A., 1987, Dolomitization: a critical view of some current views: Jour. Sed. Petrology, v. 57, p. 166-183.

HAYES, M. L., 1967, Hurricanes as geological agents, south Texas coast: Am. Assoc. Petroleum Geologists Bull., v. 51, p. 937-956.

HINTZE, L. F., 1951, Lower Ordovician detailed stratigraphic sections for western Utah: Utah Geol. and Mineralogical Survey Bull. 39, 99 p.

______, 1973, The Geologic History of Utah: Brigham Young University Geology Studies, v. 20, pt. 3, 181 p.

IDEN, R. F., and MOORE, C. H., 1983, Beach environment, in Scholle, P. A., Bebout, D. G., and Moore, C. H., eds., Carbonate Depositional Environments: Am. Assoc. Petroleum Geologists Memoir 33, p. 212-265.

IRWIN, M. L., 1965, General theory of epeiric clear water sedimentation: Am. Assoc. Petroleum Geologists Bull., v. 49, p. 445-459.

KAHLE, C. F., 1965, Possible roles of clay minerals in the formation of dolomite: Jour. Sed. Petrology, v. 35, p. 448-453.

KENNARD, J. M., and JAMES, N. P., 1986, Thrombolites and stromatolites: two distinct types of microbial structures: Palaios, v. 1, p. 492-503.

KLEIN, G. D., and RYER, T. A., 1978, Tidal circulation pattern in Precambrian, Paleozoic, and Cretaceous epeiric and mioclinal shelf seas: Geol. Soc. America Bull., v. 89, p. 1050-1058.

KNAUTH, L. P., 1979, A model for the origin of chert in limestone: Geology, v. 7, p. 274-277.

KREISA, R. D., 1981, Storm-generated sedimentary structures in subtidal marine facies with examples from the Middle and Upper Ordovician of southwest Virginia: Jour. Sed. Petrology, v. 51, p. 823-848.

KRUMBEIN, W. C., and GRAYBILL, F. A., 1965, An Introduction to Statistical Models in Geology: New York, McGraw-Hill Book Company, p. 154-158.

LANDING, E., 1981, Conodont biostratigraphy and thermal color alteration indices of the upper St. Charles and lower Garden City Formation, Bear River Range, northern Utah and southeastern Idaho: U.S. Geological Survey Open-File Report 81-740, 22 p.

LAPORTE, L. F., 1967, Carbonate deposition near mean sea-level and resultant facies mosaic: Manlius Formation (Lower Devonian) of New York State: Am. Assoc. Petroleum Geologists Bull., v. 51, p. 73-101.

______, 1969, Recognition of a transgressive carbonate sequence within an epeiric sea: Helderberg Group (Lower Devonian) of New York State, in Friedman, G. M., ed., Depositional Environments in Carbonate Rocks: Soc. Econ. Paleontologists Mineralogists Spec. Pub. No. 14, p. 98-118.

LEE, Y. I., and FRIEDMAN, G. M., 1987, Deep-burial dolomitization in the Ordovician Ellenburger Group carbonates, western Texas and southeastern New Mexico: Jour. Sed. Petrology, v. 57, p. 544-557.

LONGMAN, M. W., 1980, Carbonate diagenetic textures from nearsurface diagenetic environments: Am. Assoc. Petroleum Geologists Bull., v. 64, p. 461-485.

MANSFIELD, G. R., 1927, Geography, geology and mineral resources of sotheastern Idaho: U.S. Geol. Survey Prof. Paper 152, 453 p.

MILLER, D. M., 1984, Sedimentary and igneous rocks of the Pilot Range and vicinity, Utah and Nevada, in Kerns, G. J., and Kerns, R. L., Jr., eds., Geology of northwest Utah, southern Idaho and northeast Nevada: 1984 Field Conference, Utah Geological Assoc. Pub. 13, p. 45-63.

MOUNT, J. F., 1984, Mixing of siliciclastic and carbonate sediments in shallow shelf environments: Geology, v. 12, p. 432-435.

MULTER, H. G., 1977, Field Guide to Some Carbonate Rock Environments, Florida Keys and Western Bahamas: Dubuque, Iowa, Kendall/Hunt Pub. Co., 191 p.

OAKS, R. Q., Jr., JAMES, W. C., FRANCIS, G. G., and SCHULINGKAMP, W. J., 1977, Summary of Middle Ordovician stratigraphy and tectonics, northern Utah, southern and central Idaho, in Keisey, E. L., Lawson, D. E., Norwood, E. R., Wach, P. H., and Hale, L. A., eds., Rocky Mountain Thrust Belt Geology and Resources: Wyoming Geological Assoc. Guidebook, 29th Annual Field Conference, p. 101-118.

OSMOND, J. C., 1963, Ripple marks cut on Ordovician limestone pebble conglomerates, Stansbury Range, Utah: Jour. Sed. Petrology, v. 33, p. 105-111.

OVIATT, C. G., 1985, Preliminary notes on the Paleozoic stratigraphy and structural geology of the Honeyville quadrangle, northern Wellsville Mountain, Utah: Utah Geological Assoc. Pub. 14, p. 47-54.

PRATT, B. R., 1982a, Stromatolitic framework of carbonate mud-mounds: Jour. Sed. Petrology, v. 52, p. 1203-1227.

______, 1982b, Limestone response to stress: pressure solution and dolomitization-discussion and examples of compaction in carbonate sediments: Jour. Sed. Petrology, v. 52, p. 323-328.

PRATT, B. R., and JAMES, N. P., 1982, Cryptalgal-metazoan bioherms of early Ordovician age in the St. George Group, western Newfoundland: Sedimentology, v. 29, p. 543-569.

______. 1986, The St. George Group (Lower Ordovician) of western Newfoundland: tidal flat island model for carbonate sedimentation in shallow epeiric seas: Sedimentology, v. 33, p. 313-343.

RICHARDSON, G. B., 1913, Paleozoic section in northern Utah: Am. Jour. Sci., v. 36, p. 406-416.

RIGBY, J. K., 1958, Geology of the Stansbury Mountains, eastern Tooele County, Utah, in Rigby, J. K., ed., Geology of the Stansbury

Mountains, Tooele County, Utah: Utah Geological Soc., Guidebook to the Geology of Utah No. 13, p. 1-135.

ROSS, R. J., Jr., 1951, Stratigraphy of the Garden City Formation in northeastern Utah, and its trilobite fauna: New Haven, Yale Peabody Museum Bull. 5, 161 p.

ROSS, R. J., Jr., JAANUSSON, V., and FRIEDMAN, I., 1975, Lithology and origin of Middle Ordovician calcareous mudmound at Meiklejohn Peak, southern Nevada: U.S. Geol. Survey Prof. Paper 871, p. 48.

SCHAEFFER, F. E., 1960, Stratigraphy of the Silver Island Mountains, in Schaeffer, F. E., ed., Geology of the Silver Island Mountains, Box Elder and Toole Counties, Utah and Elko County, Nevada: Utah Geological Soc., Guidebook to the Geology of Utah No. 15, p. 15-113.

SCHOLLE, P. A., and HALLEY, R. B., 1985, Burial diagenesis: out of sight, out of mind!, in Schneidermann, M., and Harris, P. M., eds., Carbonate Cements: Soc. Econ. Paleontologists Mineralogists Spec. Pub. No. 36, p. 309-334.

SCOFFIN, T. P., 1987, An Introduction to Carbonate Sediments and Rocks: New York, Chapman and Hall, 274 p.

SCOTESE, C. R., BAMBACK, R. K., BARTON, C., VAN DERVOO, R., and ZIEGLER, A. M., 1979, Paleozoic base maps: Jour. of Geology, v. 87, p. 217-277.

SEILACHER, A., 1982, General remarks about event deposits, in Einsele, G., and Seilacher, A., eds., Cyclic and Event Stratification: New York, Springer-Verlag, p. 161-173.

SELLEY, R. C., 1976, An Introduction to Sedimentology: New York, Academic Press, 408 p.

SEPKOSKI, J. J., Jr., 1982, Flat-pebble conglomerates, storm deposits, and the Cambrian bottom fauna, in Einsele, G., and Seilacher, A., eds., Cyclic and Event Stratification: New York, Springer-Verlag, p. 371-385.

SHAW, A. B., 1964, Time in Stratigraphy: New York, McGraw-Hill, 365 p.

SHINN, E. A., and ROBBIN, D. M., 1983, Mechanical and chemical compaction in fine-grained shallow-water limestones: Jour. Sed. Petrology, v. 53, p. 595-618.

SHINN, E. A., HALLEY, R. B., HUDSON, J. H., and LIDZ, B. H., 1977, Limestone compaction: an enigma: Geology, v. 5, p. 21-24.

SLOSS, L. L., 1964, Tectonic cycles of the North American craton: Kansas Geol. Survey Bull. 169, p. 449-461.

STEWART, J. H., and POOLE, F. G., 1974, Lower Paleozoic and uppermost Precambrian cordilleran miogeocline, Great Basin, western United States, in Dickinson, W. R., ed., Tectonics and Sedimentation: Soc. Econ. Paleontologists Mineralogists Spec. Pub. No. 22, p. 28-57.

TAYLOR, M. E., and LANDING, E., 1981, Upper St. Charles and Lower Garden City Formation, Blacksmith Fork Canyon, southern Bear River Range, Utah, in Taylor, M. E., and Palmer, A. R., eds., Cambrian stratigraphy and paleontology of the Great Basin and vicinity, western United States: Guidebook for Field Trip 1, 2nd Int. Symp. on the Cambrian System, p. 141-149.

TAYLOR, M. E., LANDING, E., and GILLETT, S. L., 1981, The Cambrian-Ordovician transition in the Bear River Range, Utah-Idaho: a preliminary evaluation, in Taylor, M. E., ed., Short papers for the 2nd Int. Symp. on the Cambrian System: U.S. Geol. Survey Open-File Report 81-743, p. 222-227.

TAYLOR, M. E., GILLETT, S., LANDING, S. E., and REPETSKI, J. E., 1981, Newly discovered disconformity: Lower Paleozoic, Bear River Range, Utah-Idaho: U.S. Geol. Survey Prof. Paper 1275, p. 192.

TOOMEY, D. F., 1970, An unhurried look at a Lower Ordovician mound horizon, southern Franklin Mountains, west Texas: Jour. Sed. Petrology, v. 40, p. 1318-1334.

WANLESS, H. R., 1969, Sediments of Biscayne Bay, distribution and depositional history, in Multer, H. G., ed., Field Guide to Some Carbonate Rock Environments, Florida Keys and Western Bahamas: Dubuque, Iowa, Kendall/Hunt Pub. Co., p. 146-151.

______, 1979, Limestone response to stress: pressure solution and dolomitization: Jour. Sed. Petrology, v. 49, p. 437-462.

WILLIAMS, J. S., 1948, Geology of the Paleozoic rocks, Logan Quadrangle, Utah: Geol. Soc. America Bull., v. 59, p. 1121-1164.

______, 1955, Resume of Paleozoic stratigraphy, Ordovician to Pennsylvanian of the Green River Basin Area, Wyoming, in Green River Basin: Wyoming Geological Assoc. Guidebook, 10th Annual Field Conference, p. 43-47.

WILSON, J. L., 1969, Microfacies and sedimentary structures in "deeper water" lime mudstones, in Friedman, G. M., ed., Depositional Environments in Carbonate Rocks: Soc. Econ. Paleontologists Mineralogists Spec. Pub. No. 14, p. 4-19.

______, 1975, Carbonate Facies in Geologic History: New York, Springer-Verlag, 471 p.

WRAY, J. L., 1977, Calcareous Algae: New York, Elsevier, 185 p.

APPENDICES

Appendix A

Petrographic, Insoluble Residue, and X-ray Data

Explanation

Thin sections were made from all samples from the High Creek Section. Sample numbers followed by an asterisk (*) were point counted with a minimum of 300 points. Petrologic data from samples in the remaining sections were estimated using acetate peels. The term bioclast refers to unidentified fossil fragments.

The column after the sample number indicates the location (given in feet and meters) within the section that the sample was taken. Zero is always the bottom of the section.

Insoluble residue compositions are listed in order of decreasing relative peak heights.

Sample Number	Feet (Meters)	Rock Name	Percent Insoluble	Insoluble Residue Composition
BF-15	384 (117.0)	Limestone: clay-, bioclast-bearing burrowed stylonodular mudstone	10.3	Quartz, microcline, illite, chlorite trace
BF-16	411 (125.3)	Limestone: quartz-, brachiopod-, peloid-, trilobite-, pelmatozoan-bearing intraclast grainstone with stylolites	5.5	Quartz, microcline
BF-17	440 (134.0)	Limestone: dolomite-rhomb-, clay-bearing burrowed mudstone with stylolites	5.4	Quartz, microcline, plagioclase, illite
BF-18	444 (135.3)	Limestone: brachiopod-, pelmatozoan-, trilobite-bearing intraclast grainstone with stylolites	6.0	Quartz, microcline, illite
BF-19	447 (136.2)	Limestone: burrowed stylonodular mudstone	19.0	Quartz, microcline, illite
BF-20	474 (144.5)	Limestone: quartz-, dolomite-rhomb-, brachiopod-, peloid-bearing intraclast-, trilobite-rich pelmatozoan burrowed grainstone with stylolites	18.3	Quartz, microcline, kaolinite
BF-21	485 (147.8)	Limestone: trilobite-, quartz-, dolomite-rhomb-, peloid-, pelmatozoan-bearing intraclast grainstone with stylolites	11.3	Quartz, microcline, illite
BF-22	504 (153.6)	Limestone: quartz-, bioclast-bearing stylonodular burrowed wackestone	12.8	Quartz, microcline, illite trace

Sample Number	Feet (Meters)	Rock name	Percent Insoluble	Insoluble Residue Composition
BF-23	195 (59.0)	Limestone: Nuia-, spicule-, quartz-bearing sponge (?)-, algal mat-rich wackestone with floored fenestrae and stylolites	11.9	Quartz, microcline, illite
BF-09	208 (63.4)	Limestone: clay-, quartz-, dolomite-rhomb-, trilobite-, Nuia-, bioclast-bearing pelmatozoan wackestone with stylolites	9.5	Quartz, microcline, illite, chlorite, mixed clay, unid. pk. @ 10.9
BF-10	235 (71.6)	Limestone: molluscan-, peloid-, intraclast-, quartz-bearing pelmatozoan trilobite thin-laminated burrowed packstone with stylolites	7.0	Quartz, microcline
BF-11	275 (83.8)	Limestone: pelmatozoan-, chert-rich trilobite intraclast grainstone with stylolites	19.6	Quartz, microcline
BF-12	301 (91.7)	Limestone: peloid-, dolomite-rhomb-, trilobite-, pelmatozoan-, quartz-bearing intraclast grainstone with lower laminated silty mudstone with stylolites	13.8	Quartz, microcline, illite trace
BF-13	330 (100.6)	Limestone: trilobite-, molluscan-bearing pelmatozoan-rich intraclast packstone with stylolites	17.3	Quartz, microcline, illite
BF-14	361 (110.0)	Limestone: quartz-, brachiopod-bearing trilobite-rich pelmatozoan graded burrowed thin-laminated grainstone	3.0	Quartz, microcline, plagioclase, illite

BLACKSMITH FORK SECTION 1

Sample Number	Feet (Meters)	Rock Name	Percent Insoluble	Insoluble Residue Composition
BF-03	74 (22.6)	Limestone: quartz-bearing burrowed stylolaminated mudstone	17.2	Quartz, microcline, chlorite, illite
BF-04	104 (31.7)	Limestone: trilobite-, pelmatozoan-, peloid-bearing intraclast packstone with stylolites	5.1	Quartz, microcline, illite, chlorite
BF-05	130 (39.6)	Dolostone: quartz-, pyrite-bearing thin-laminated vuggy crystalline	10.2	Quartz, microcline, pyrite
BF-06	134 (39.7)	Limestone: *Nuia*-bearing peloid-, pelmatozoan-, trilobite-rich intraclast laminated, burrowed packstone with stylolites	4.3	Quartz, microcline, chlorite and illite traces
BF-07	148 (45.0)	Limestone: trilobite-, clay-, peloid-, dolomite-rhomb-bearing pelmatozoan-rich intraclast imbricated packstone with stylolites	7.5	Quartz, microcline, plagioclase, chlorite and illite traces
BF-01	167 (50.9)	Limestone: brachiopod-, trilobite-, intraclast-, quartz-, bioclast-, pelmatozoan-bearing peloid-rich dasycladacean alga packstone/wackestone	9.3	Quartz, microcline, illite
BF-08	178 (54.2)	Limestone: quartz-, bioclast-bearing trilobite-, intraclast-rich pelmatozoan peloid packstone with stylolites	8.4	Quartz, microcline

Sample Number	Feet (Meters)	Rock Name	Percent Insoluble	Insoluble Residue Composition
BF-24	534 (162.8)	Limestone: quartz-bearing peloid-rich pelmatozoan thin-laminated grainstone	10.0	Quartz, microcline
BF-25	563 (171.6)	Limestone: brachiopod-, trilobite-, intraclast-, quartz-bearing peloid-, pelmatozoan-rich chert thin-laminated packstone with stylolites	19.5	Quartz, microcline, chlorite trace
BF-26	595 (181.3)	Limestone: trilobite-, bioclast-, clay-, dolomite-rhomb-bearing quartz-rich pelmatozoan burrowed packstone with stylolites	43.5	Quartz, microcline, plagioclase, chlorite
BF-27	624 (190.2)	Limestone: trilobite-, peloid-bearing quartz-, chert-rich pelmatozoan thin-laminated grainstone	24.2	Quartz, microcline
BF-28	654 (199.3)	Limestone: Nuia-, quartz-, peloid-bearing trilobite-rich intraclast pelmatozoan faintly-laminated graded grainstone with stylolites	31.4	Quartz, microcline
BF-29	647 (197.2)	Limestone: Facies A: Nuia-, trilobite-, quartz-, peloid-, pelmatozoan-bearing intraclast bioturbated grainstone with stylolites Facies B: pelmatozoan-, quartz-bearing burrowed mudstone with stylolites Facies C: quartz-, trilobite-bearing, Nuia-, intraclast-rich pelmatozoan peloid packstone with stylolites	9.8	Quartz, microcline

Sample Number	Feet (Meters)	Rock Name	Percent Insoluble	Insoluble Residue Composition
BF-30	684 (208.5)	Limestone: bioclast-, quartz-bearing clay-rich nodular mudstone with stylolites and laminated lenses	30.0	Quartz, microcline, illite, kaolinite, chlorite trace
BF-31	714 (217.6)	Limestone: brachiopod-, quartz-, trilobite-, intraclast-bearing peloid-rich pelmatozoan thin-laminated hummocky cross stratified grainstone	5.3	Quartz, microcline
BF-32	744 (226.8)	Limestone: brachiopod-, quartz-, dolomite-bearing trilobite-, *Nuia*-rich pelmatozoan burrowed packstone with stylolites	11.9	Quartz, microcline
BF-33	774 (235.9)	Limestone: quartz-, molluscan-, trilobite-bearing pelmatozoan-rich chert *Nuia* grainstone with stylolites	11.6	Quartz, microcline
BF-34	805 (245.4)	Limestone: trilobite-, pelmatozoan-, intraclast-, quartz-bearing *Nuia*-rich burrowed wackestone with stylolites	13.5	Quartz, microcline, illite, chlorite trace
BF-35	836 (254.8)	Limestone: quartz-, bioclast-, peloid-bearing chert burrowed wackestone with stylolites and laminated lenses	21.8	Quartz, microcline
BF-36	870 (265.2)	Cherty Dolostone: bioclast-bearing burrowed algal mat (?) laminated cherty dolostone	21.8	Quartz, microcline

Sample Number	Feet (Meters)	Rock Name	Percent Insoluble	Insoluble Residue Composition
BF-37	862 (262.7)	Limestone: molluscan-, ostracod-, trilobite-, chert-, quartz-, intraclast-bearing burrowed bioturbated wackestone with stylolites	24.9	Quartz, microcline
BF-38	890 (271.3)	Dolostone: bioclast-, quartz-bearing chert-rich bioturbated burrowed with stylolites	21.1	Quartz, microcline
BF-39	902 (274.9)	Limestone: dolomite-rhomb-, quartz-, peloid-, brachiopod-bearing intraclast pelmatozoan trilobite burrowed packstone with stylolites	12.1	Quartz, microcline
BF-40	920 (280.4)	Limestone: peloid-. trilobite-. pelmatozoan-, dolomite-bearing *Nuia*-, chert-rich intraclast burrowed packstone with stylolites	7.6	Quartz, microcline
BF-41	950 (289.6)	Limestone: Facies A: trilobite-, peloid-, quartz-, bioclast-bearing pelmatozoan-rich bioturbated wackestone with stylolites Facies B: brachiopod-, quartz-bearing, trilobite-, pelmatozoan-, *Nuia*-, intraclast-rich packstone with stylolites	17.9	Quartz, microcline, chlorite trace
BF-42	980 (298.7)	Limestone: quartz-, dolomite-rhomb-, trilobite-, peloid-, intraclast-, pelmatozoan-bearing bioclast-rich bioturbated burrowed wackestone with stylolites	6.6	Quartz, microcline

Sample Number	Feet (Meters)	Rock Name	Percent Insoluble	Insoluble Residue Composition
BF-43	1010 (307.8)	Limestone: bioclast-, quartz-, dolomite-rhomb-bearing burrowed bioturbated wackestone with stylolites	22.6	Quartz, microcline, plagioclase trace
BF-44	1040 (317.0)	Limestone: ostracod-, pelmatozoan-, trilobite-, quartz-, bioclast-bearing intraclast-rich peloid dolomite burrowed burrowed bioturbated packstone with stylolite	11.3	Quartz, microcline, illite trace
BF-46	1045 (318.5)	Limestone: trilobite-, bioclast-, peloid-bearing pelmatozoan-rich *Nuia* quartz packstone with stylolites	31.0	Quartz, microcline
BF-45	1047 (319.1)	Limestone: hematite-, peloid-, trilobite-, *Nuia*-bearing bioclast-, pelmatozoan-rich quartz wackestone with stylolites	29.1	Quartz, microcline

GREEN CANYON SECTION 2

Sample Name	Feet (Meters)	Rock Name	Percent Insoluble	Insoluble Residue Composition
GC-01	0.5 (0.2)	Dolostone: burrowed with stylolites	6.6	Quartz, microcline, illite
GC-02	3 (0.9)	Dolostone: silty	44.0	Quartz, microcline, illite
GC-03	5 (1.5)	Limestone: clay-, quartz-, pelmatozoan-bearing brachiopod-, intraclast-rich bioclast bioturbated packstone with stylolites	15.0	Quartz, microcline, illite
GC-05	55 (16.8)	Limestone: molluscan-, spicule-, intraclast-, pelmatozoan-, bioclast-bearing bored wackestone/packstone with stylolaminations	11.8	Quartz, microcline, chlorite ?
GC-06	85 (25.9)	Limestone: bioclast-, molluscan-, pelmatozoan-bearing trilobite-rich intraclast grainstone with stylolites	7.8	Quartz, microcline, illite, kaolinite, chlorite
GC-07	123 (37.9)	Limestone: clay/limonite-, dolomite-rhomb-bearing burrowed mudstone with stylolites	11.8	Quartz, microcline, plagioclase, kaolinite, illite, chlorite
GC-08	145 (44.2)	Limestone: bioclast-, molluscan-, pelmatozoan-bearing intraclast burrowed grainstone with stylolites	7.6	Quartz, plagioclase, microcline, kaolinite and chlorite traces

Sample Number	Feet (Meters)	Rock Name	Percent Insoluble	Insoluble Residue Composition
GC-09	175 (53.3)	Limestone: Facies A: molluscan-, trilobite-, peloid-, pelmatozoan-bearing intraclast packstone with stylolites Facies B: molluscan-, trilobite-, spicule-bearing Nuia-, intraclast-rich packstone/wackestone with stylolites Facies C: bioclast-, nautiloid-bearing Nuia grainstone with stylolites	6.9	Quartz, microcline, plagioclase, illite, chlorite trace
GC-10	205 (62.5)	Limestone: spicule-, pelmatozoan-, intraclast-, bioclast-bearing burrowed wackestone/packstone with stylolites	6.9	Quartz, microcline, plagioclase, illite, chlorite, kaolinite
GC-11	227 (69.2)	Limestone: peloid-, brachiopod-, bioclast-bearing pelmatozoan-rich intraclast grainstone with stylolites	3.5	Quartz, plagioclase, microcline, chlorite, illite, kaolinite
GC-12	256 (78.0)	Limestone: nodular burrowed mudstone with stylolites	11.3	Quartz, microcline, illite, plagioclase, kaolinite, chlorite
GC-13	286 (87.2)	Limestone: clay-, trilobite-, bioclast-, spicule-bearing pelmatozoan-, peloid-, intraclast-rich burrowed wackestone/packstone with stylolites	4.8	Quartz, microcline, plagioclase, illite, chlorite, kaolinite
GC-14	310 (94.5)	Limestone: brachiopod-, trilobite-, bioclast-bearing pelmatozoan-, intraclast-rich burrowed packstone	6.5	Quartz, microcline, plagioclase, kaolinite, chlorite, illite

Sample Number	Feet (Meters)		Percent Insoluble	Insoluble Residue Composition
GC-15	347 (105.8)	Limestone: molluscan-, trilobite-bearing peloid-, pelmatozoan-rich intraclast planar-laminated grainstone	4.5	Quartz, plagioclase, microcline, chlorite, kaolinite
GC-16	377 (114.9)	Limestone: clay-, brachiopod-, Nuia-, peloid-bearing pelmatozoan-rich grainstone/packstone with stylolites	6.7	Quartz, chlorite, plagioclase, microcline, kaolinite trace
GC-17	407 (124.0)	Limestone: peloid-, bioclast-bearing trilobite-, pelmatozoan-rich intraclast grainstone with stylolites	5.2	Quartz, plagioclase, microcline, illite trace
GC-18	437 (133.2)	Calcareous Shale	31.4	Quartz, kaolinite, chlorite, plagioclase, illite
GC-19	467 (142.3)	Limestone: quartz-, bioclast-bearing pelmatozoan-rich intraclast grainstone with stylolites	12.5	Quartz, plagioclase, microcline, illite, mixed clay ?
GC-20	497 (151.5)	Limestone: molluscan-, trilobite-, pelmatozoan-bearing bioclast-rich burrowed (?) grainstone/packstone with stylolites	19.5	Quartz, plagioclase, kaolinite, chlorite, microcline, illite
GC-21	527 (160.6)	Limestone: clay-rich burrowed mudstone with stylolites	27.1	Quartz, illite, unid. pk. @ 13, plagioclase, chlorite
GC-22	563 (171.6)	Limestone: bioclast-, pelmatozoan-bearing intraclast grainstone/packstone with stylolites	8.7	Quartz, plagioclase, chlorite, illite, microcline, kaolinite

Sample Number	Feet (Meters)	Rock Name	Percent Insoluble	Insoluble Residue Composition
GC-23	590 (179.8)	Limestone: dolomite-rhomb-, trilobite-, molluscan-, peloid-, bioclast-, pelmatozoan-bearing intraclast imbricated grainstone with stylolites	8.5	Quartz, kaolinite, plagioclase, microcline
GC-25	617 (188.1)	Calcareous Shale: limy with stylolaminations	35.0	Quartz, kaolinite, illite, plagioclase, chlorite, microcline trace
GC-26	647 (197.2)	Limestone: chert-, trilobite-, peloid-, bioclast-, molluscan-bearing pelmatozoan-rich intraclast grainstone with stylolites	6.7	Quartz, plagioclase, microcline, illite
GC-27	677 (206.3)	Limestone: chert-, bioclast-, peloid-bearing pelmatozoan-rich intraclast grainstone/packstone with stylolites	13.7	Quartz, plagioclase, microcline, illite
GC-28	706 (215.2)	Limestone: bioclast-bearing Nuia-rich pelmatozoan intraclast packstone with stylolites	10.4	Quartz, kaolinite, illite, microcline, chlorite trace
GC-29	737 (224.6)	Limestone: trilobite-, quartz-, Nuia-, bioclast-, peloid-, molluscan-bearing pelmatozoan intraclast grainstone/packstone with stylolites	7.1	Quartz, microcline, plagioclase, illite, kaolinite, chlorite
GC-30	766 (233.5)	Limestone: Nuia-, molluscan-bearing pelmatozoan-rich intraclast grainstone with a burrowed fossiliferous wackestone upper with stylolites	9.7	Quartz, plagioclase, microcline, illite

Sample Number	Feet (Meters)	Rock Name	Percent Insoluble	Insoluble Residue Composition
GC-31	807 (246.0)	Limestone: quartz-, brachiopod-, gastropod-, peloid-, pelmatozoan-, intraclast-bearing clay/shale-rich bioturbated burrowed packstone/ wackestone with stylolites	23.1	Quartz, microcline, chlorite, kaolinite, plagioclase, illite trace
GC-32	857 (261.2)	Limestone: Facies A: trilobite- Nuia-, molluscan-, brachiopod-bearing peloid-, grastropod-rich pelmatozoan packstone with stylolites Facies B: clay-, intraclast-bearing molluscan-rich Nuia pelmatozoan burrowed bioturbated grainstone/packstone with stylolites	14.4	Quartz, microcline, kaolinite, illite, chlorite
GC-33	887 (270.4)	Limestone: spicule-, molluscan-, gastropod-, intraclast-, bioclast-bearing peloid-, shale-rich burrowed bioturbated packstone with stylolites	30.0	Quartz, microcline, illite trace
GC-34	918 (279.8)	Limestone: molluscan-, intraclast-bearing pelmatozoan-rich Nuia grainstone with stylolites	2.5	Quartz, microcline
GC-35	947 (288.6)	Limestone: spicule-, bioclast-, dolomite-rhomb-, clay-, peloid-bearing burrowed bioturbated wackestone with stylolites	9.7	Quartz, microcline, chlorite, illite trace
GC-36	958 (292.0)	Limestone: quartz-, limonite-, peloid-bearing bioclast-rich burrowed wackestone with stylolites	19.5	Quartz, microcline

Sample Number	Feet (Meters)	Rock Name	Percent Insoluble	Insoluble Residue Composition
GC-37	988 (301.1)	Limestone: quartz-, spicule-, clay-, pelmatozoan-bearing bioclast burrowed stylobrecciated wackestone	13.6	Quartz, microcline, chlorite, kaolinite
GC-38	1016 (309.7)	Dolostone: burrowed cherty with stylolites	45.4	Quartz, microcline, illite
GC-39	1036 (315.8)	Limestone: clay-, bioclast-, dolomite-bearing burrowed peloid packstone with stylolites	15.6	Quartz, microcline, chlorite trace
GC-40	1044 (318.2)	Limestone: Facies A: Nuia-, trilobite-, spicule-, peloid-bearing bioclast pelmatozoan-rich burrowed wackestone with stylolites Facies B: trilobite-bearing nautiloid (?) wackestone with stylolites	22.8	Quartz, kaolinite, microcline, chlorite trace
GC-41	1074 (327.3)	Limestone: Nuia-, trilobite-, brachiopod-, quartz-, molluscan-, dolomite-, intraclast-, peloid-bearing bioclast-, pelmatozoan-rich wackestone with stylolites	10.7	Quartz, microcline
GC-42	1127 (343.5)	Limestone: peloid-, trilobite-, spicule-, gastropod-, pelmatozoan-bearing dolomite wackestone with stylolites	21.9	Quartz, microcline, illite trace
GC-43	1157 (352.6)	Limestone: gastropod-, quartz, pelmatozoan-, bioclast-bearing clay-rich burrowed bioturbated wackestone/packstone with stylolites	9.8	Quartz, microcline, illite

Sample Number	Feet (Meters)	Rock Name	Percent Insoluble	Insoluble Residue Composition
GC-44	1187 (361.8)	Limestone: quartz-, pelmatozoan-bearing bioclast dolomite burrowed bioturbated packstone/wackestone with stylolites	23.9	Quartz, microcline, illite trace
GC-45	1194 (363.9)	Dolostone: chert-bearing bioclast crystalline with stylolites	11.8	Quartz, microcline
GC-46	1213 (369.7)	Limestone: quartz-, molluscan-, trilobite-, _Nuia_-, pelmatozoan-, bioclast-bearing dolomite-rich burrowed wackestone with stylolites	8.2	Quartz, microcline
GC-47	1224 (373.1)	Limestone: _Nuia_-, pelmatozoan-, bioclast-bearing quartz-rich peloid burrowed bioturbated wackestone with stylolites	7.8	Quart, microcline

HIGH CREEK SECTION 3

Sample Number	Feet (Meters)	Rock Name	Percent Insoluble	Insoluble Residue Composition
HC-01*	3 (0.9)	Dolostone: crystalline with relict intraclasts, wavy silty partings	1.8	Quartz. microcline
HC-02*	4 (1.2)	Dolostone: quartz-bearing crystalline thin-laminated	29.4	Quartz, microcline, illite, kaolinite trace
HC-03*	04.5 (1.4)	Dolostone: quartz-bearing crystalline thin-laminated to wavy silty partings burrowed with stylolites	12.1	Quartz, microcline, illite, chlorite
HC-04*	13 (4)	Limestone: Facies A: quartz-, dolomite-rhomb-, clay-bearing thin-laminated mudstone with stylolites Facies B: quartz-, pelmatozoan-, trilobite-, dolomite-rhomb-bearing graded wackestone with stylolites	25.7	Quartz, microcline, illite, chlorite, kaolinite
HC-05*	16 (4.9)	Dolostone: clay-bearing bioclast-rich crystalline intraclastic with stylolites	5.2	Quartz, microcline, illite, chlorite trace
HC-06*	37 (11.9)	Limestone: bioclast-bearing peloid laminated burrowed wackestone	11.1	Quartz, microcline, chlorite, kaolinite, illite
HC-07*	67 (20.4)	Limestone: trilobite-bearing pelmatozoan-rich intraclast grainstone with stylolites	3.5	Quartz, microcline, illite
HC-09	97 (29.6)	Limestone: peloid-, intraclast-bearing trilobite-rich pelmatozoan faintly-laminated grainstone with stylolites	2.2	Quartz, microcline, kaolinite, chlorite, illite

Sample Number	Feet (Meters)	Rock Name	Percent Insoluble	Insoluble Residue Composition
HC-10*	127 (38.7)	Limestone: quartz-, limonite-, dolomite-, bioclast-bearing burrowed wackestone with stylolites	9.4	Quartz, microcline, chlorite, illite, unid. pk. @ 7.7
HC-11*	157 (47.8)	Limestone: Facies A: hematite-, peloid-, pelmatozoan-bearing quartz-rich laminated packstone with stylolites Facies B: trilobite-, conodont/lingula-, peloid-, bioclast-, quartz-bearing faintly-laminated burrowed packstone with stylolites	2.8	Quartz, microcline, kaolinite, chlorite, plagioclase, illite, smectite ?
HC-12	187 (57.0)	Limestone: lingula-, dolomite-, trilobite-, bioclast-, clay-, quartz-, intraclast-bearing peloid burrowed packstone with stylolites	13.8	Quartz, kaolinite, microcline, chlorite, plagioclase
HC-13	218 (66.4)	Limestone: conodont/lingula-, quartz-, pelmatozoan-bearing bioclast-, peloid-, dolomite-rich clay burrowed wackestone with stylolaminations	16.4	Quartz. ,microcline, chlorite, kaolinite, plagioclase, illite
HC-14	248 (75.6)	Limestone: conodont/lingula-, hematite-, pelmatozoan-, quartz-, dolomite-bearing bioclast clay burrowed wackestone with stylolaminations	17.0	Quartz, microcline kaolinite, illite and chlorite traces
HC-15*	278* (84.7)	Limestone: clay-, bioclast-, dolomite-bearing burrowed wackestone	9.1	Quartz, chlorite, microcline, kaolinite, illite, plagioclase

Sample Number	Feet (Meters)	Rock Name	Percent Insoluble	Insoluble Residue Composition
HC-16	308 (93.9)	Limestone: clay-, bioclast-, peloid-, trilobite-bearing intraclast-, pelmatozoan-rich burrowed wackestone with lenses of fossiliferous packstone stylolaminated to stylonodular	6.9	Quartz, microcline, plagioclase, kaolinite, chlorite, illite trace
HC-17*	338 (103.0)	Limestone: clay-, peloid-, intraclast-, trilobite-, pelmatozoan-bearing bioclast-rich partially-laminated burrowed wackestone with stylolites	4.1	Quartz, plagioclase, microcline, illite, chlorite, kaolinite
HC-18*	368 (112.2)	Limestone: lenses of pelmatozoan-bearing packstone in kaolinite-, quartz-, dolomite-, spicule-bearing burrowed wackestone with stylolaminations	28.3	Quartz, microcline, kaolinite, plagioclase, chlorite, illite
HC-19*	386 (117.6)	Limestone: dolomite-rhomb-, clay-, bioclast-, trilobite-, pelmatozoan-bearing sparite packstone with few stylolites	3.5	Quartz, kaolinite, unid. pk. @ 7.7, chlorite, microcline and plagioclase traces
HC-20*	398 (121.3)	Limestone: lenses of pelmatozoan-bearing packstone in limonite-, dolomite-, peloid-, bioclast-, spicule-bearing burrowed wackestone with stylolaminations	19.3	Quartz, chlorite, kaolinite, plagioclase, microcline, illite

Sample Number	Feet (Meters)	Rock Name	Percent Insoluble	Insoluble Residue Composition
HC-21*	428 (130.4)	Limestone: Facies A: burrowed mudstone Facies B: Nuia-, trilobite-, brachiopod-, peloid-bearing pelmatozoan-, intraclast-rich packstone Facies C: quartz-, dolomite-, peloid-, bioclast-, pelmatozoan-bearing clay-rich Nuia laminated bioturbated packstone with stylolites	19.3	Quartz, plagioclase, chlorite, illite, microcline, kaolinite
HC-22*	458 (139.6)	Limestone: bioclast-, peloid-, trilobite-, molluscan-bearing pelmatozoan-rich intraclast faintly imbricated grainstone with stylolites	5.6	Quartz, plagioclase, chlorite, kaolinite, illite
HC-24	488 (148.7)	Limestone: quartz-, pelmatozoan-bearing kaolinite-rich bioclast stylolaminated wackestone with lenses of thin-laminated fossiliferous packstone	24.8	Quartz, plagioclase, kaolinite, microcline, chlorite, illite
HC-25*	518 (157.0)	Limestone: molluscan-, trilobite-bioclast-, peloid-, chert-bearing pelmatozoan-rich intraclast bioturbated packstone with stylolites	12.3	Quartz, plagioclase, kaolinite, chlorite, microcline, illite
HC-26	548 (167.0)	Limestone: dolomite-, peloid-, quartz-bearing bioclast-, clay-, pelmatozoan-rich laminated packstone with stylolaminations	27.8	Quartz, kaolinite, plagioclase, chlorite, microcline

Sample Number	Feet (Meters)	Rock Name	Percent Insoluble	Insoluble Residue Composition
HC-27*	579 (176.5)	Limestone: molluscan-, bioclast-, gastropod-bearing pelmatozoan-rich intraclast grainstone with lenses of fossiliferous quartz stylolaminated wackestone	6.8	Quartz, plagioclase chlorite, kaolinite, illite and microcline traces
HC-28	608 (185.3)	Limestone: molluscan-, trilobite-, pelmatozoan-bearing intraclast laminated packstone with stylolites	18.5	Quartz, plagioclase, chlorite, illite, kaolinite, microcline
HC-29*	638 (194.5)	Limestone: *Nuia*-, molluscan-, bioclast-, clay-, peloid-, trilobite-, dolomite-rhomb-bearing pelmatozoan-rich intraclast grainstone with stylolites	12.6	Quartz, plagioclase chlorite, illite, microcline
HC-30	667 (203.3)	Limestone: peloid-, dolomite-rhomb-, trilobite-, *Nuia*-bearing pelmatozoan-rich intraclast imbricated grainstone with stylolites	4.9	Quartz, kaolinite, plagioclase, chlorite, illite, unid. pk. @ 4, microcline trace
HC-31*	698 (212.7)	Limestone: trilobite-, peloid-, pelmatozoan-bearing intraclastic burrowed stylolitic packstone with lower lense of stylolaminated fossiliferous wackestone	8.8	Quartz, plagioclase, chlorite, kaolinite, microcline, illite
HC-32	728 (221.9)	Limestone: bioclast-, spiculite-bearing burrowed stylolaminated mudstone	24.2	Quartz, kaolinite, plagioclase, chlorite, illite and microcline traces

Sample Number	Feet (Meters)	Rock Name	Percent Insoluble	Insoluble Residue Composition
HC-33	758 (231.0)	Limestone: dolomite-rhomb-, peloid-, trilobite-bearing pelmatozoan-rich intraclastic packstone with stylolites	4.6	Quartz, plagioclase kaolinite, microcline illite, chlorite, unid. pk.
HC-34*	788 (240.2)	Limestone: quartz-, lingula-, intraclast-, clay-, bioclast-, trilobite-, peloid-, Nuia-, pelmatozoan-bearing laminated burrowed grainstone/packstone with stylolites	11.6	Quartz, kaolinite plagioclase, chlorite, illite
HC-35	818 (249.3)	Limestone: quartz-, trilobite-, kaolinite/limonite-, pelmatozoan-bearing peloid planar-laminated packstone with stylolites	19.9	Quartz, kaolinite, chlorite, mixed clays, plagioclase, microcline
HC-36A*	848 (258.5)	Limestone: clay/limonite-, dolomite-, bioclast-, spicule-bearing burrowed wackestone with stylolites	8.8	Quartz, plagioclase, microcline, kaolinite, illite, chlorite, mixed clays
HC-37*	878 (267.6)	Limestone: dasycladacean algae-, Nuia-, peloid-, trilobite-, pelmatozoan-bearing intraclastic burrowed grainstone with stylolites	9.1	Quartz, microcline, plagioclase, kaolinite, chlorite, mixed clays
HC-38*	908 (276.7)	Limestone: conodont/lingula-, dolomite-rhomb-, trilobite-, quartz-, bioclast-bearing clay-, pelmatozoan-, Nuia-rich burrowed bioturbated packstone with stylolites	17.4	Quartz, kaolinite, microcline, plagioclase, chlorite

Sample Number	Feet (Meters)	Rock Name	Percent Insoluble	Insoluble Residue Composition
HC-39	938 (285.9)	Limestone: dolomite-, spiculite, bioclast-, clay-, intraclast-bearing burrowed wackestone with stylolites	15.9	Quartz, kaolinite, mixed clay microcline, plagioclase, chlorite
HC-40*	968 (295.0)	Limestone: dolomite-rhomb-, Nuia-, bioclast-, chert-, clay-, peloid-, brachiopod-, trilobite-bearing intraclast-, pelmatozoan-rich packstone with stylolites	16.5	Quartz, plagioclase, microcline, kaolinite, chlorite, illite trace
HC-41*	998 (304.2)	Limestone: limonite-rhomb-, Nuia-, peloid-, trilobite-bearing intraclast-, pelmatozoan-rich cherty burrowed packstone with stylolites	24.3	Quartz, plagioclase, microcline, kaolinite, chlorite
HC-42*	1028 (313.3)	Limestone: chert-, dolomite-, pelmatozoan-, trilobite-, peloid-, bioclast-bearing packstone lenses in clay-rich burrowed stylolaminated wackestone	30.3	Quartz, kaolinite, microcline, chlorite, illite
HC-43A	1058 (322.5)	Limestone: peloid-, pelmatozoan-, dolomite-, bioclast-, quartz-bearing planar-laminated graded grainstone lenses in clay-rich wackestone with stylolites	27.7	Quartz, kaolinite, microcline, chlorite, illite, mixed clay
HC-44*	1088 (331.6)	Limestone: hematite-, Nuia-, trilobite-, quartz-bearing peloid-rich pelmatozoan planar-laminated grainstone with stylolites	4.5	Quartz, microcline, kaolinite, chlorite, illite, mixed clay

Sample Number	Feet (Meters)	Rock Name	Percent Insoluble	Insoluble Residue Composition
HC-45	1118 (340.8)	Limestone: pelmatozoan-, bioclast-, clay-, quartz-bearing graded planar-laminated burrowed wackestone with stylolaminations	22.4	Quartz, microcline, kaolinite, chlorite, plagioclase
HC-46*	1125 (342.9)	Limestone: gastropod-, trilobite-, peloid-, bioclast-, dolomite-rhomb-, intraclast-bearing Nuia-rich pelmatozoan burrowed packstone with stylolites	5.2	Quartz, microcline, kaolinite, chlorite, illite
HC-47	1155 (352.0)	Limestone: trilobite-, bioclast-bearing recrystallized bioclast-rich intraclast packstone with stylolites	7.8	Quartz, microcline, kaolinite, chlorite
HC-48*	1185 (361.2)	Limestone: quartz-, peloid-, trilobite-, calcite-rhomb-, clay-, dolomite-rhomb-, intraclast-bearing Nuia burrowed packstone with stylolites	10.5	Quartz, microcline, kaolinite, chlorite
HC-49	1197 (364.8)	Limestone: pelmatozoan-, clay-, trilobite-, quartz-bearing sponge-rich dasycladacean algae burrowed packstone with stylolites	14.4	Quartz, microcline, kaolinite, chlorite, illite, mixed clay
HC-50*	1215 (370.3)	Limestone: pelmatozoan-, dolomite-, trilobite- recrystallized bioclast-, quartz-, spicule-bearing dolomite-rhomb laminated burrowed wackestone with stylolites	8.1	Quartz, microcline, chlorite, illite, kaolinite

Sample Number	Feet (Meters)	Rock Name	Percent Insoluble	Insoluble Residue Composition
HC-51*	1257 (383.1)	Limestone: Facies A: quartz-, peloid-, brachiopod-, intraclast-, pelmatozoan-, bioclast-, *Nuia*-, trilobite-, dolomite-bearing cherty burrowed grainstone Facies B: trilobite-, bioclast-, dolomite-, quartz-bearing chert-rich burrowed wackestone with stylolites	23.0	Quartz, microcline, trace of chlorite
HC-52*	1287 (392.3)	Limestone: ostracod-, peloid-, quartz-, pelmatozoan-, calcite-rhomb-, spicule-, bioclast-bearing burrowed partially-laminated packstone with stylolites	9.4	Quartz, microcline, chlorite, kaolinite, illite
HC-53	1323 (403.2)	Limestone: trilobite-, pelmatozoan-, bioclast-, quartz-, ostracod-bearing peloid-, chert-rich burrowed packstone	21.0	Quartz, microcline, chlorite and illite and kaolinite traces
HC-54	1353 (412.4)	Chert: dolomite-, calcite-bearing spicule-rich laminated mega, chalcedony and microcrystalline chert	78.2	Quartz, microcline, illite, mixed clay
HC-55*	1380 (420.6)	Dolomitic Calcareous Chert: lenses of bioclast-, peloid-bearing packstone in limonite-bearing dolomite-, spicule-rich chert with stylolites	72.2	Quartz, microcline
HC-56*	1406 (428.5)	Limestone: ostracod-, bioclast-, pelmatozoan-, spicule-, limonite-, trilobite-, peloid-bearing dolomite-rhomb burrowed partially-laminated packstone with stylolites	7.5	Quartz, microcline, illite and kaolinite traces

Sample Number	Feet (Meters)	Rock Name	Percent Insoluble	Insoluble Residue Composition
HC-57	1414 (431.0)	Limestone: quartz-, bioclast-, pelmatozoan-, peloid-, spicule-, calcite-rhomb-, clay-bearing burrowed wackestone with stylolites	13.0	Quartz, microcline, chlorite, kaolinite, illite trace
HC-58*	1444 (440.1)	Limestone: quartz-, pelmatozoan-, ostracod-, limonite-, bioclast-, spicule-, peloid-bearing dolomite-rich cherty burrowed packstone with stylolites	29.5	Quartz, microcline
HC-59*	1474 (449.3)	Limestone: clay-, trilobite-, spicule-, dolomite-rhomb-, Nuia-, pyrite-, pelmatozoan-, bioclast-bearing quartz-rich burrowed wackestone with stylolites	16.4	Quartz, microcline, chlorite
HC-60	1504 (458.4)	Limestone: clay-, quartz-, intraclast-, peloid-, ostracod-, trilobite-, spicule-bearing burrowed wackestone with stylolites	14.9	Quartz, microcline, chlorite
HC-61*	1534 (467.6)	Limestone: brachiopod-, clay-, trilobite-, pelmatozoan-, calcite-rhomb-, quartz-, ostracod-bearing bioclast-, spicule-rich burrowed bioturbated wackestone	10.0	Quartz, microcline, chlorite and kaolinite traces
HC-62	1565 (477.0)	Dolostone: chert, quartz-bearing burrowed crystalline with stylolites	7.6	Quartz, microcline
HC-63	1582 (482.2)	Dolostone: chert-, quartz-, sparite-bearing micrite-rich fossiliferous burrowed with stylolites	7.9	Quartz, microcline, kaolinite, illite

Sample Number	Feet (Meters)	Rock Name	Percent Insoluble	Insoluble Residue Composition
HC-64	1612 (491.3)	Dolostone: chert-, sparite-, quartz-, bearing burrowed bioturbated with stylolites	6.6	Quartz, microcline, illite trace
HC-65	1631 (497.2)	Siliceous Dolostone: quartz burrowed bioturbated with stylolites	22.7	Quartz, microcline, chlorite and illite traces
HC-66*	1633 (497.7)	Siliceous Limestone: brachiopod-, pelmatozoan-, Nuia-, bioclast-, dolomite-bearing quartz burrowed wackestone	38.7	Quartz, microcline, illite

MANTUA SECTION 4

Sample Number	Feet (Meters)	Rock Name	Percent Insoluble	Insoluble Residue Composition
M-01	2 (0.6)	Dolostone: bioclast-, intraclast-bearing crystalline with stylolites	8.8	Quartz, illite, kaolinite, microcline
M-02	10 (3.0)	Dolostone: stromatolitic chert crystalline	--	------
M-03	40 (12.2)	Limestone: bioclast-, spicule-bearing chert-rich graded burrowed wackestone with stylolites	15.7	Quartz, microcline, illite
M-04	70 (21.3)	Limestone: molluscan-, peloid-bearing trilobite-, intraclast-rich pelmatozoan grainstone with stylolites and laminated lenses	7.7	Microcline, quartz, illite
M-05	100 (30.5)	Limestone: pelmatozoan-, molluscan-, trilobite-, quartz-, dolomite-rhomb-bearing intraclast packstone with lenses of nodular stylolitic wackestone	8.6	Quartz, microcline, illite chlorite, kaolinite
M-06	131 (39.9)	Limestone: *Nuia*-, trilobite-, pelmatozoan- bioclast-bearing peloid-rich intraclast burrowed packstone with stylolites	3.5	Quartz, microcline, chlorite, illite, kaolinite
M-07	150 (45.7)	Limestone: pelmatozoan-, quartz-, molluscan-bearing bioclast grainstone in quartz-, clay-, bioclast-bearing nodular packstone with stylolites	9.5	Quartz, microcline, kaolinite, chlorite, illite trace

Sample Number	Feet (Meters)	Rock Name	Percent Insoluble	Insoluble Residue Composition
M-08	152 (46.3)	Limestone: trilobite-, pelmatozoan-, clay-bearing intraclast grainstone with stylolites	4.6	Quartz, microcline, plagioclase, illite and chlorite traces
M-11	180 (54.9)	Limestone: pelmatozoan-, bioclast-, spicule-bearing sponge (?)-rich wackestone with stylolites	6.5	Quartz, microcline, chlorite trace
M-09	182 (55.5)	Limestone: clay-, hematite-, bioclast-, quartz-bearing nodular wackestone with stylolites	16.0	Quartz, microcline, plagioclase, kaolinite, illite, chlorite trace
M-10	212 (64.6)	Limestone: peloid-bearing nodular wackestone with stylolites	6.4	Quartz, microcline, illite, chlorite trace
M-13	241 (73.5)	Limestone: Facies A: clay-bearing burrowed mudstone with stylolites Facies B: molluscan-, peloid-, dolomite-rhomb-, trilobite-, pelmatozoan-bearing bioclast-rich burrowed packstone with stylolites Facies C: peloid-, *Nuia*-, hematite-, dolomite-rhomb-, molluscan-, pelmatozoan-bearing bioclast-, trilobite-, gastropod-rich packstone with stylolites	7.5	Quartz, microcline, illite, kaolinite
M-12	242 (73.8)	Limestone: hematite-, peloid-, molluscan, trilobite-, pelmatozoan-, clay-bearing nodular wackestone with stylolites	11.3	Quartz, microcline, kaolinite, chlorite, illite

Sample Number	Feet (Meters)	Rock Name	Percent Insoluble	Insoluble Residue Composition
M-14	272 (82.9)	Limestone: Nuia-, trilobite-, molluscan-, peloid-bearing gastropod packstone with stylolites	5.9	Quartz, microcline, plagioclase, kaolinite, chlorite and illite traces
M-15	302 (92.0)	Limestone: pelmatozoan-, bioclast-bearing peloid-, clay-rich thin-laminated grainstone with mud cracked (?) burrowed clay seams with stylolites	58.0	Quartz, chlorite, plagioclase, illite, microcline, kaolinite
M-16	332 (101.2)	Limestone: pelmatozoan-, bioclast-bearing Nuia-rich clay burrowed nodular wackestone with stylolites	31.0	Quartz, kaolinite, chlorite, microcline, plagioclase, illite
M-17	362 (110.3)	Limestone: clay/limonite-, dolomite-rhomb-, molluscan-, peloid-, brachiopod-, intraclast-, trilobite-, gastropod-, Nuia-bearing pelmatozoan-rich grainstone/packstone	3.8	Quartz, microcline, kaolinite, illite, chlorite, plagioclase
M-18	392 (119.5)	Shale: bioclast-bearing quartz-rich planar-laminated grainstone (limestone) lenses in shale	65.5	Quartz, illite, kaolinite, chlorite, microcline, plagioclase
M-19	422 (128.6)	Limestone: shaly burrowed nodular mudstone	32.1	Quartz, kaolinite, illite, chlorite, plagioclase, microcline trace
M-20	452 (137.8)	Limestone: shaly burrowed nodular mudstone with stylolites	37.2	Quartz, illite, kaolinite, plagioclase, microcline
M-21	482 (146.9)	Limestone: bioclast-bearing shaly burrowed thin-laminated mudstone with stylolites	22.2	Quartz, illite, plagioclase, microcline, kaolinite, chlorite

Sample Number	Feet (Meters)	Rock Name	Percent Insoluble	Insoluble Residue Composition
M-22	512 (156.1)	Limestone: trilobite-, peloid-, bioclast-bearing pelmatozoan intraclast imbricated grainstone with stylolites	4.6	Quartz, plagioclase, illite, microcline, kaolinite, chlorite
M-23	542 (165.2)	Limestone: trilobite-, quartz-, pelmatozoan-, peloid-, molluscan-bearing shale-rich intraclast grainstone/packstone	15.8	Quartz, plagioclase, microcline, kaolinite, illite, chlorite
M-24	572 (174.3)	Limestone: quartz-, clay-, bioclast-bearing intraclast planar-laminated and nodular wackestone with stylolites	37.1	Quartz, illite, plagioclase, kaolinite, microcline, chlorite
M-25	602 (183.5)	Limestone: trilobite-, peloid-, brachiopod-, bioclast-, *Nuia*-bearing intraclast grainstone with lenses of planar-laminated shale-, bioclast-bearing packstone with stylolites	25.0	Quartz, plagioclase, illite, kaolinite, chlorite
M-26	632 (192.6)	Limestone: bioclast-, pelmatozoan-, molluscan-, trilobite-, quartz-bearing shaly planar-laminated nodular wackestone with lenses of fossiliferous grainstone with stylolites	42.5	Quartz, plagioclase, microcline, illite, kaolinite, chlorite
M-27	662 (201.8)	Shale: clay-, trilobite-, quartz-, pelmatozoan-, bioclast-bearing packstone lenses in faintly-laminated shale	59.8	Quartz, kaolinite, illite, chlorite, plagioclase, microcline

Sample Number	Feet (Meters)	Rock Name	Percent Insoluble	Insoluble Residue Composition
M-28	692 (210.9)	Limestone: trilobite-, pelmatozoan-, molluscan-, quartz-, bioclast-bearing intraclast-rich shaly bioturbated packstone with stylolites	28.7	Quartz, plagioclase, kaolinite, microcline, chlorite, illite
M-29	722 (220.1)	Limestone: trilobite-, molluscan-, quartz-bearing bioclast-, shale-rich planar thin-laminated nodular mudcracked(?) burrowed (?) wackestone with stylolites	37.8	Quartz, chlorite, kaolinite, illite, microcline, plagioclase
M-30	752 (229.2)	Limestone: peloid-, *Nuia*-, molluscan-, trilobite-bearing pelmatozoan-rich intraclast grainstone with stylolites	10.6	Quartz, microcline, illite, kaolinite and chlorite traces
M-31	782 (238.4)	Limestone: trilobite-, quartz-, clay-, molluscan-, intraclast-, pelmatozoan-bearing bioclast-rich burrowed bioturbated packstone/wackestone with stylolites	14.0	Quartz, microcline, chlorite, illite, kaolinite
M-32	812 (247.5)	Limestone: bioclast-, molluscan-, spicule-, trilobite-, peloid-, gastropod-bearing pelmatozoan-, intraclast-rich burrowed packstone/wackestone with stylolites	5.9	Quartz, microcline, kaolinite, illite, chlorite
M-33	842 (256.6)	Limestone: gastropod-, peloid-, intraclast-, molluscan-, *Nuia*-bearing bioclast-, pelmatozoan-rich grainstone with stylolites	9.3	Quartz, microcline, kaolinite, illite and chlorite traces

Sample Number	Feet (Meters)	Rock Name	Percent Insoluble	Insoluble Residue Composition
M-34	872 (265.8)	Limestone: quartz-, bioclast-bearing shaly nodular bedded wackestone with quartz-, pelmatozoan-bearing peloid-rich hummocky cross-stratified lenses of packstone	24.5	Quartz, microcline, illite, chlorite, kaolinite
M-35	902 (274.9)	Limestone: pelmatozoan-, quartz-bearing shaly nodular bedded rippled (?) laminated wackestone with stylolites	33.9	Quartz, microcline, chlorite, illite, kaolinite, plagioclase
M-36	932 (284.1)	Limestone: trilobite-, quartz-, spicule-bearing pelmatozoan-, peloid-rich intraclast burrowed packstone/grainstone with stylolites	2.9	Quartz, microcline, kaolinite, illite, chlorite
M-37	958 (292.0)	Limestone: quartz-, dolomite-rhomb-, brachiopod-, molluscan-, peloid-, intraclast-bearing trilobite-, bioclast-, pelmatozoan-rich burrowed grainstone/packstone with stylolites	13.2	Quartz, microcline
M-38	982 (299.3)	Limestone: quartz-, dolomite-rhomb-, *Nuia*-, intraclast-, peloid-, brachiopod-, trilobite-bearing molluscan-rich pelmatozoan burrowed grainstone with stylolites	5.9	Quartz, microcline
M-39	1012 (308.5)	Limestone: *Nuia*-, clay-, trilobite-, dolomite-rhomb-, gastropod-, molluscan-bearing intraclast-rich pelmatozoan burrowed packstone with stylolites	15.8	Quartz, microcline, kaolinite

Sample Number	Feet (Meters)	Rock Name	Percent Insoluble	Insoluble Residue Composition
M-40	1042 (317.6)	Limestone: clay-bearing Nuia burrowed grainstone with stylolites	7.9	Quartz, microcline, illite, chlorite trace
M-41	1072 (326.7)	Limestone: clay-, quartz-, molluscan-, bioclast-, peloid-, pelmatozoan-bearing Nuia-rich burrowed bioturbated wackestone/packstone with stylolites	18.2	Quartz, microcline, illite
M-42	1102 (335.9)	Limestone: ostracod-, clay-, dolomite-rhomb-, peloid-, molluscan-, pelmatozoan-, spicule-bearing bioclast-rich burrowed bioturbated wackestone with stylolites	8.9	Quartz, microcline, illite
M-43	1128 (343.8)	Limestone: trilobite-, gastropod-, pelmatozoan-, spicule-, quartz-bearing chert bioturbated burrowed wackestone/packstone with stylolites	22.4	Quartz, microcline
M-44	1158 (353.0)	Limestone: quartz-, spicule-, bioclast-, peloid-, chert-bearing burrowed wackestone	11.6	Quartz, microcline
M-45	1188 (362.1)	Chert: quartz-bearing peloid-rich packstone limestone lenses in chert with stylolites	63.3	Quartz, microcline, mixed clay (?)
M-46	1218 (371.2)	Limestone: clay-, shale-, quartz-, molluscan-, pelmatozoan-, spicule-bearing bioclast-rich burrowed bioturbated wackestone with stylolites	17.1	Quartz, microcline, illite trace

Sample Number	Feet (Meters)	Rock Name	Percent Insoluble	Insoluble Residue Composition
M-47	1227 (374.0)	Limestone: pelmatozoan-, ostracod-, shale-, quartz-, spicule-bearing bioclast-rich bioturbated burrowed wackestone with stylolites	30.9	Quartz, microcline, illite
M-48	1247 (380.1)	Limestone: quartz-, shale-, bioclast-, bearing *Nuia*-, chert-rich burrowed bioturbated wackestone/packstone with stylolites	30.9	Quartz, microcline, illite
M-49	1257 (383.1)	Limestone: trilobite-, spicule-, shale-, pelmatozoan-, peloid-, quartz-, *Nuia*-bearing bioclast-rich burrowed bioturbated wackestone with stylolites	17.5	Quartz, microcline, illite
M-50	1287 (392.3)	Dolostone: hematite-, quartz-bearing bioclast-rich burrowed bioturbated crystalline with stylolites	20.5	Quartz, microcline, chlorite trace
M-51	1307 (398.4)	Dolostone: shale-bearing quartz-rich with stylolites	7.7	Quartz, microcline, illite
M-52	1347 (410.5)	Dolostone	22.4	Quartz, microcline
M-53	1377 (419.7)	Dolostone: quartz-, calcite-bearing, crystalline with wavy horizontal void fillings (stromatactis ?) and stylolites	4.1	Quartz, microcline, illite trace
M-54	1407 (428.8)	Dolostone: quartz-rich crystalline	6.3	Quartz, microcline, illite trace

WELLSVILLE SECTION 5

Sample Number	Feet (Meters)	Rock Name	Percent Insoluble	Insoluble Residue Composition
W-01	1 (0.3)	Dolostone: calcite-bearing intraclast crystalline with stylolites	4.5	Quartz, microcline
W-02	21 (6.4)	Dolostone: intraclast crystalline with stylolites	8.1	Quartz, microcline, illite, trace
W-03	48 (14.6)	Limestone: clay-, trilobite-, quartz-, molluscan-, spicule-bearing bioclast-rich burrowed bioturbated wackestone with a lower thin-laminated pelmatozoan-rich packstone with stylolites	5.4	Quartz, microcline, chlorite, illite, kaolinite
W-04	78 (23.8)	Limestone: pelmatozoan-, spicule-, shale-bearing clay-, bioclast-rich nodular wackestone with stylolites	19.3	Quartz, microcline, kaolinite, chlorite, illite
W-05	108 (32.9)	Limestone: clay-, spicule-, quartz-, dolomite/calcite-rhomb-, hematite-, peloid-, bioclast-, pelmatozoan-bearing intraclast burrowed planar-laminated packstone/wackestone with stylolites	18.7	Quartz, microcline, illite, kaolinite
W-06	137 (41.8)	Limestone: quartz-, molluscan-, trilobite-, spicule-, bioclast-, peloid-, pelmatozoan-bearing graded faintly-laminated wackestone/packstone with stylolites	8.3	Quartz, microcline, illite, chlorite, kaolinite, plagioclase ?

Sample Number	Feet (Meters)	Rock Name	Percent Insoluble	Insoluble Residue Composition
W-07	140 (42.7)	Limestone: Nuia-, trilobite-, spicule-, intraclast-, pelmatozoan-, bioclast-, peloid-bearing burrowed clotted fabric wackestone with stylolites	5.8	Quartz, microcline, illite
W-08	169 (51.5)	Limestone: pelmatozoan-, spicule-, bioclast-, trilobite-bearing peloid-rich intraclast burrowed packstone/wackestone with stylolites	6.3	Quartz, microcline, illite, chlorite, kaolinite trace
W-09	180 (23.5)	Limestone: brachiopod-, quartz-, trilobite-, molluscan-bearing intraclast-, peloid-rich pelmatozoan planar-laminated grainstone with stylolites	7.6	Quartz, microcline, chlorite, kaolinite, illite
W-10	210 (64.0)	Limestone: quartz-, clay-bearing bioclast-rich stylonodular burrowed wackestone/packstone	16.1	Quartz, microcline, illite, kaolinite, chlorite
W-12	237 (72.2)	Limestone: pelmatozoan-, bioclast-bearing sponge (?) wackestone with stylolites	12.8	Quartz, illite, kaolinite, microcline
W-11	240 (73.1)	Limestone: spicule-, hematite-, clay-, peloid-, bioclast-bearing burrowed stylonodular wackestone	8.9	Quartz, microcline, chlorite, illite, kaolinite
W-13	270 (82.3)	Limestone: trilobite-, molluscan-bearing pelmatozoan-, peloid-rich intraclast grainstone/packstone	5.1	Quartz, microcline, illite, kaolinite

Sample Number	Feet (Meters)	Rock Name	Percent Insoluble	Insoluble Residue Composition
W-14	300 (91.4)	Limestone: spicule-, peloid-, trilobite-, pelmatozoan-, chert-, bioclast-bearing intraclast-rich burrowed bioturbated wackestone/ packstone with stylolites	10.5	Quartz, microcline, illite, kaolinite, chlorite trace
W-16	327 (99.7)	Limestone: bioclast-, peloid-, trilobite-, molluscan-bearing gastropod-, pelmatozoan-rich intraclast shell-cast grainstone/ packstone with stylolites	5.3	Quartz, microcline, kaolinite, illite, chlorite trace
W-17	360 (109.7)	Limestone: intraclast-, clay-, bioclast-, dolomite-rhomb-bearing pelmatozoan-rich *Nuia* bioturbated packstone with stylolites	16.9	Quartz, illite, microcline
W-18	390 (118.9)	Limestone: spicule-, bioclast-, clay-bearing stylolaminated burrowed wackestone	18.3	Quartz, illite, microcline, chlorite
W-19	425 (129.5)	Limestone: Facies A: bioclast-bearing pelmatozoan-, peloid-rich intraclast burrowed grainstone/ packstone with stylolites Facies B: chert-, peloid-, brachiopod-bearing pelmatozoan grainstone	4.2	Quartz, microcline, kaolinite, illite, chlorite trace
W-20	437 (133.2)	Shale: quartz-, trilobite-, bioclast-pelmatozoan-bearing graded faintly-laminated lenses of packstone in shale	66.2	Quartz, kaolinite, illite, chlorite, microcline

Sample Number	Feet (Meters)	Rock Name	Percent Insoluble	Insoluble Residue Composition
W-37	455 (138.7)	Limestone: spicule-, dolomite-rhomb-, clay-, peloid-, pelmatozoan-, bioclast-bearing intraclast-rich burrowed bioturbated faintly planar-laminated grainstone/wackestone with stylolites	20.5	Quartz, plagioclase, microcline, illite, chlorite trace
W-36	485 (147.8)	Limestone: molluscan-, peloid-, clay-, trilobite-, pelmatozoan-bearing intraclast faulted grainstone with stylolites	9.5	Quartz, microcline, kaolinite, illite, chlorite
W-35	516 (157.3)	Limestone: pelmatozoan-, peloid-, molluscan-, clay-, bioclast-, shale-bearing wackestone/packstone with stylolites	39.1	Quartz, microcline, illite, plagioclase, kaolinite
W-34	545 (166.1)	Limestone: spicule-, quartz-, pelmatozoan-, bioclast-bearing shale-, clay-rich burrowed nodular wackestone with stylolites	28.1	Quartz, plagioclase, illite, microcline, kaolinite
W-33	575 (175.3)	Limestone: hematite-, spicule-, tiolobite-, peloid-, clay-, brachiopod-bearing bioclast-, pelmatozoan-, shale-rich burrowed bioturbated stylonodular packstone	20.7	Quartz, microcline, illite, plagioclase, mixed clay ?
W-32	605 (184.4)	Limestone: trilobite-, brachiopod-, quartz-. clay-, bioclast-, pelmatozoan-bearing intraclast planar-laminated packstone with stylolites	11.2	Quartz, microcline, illite, chlorite trace

Sample Number	Feet (Meters)	Rock Name	Percent Insoluble	Insoluble Residue Composition
W-31	635 (193.5)	Limestone: trilobite-, clay-, bioclast-, brachiopod-, molluscan-, shell-cast-, pelmatozoan-bearing intraclast grainstone with stylolites with a lower and upper micrite-clay mudstone with stylolites	8.2	Quartz, microcline, illite, chlorite trace
W-30	665 (202.7)	Limestone: dolomite-rhomb-, trilobite-, brachiopod-, molluscan-, bioclast-, pelmatozoan- bearing intraclast burrowed packstone/wackestone with stylolites	10.9	Quartz, microcline, illite
W-29	695 (211.8)	Limestone: clay-, trilobite-, molluscan-, peloid-, pelmatozoan-bearing intraclast bioturbated packstone with stylolites with a lower bioclast-bearing faintly-laminated wackestone with stylolites	19.7	Quartz, illite, microcline, plagioclase
W-28	725 (221.0)	Limestone: molluscan-, spicule-, trilobite-, gastropod-, dolomite-rhomb-, pelmatozoan-bearing intraclast-, Nuia-rich packstone with stylolites	6.3	Quartz, microcline, illite
W-27	755 (230.1)	Limestone: clay-, pelmatozoan-bearing spicule-rich peloid burrowed bioturbated packstone with stylolites	15.8	Quartz, microcline, illite

Sample Number	Feet (Meters)	Rock Name	Percent Insoluble	Insoluble Residue Composition
W-26	785 (239.3)	Limestone: clay-, chert-, quartz-, calcite-rhomb-, Nuia-, peloid-, bioclast-, pelmatozoan-bearing intraclast packstone with stylolites	15.6	Quartz, microcline, illite, chlorite trace
W-25	815 (248.4)	Limestone: molluscan-bearing peloid-, pelmatozoan-, bioclast-rich shaly bioturbated burrowed packstone	24.4	Quartz, microcline
W-24	845 (257.6)	Limestone: quartz-, molluscan-, peloid-bearing bioclast-, pelmatozoan-rich shaly burrowed bioturbated packstone with stylolites	36.1	Quartz, microcline, illite
W-23	875 (266.7)	Limestone: molluscan-, bioclast-, peloid-, shale-, pelmatozoan-bearing intraclast inbricated grainstone with stylolites	9.3	Quartz, microcline, illite, kaolinite trace
W-22	905 (275.8)	Limestone: molluscan-, shale-, trilobite-, peloid-bearing pelmatozoan-rich intracalst imbricated grainstone/ packstone with stylolites	8.6	Quartz, microcline, illite and kaolinite and chlorite traces
W-59	912 (278.0)	Limestone: clay-, molluscan-, trilobite-bearing pelmatozoan-rich Nuia burrowed grainstone with stylolites	9.2	Quartz, kaolinite, chlorite, microcline, illite
W-21	913 (278.3)	Limestone: peloid-, bioclast-, trilobite-bearing pelmatozoan-rich intraclast imbricated grainstone with stylolites	7.4	Quartz, microcline, illite

Sample Number	Feet (Meters)	Rock Name	Percent Insoluble	Insoluble Residue Composition
W-58	942 (287.1)	Limestone: shaly mudstone with stylolites	37.1	Quartz, kaolinite, microcline, chlorite, illite
W-57	972 (296.3)	Limestone: trilobite-, bioclast-, peloid-, gastropod-, pelmatozoan-bearing clay-rich planar-laminated packstone with stylolites	5.4	Quartz, microcline, kaolinite, chlorite, illite trace
W-56	984 (300.0)	Limestone: bioclast-, dolomite-bearing *Nuia*-, pelmatozoan-rich clay burrowed grainstone/packstone with stylolites	25.9	Quartz, microcline, kaolinite, chlorite, illite
W-55	1015 (309.1)	Limestone: bioclast-, dolomite-bearing *Nuia* burrowed grainstone with stylolites	8.5	Quartz, microcline, kaolinite, chlorite
W-54	1043 (317.9)	Limestone: quartz-, pelmatozoan-, bioclast-bearing peloid-rich *Nuia* planar-laminated grainstone/packstone with stylolites	10.5	Quartz, microcline, kaolinite, chlorite
W-53	1044 (318.2)	Limestone: clay-, molluscan-, gastropod-, pelmatozoan-, bioclast-bearing *Nuia* burrowed grainstone/ packstone with stylolites	3.9	Quartz, microcline
W-52	1074 (327.3)	Limestone: trilobite-, spicule-, gastropod-, pelmatozoan-, *Nuia*-, dolomite-, peloid-, clay-, bioclast-bearing burrowed bioturbated wackestone with stylolites	7.2	Quartz, microcline, illite trace

Sample Number	Feet (Meters)	Rock Name	Percent Insoluble	Insoluble Residue Composition
W-51	1104 (336.5)	Limestone: clay-, brachiopod-, gastropod-, spicule-, dasycladacean-, bioclast-bearing burrowed bioturbated wackestone with stylolites	9.8	Quartz, microcline
W-50	1123 (342.3)	Limestone: pelmatozoan-, clay-, peloid-, gastropod-, bioclast-bearing spicule-rich burrowed bioturbated wackestone/packstone with stylolites	9.7	Quartz, microcline, kaolinite, chlorite, illite
W-49	1153 (351.4)	Chert: with ostracod-, quartz-bearing peloid-rich grainstone lenses with stylolites	55.0	Quartz, microcline, illite trace
W-48	1183 (360.6)	Limestone: molluscan-, gastropod-, spicule-, trilobite-, peloid-, pelmatozoan-, bioclast-bearing burrowed bioturbated wackestone with stylolites	12.8	Quartz, microcline, illite, kaolinite trace
W-47	1203 (366.7)	Limestone: trilobite-, clay-, ostracod-, quartz-, gastropod-, brachiopod-, pelmatozoan-, peloid-, molluscan-, spicule-, bioclast-bearing burrowed bioturbated wackestone with stylolites	16.1	Quartz, microcline, kaolinite trace
W-46	1233 (375.8)	Limestone: clay-, molluscan-, bioclast-bearing peloid-rich cherty burrowed wackestone with stylolites	34.6	Quartz, kaolinite, microcline

Sample Number	Feet (Meters)	Rock Name	Percent Insoluble	Insoluble Residue Composition
W-45	1248 (380.4)	Limestone: clay-, brachiopod-, quartz, molluscan-, chert-, pelmatozoan-, intraclast-, peloid-bearing Nuia-rich burrowed bioturbated packstone/wackestone with stylolites	18.5	Quartz, microcline, illite and kaolinite traces
W-44	1266 (385.9)	Dolostone: stromatactis (?) cavities, crystalline	7.4	Quartz, microcline
W-43	1296 (395.0)	Dolostone: burrowed crystalline with stylolites	22.7	Quartz, microcline
W-42	1326 (404.2)	Dolostone: bioclast-bearing burrowed bioturbated crystalline with stylolites	10.1	Quartz, microcline
W-41	1356 (413.3)	Dolostone: bioclast-bearing burrowed bioturbated crystalline with stylolites	16.8	Quartz, microcline, illite
W-40	1367 (416.8)	Dolostone: Facies A: clay-, quartz-bearing brachiopod-rich burrowed with stylolites Facies B: dolomite-, hematite-bearing stylolaminated chert	45.7	Quartz, microcline, chlorite and illite traces

Appendix B

Measured Stratigraphic Sections

Explanation

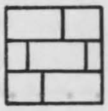
Limestone

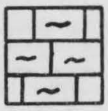
Nodular and sedimentary boudinage limestone with some shale interbeds

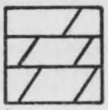
Dolostone

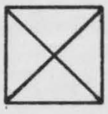
Covered Slope, float present


Mud mounds


Chert


Stromatolite

BLACKSMITH FORK
SECTION 1

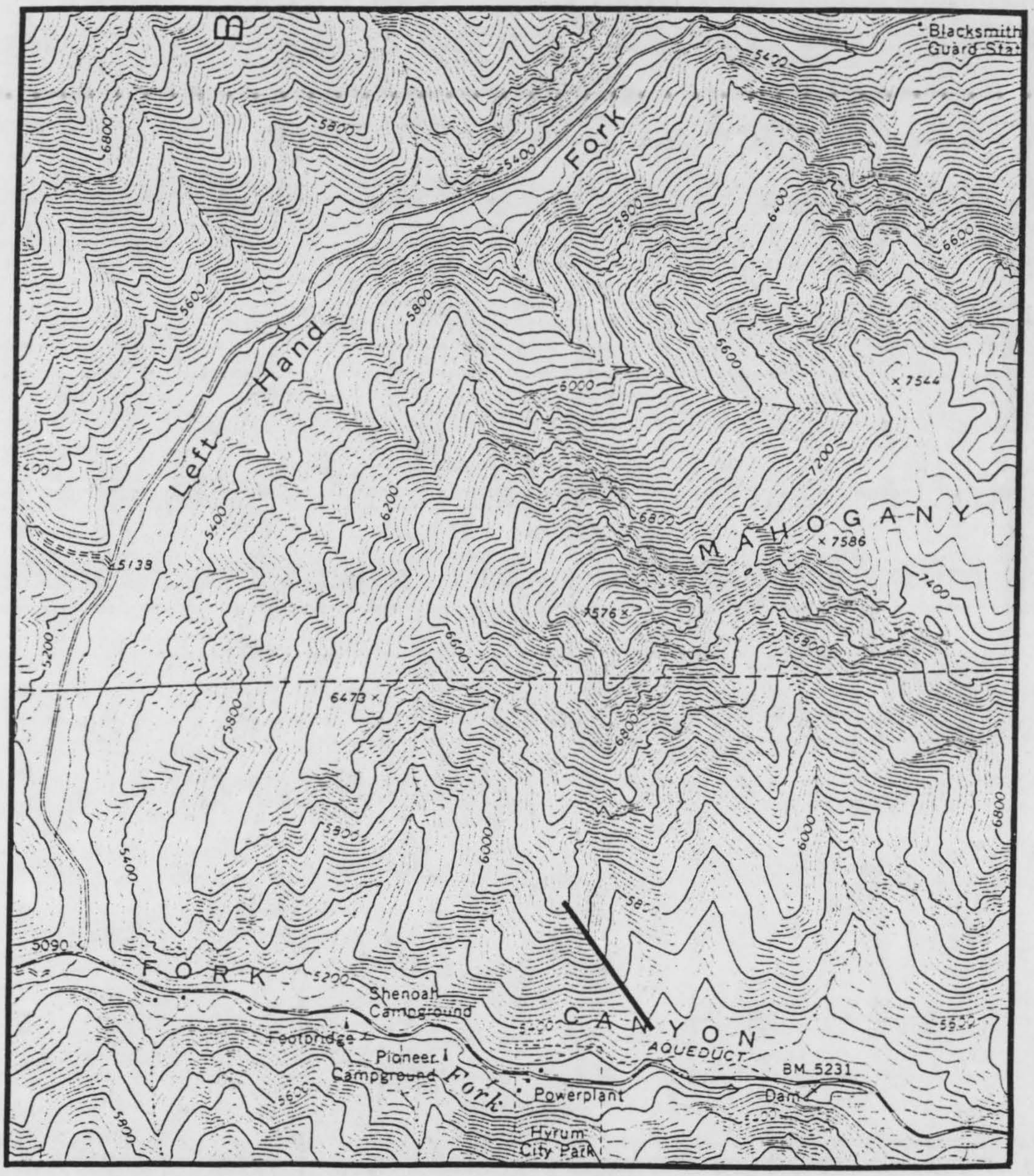

Location: Blacksmith Fork Canyon, Highway 101, northeast of Hyrum City Park, measured on a southeast-facing ridge (Logan Peak 7 1/2 minute quadrangle).

Swan Peak Formation

Abrupt contact

Garden City Limestone

	Thickness in feet	and (meters)
Irregular contact to blocky dolostone with some thin-bedded, silty, fine-grained limestone	17	(5.2)
Fine-grained limestone mixed with coarse-grained fossiliferous lenses, silty wavy partings, fractures filled with white calcite	105	(32.0)
Thin- to thick-bedded, fossiliferous limestone, fine-grained to coarse-grained with small amounts of silt, small (2.5 by 30 cm) lenses of intraformational conglomerate, ~15% black chert in scattered nodules	38	(11.6)
Banded and anastomosing black chert, makes up ~50% of the rock with fine- to medium-grained, fossiliferous limestone in between	39	(11.9)
Mixed, fine- to coarse-grained, fossiliferous limestone with some intraclasts, ~15% grey to black banded to nodular chert	34	(10.4)
Thin- to thick-bedded, fine-grained to coarse-grained, fossiliferous limestone with irregular small intraclasts, interbedded with a few bladed large intraclast intraformational conglomerate beds, 2 to 20 cm thick, erosional to gradational contacts, silty wavy partings, very burrowed	144	(43.9)
Intraformational conglomerate limestone layers and lenses, large bladed to small irregular to rounded intraclasts set in a fossiliferous groundmass, interbedded with fine-grained, nodular silty layers from 30 cm to 1.5 m thick and planar-laminated coarse-grained layers from 5 to 20 cm thick, abrupt, erosional to gradational contacts, light grey chert nodules, occasional ripple marks, trace fossils and burrows . .	380	(115.8)
Covered slope	69	(21.0)
Coarse-grained, fossiliferous (fossil hash) limestone with some intraclasts, interbedded with 4 to 14 cm thick lenses of intraformational conglomerate with bladed to rounded intraclasts, and nodular to planar-laminated		

	Thickness in feet and (meters)	
limestone with varying amounts of silt , mud mounds covered by fossil hash at 58.8 meters	89	(27.1)
Covered slope	7	(2.1)
Mixed, fine- to coarse-grained limestone with silty wavy partings, interbedded with intraformational conglomerate with large bladed to rounded intraclasts with silty partings, occasional nodules and stringers of white and black chert, abrupt to erosional contacts, interbedded with some nodular silty fine-grained limestone	75	(22.9)
Mud mound draped with fine- to coarse-grained planar-laminated limestone, trace fossils	5	(1.5)
Mixed, fine- to coarse-grained limestone, massive with wavy silty partings, scattered fossils	7	(2.1)
Mixed, fine- to coarse-grained limestone with silty wavy partings, interbedded with intraformational conglomerate lenses and layers, erosional contacts . .	31	(9.5)
Crystalline dolostone, thin-laminated with some intraformational conglomerate in thin beds	17	(5.1)
Total	1057	(322.1)

Disconformity

Saint Charles Formation

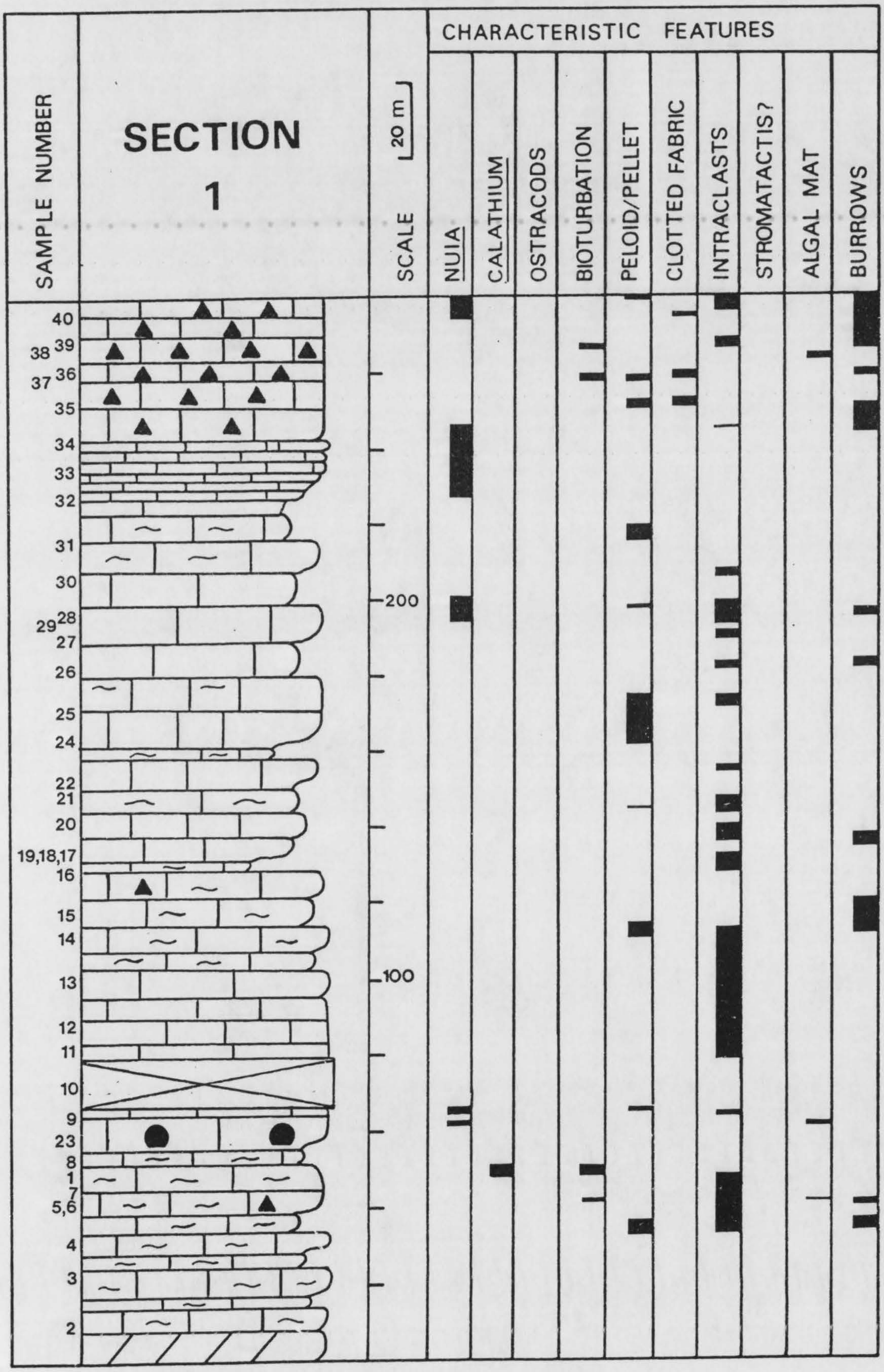
SAMPLE NUMBER
SECTION 1
SCALE
20 m
CHARACTERISTIC FEATURES
NUIA
CALATHIUM
OSTRACODS
BIOTURBATION
PELOID/PELLET
CLOTTED FABRIC
INTRACLASTS
STROMATACTIS?
ALGAL MAT
BURROWS
40
38 39
37 36
35
34
33
32
31
30
29 28
27
26
25
24
22
21
20
19,18,17
16
15
14
13
12
11
10
9
23
8
1
7
5,6
4
3
2
200
100

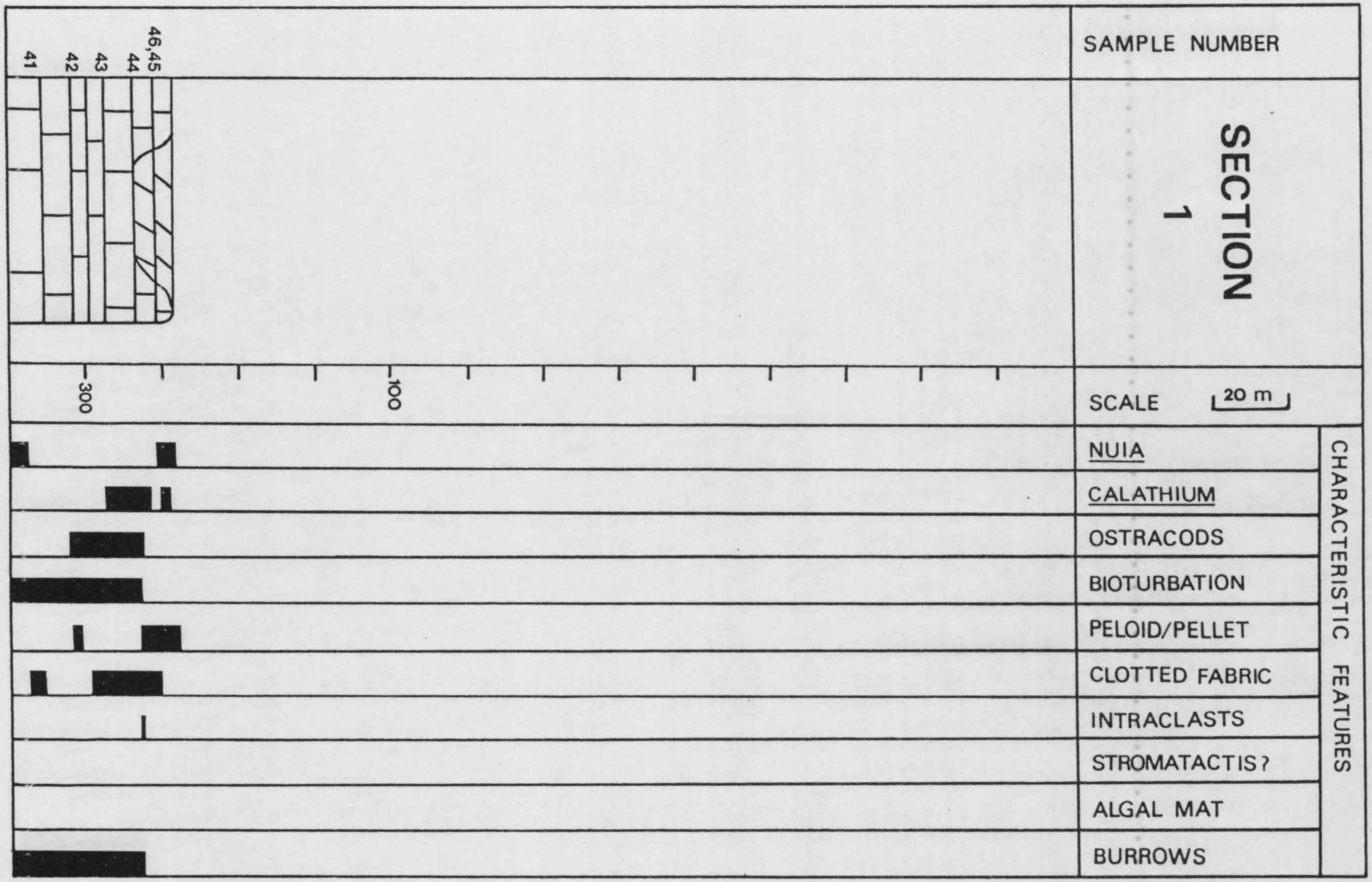
SAMPLE NUMBER
41
42
43
44
46,45
SECTION 1
SCALE
20 m
300
100
CHARACTERISTIC FEATURES
NUIA
CALATHIUM
OSTRACODS
BIOTURBATION
PELOID/PELLET
CLOTTED FABRIC
INTRACLASTS
STROMATACTIS?
ALGAL MAT
BURROWS

GREEN CANYON
SECTION 2

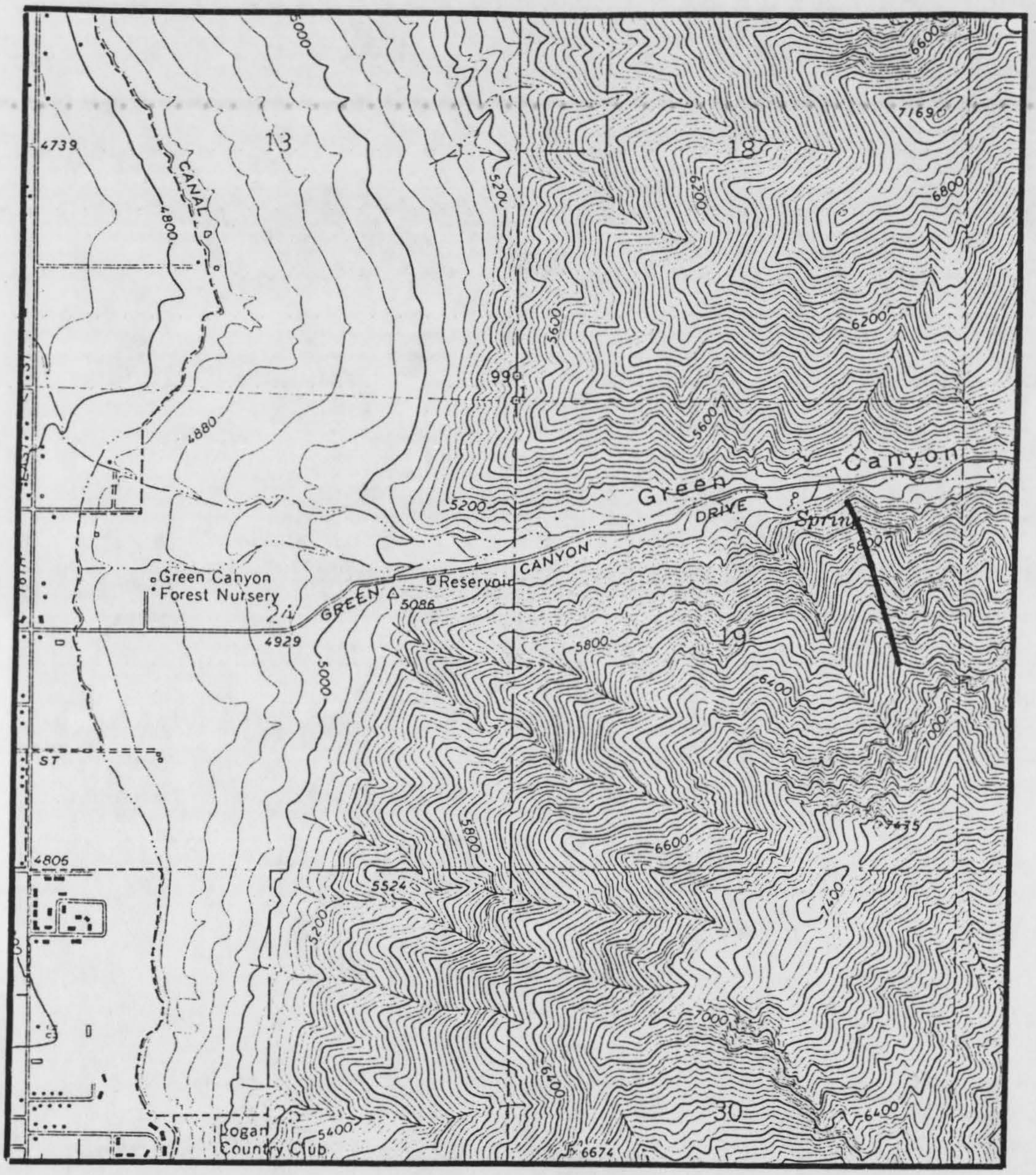

Location: One mile from the mouth of Green Canyon, measured on a north-facing slope, NE 1/4, Sec 19, T. 12 N., R. 2 E. (Smithfield 7 1/2 minute quadrangle).

Swan Peak Formation

Abrupt contact

Garden City Formation

	Thickness in feet	and (meters)
Covered, sandy mudstone limestone float, dug to contact with sandy shale	6	(1.8)
Fine- to coarse-grained, fossiliferous limestone, silty wavy partings, burrowed, laterally irregularly alternating to dolostone, horizontal calcite veins (stromatactics ?)	15	(4.6)
Crystalline dolostone with some calcite nodules and veins (stromatactics ?)	15	(4.6)
Mixed, fine- to coarse-grained limestone with scattered fossils and silty wavy partings, some calcite veins . .	89	(27.1)
Fine-grained limestone with scattered fossils, burrowed, black chert in nodules and stringers decreasing in amount upwards, few silty partings . . .	64	(19.6)
Black banded and anastomosing chert, comprises ~40% of the rock, limestone between the chert is fine-grained with some fossil fragments	27	(8.3)
Fossiliferous, fine-grained limestone with silty wavy partings between banded black chert, chert comprises ~15% of the rock	52	(15.8)
Thin-bedded, very fossiliferous limestone, very fossiliferous	49	(14.9)
Covered slope	21	(6.4)
Fine-grained, nodular silty limestone with trace fossils	2	(0.6)
Covered slope	5	(1.5)
Intraformational conglomerate limestone with large bladed intraclasts in a fossil groundmass, some imbrication, erosional surfaces, interbedded with nodular silty limestone with some burrows and trace fossils	7	(2.1)
Covered slope	8	(2.4)

	Thickness in feet	and (meters)
Mixed, fine-grained and fossiliferous limestone with some scattered intraclasts, thin-bedded, silty partings, burrowed, grades to nodular fine-grained silty limestone	11	(3.4)
Covered slope	41	(12.5)
Thin-bedded, fossiliferous limestone with some intraclasts, wavy silty partings, very burrowed, grades to fine-grained nodular silty limestone	6	(1.8)
Covered slope	40	(12.2)
Intraformational conglomerate layers and lenses, interbedded with thick-bedded, mixed, fine- to coarse-grained limestone with some lenses of fossil hash and small intraclasts, burrowed, interbedded with fine-grained nodular to planar-laminated limestone with trace fossils and some possible ripple marks, scattered black chert nodules .	366	(111.6)
Fine-grained, nodular silty limestone interbedded with fossil hash and intraformational conglomerate, some green shale in layers from 1 to 3 cm thick, burrowed, trace fossils and some possible ripple marks, scattered grey chert in nodules and stringers	76	(23.2)
Low angle bedding plane fault, covered slope	15	(4.6)
Thin- to thick-bedded intraformational conglomerate with large and small intraclasts in a fossiliferous groundmass, interbedded with nodular to planar-laminated, fine- to course-grained limestone. Mud mounds covered by fossil hash appear at 76.2 meters, gastropods common at 87.2 meters	83	(25.3)
Fine-grained, nodular silty limestone, thin- to thick-bedded with trace fossils and possible ripple marks, interbedded with intraformational conglomerate layers and lenses 30.5 to 254 cm thick, gradational to abrupt and erosional contacts, scattered chert nodules and stringers	104	(31.7)
Covered slope	20	(6.1)
Mixed, fine- to coarse-grained limestone with intraformational conglomerate layers and small lenses, scattered fossils, banded black chert at 27.9 meters .	42	(12.8)

	Thickness in feet	and (meters)
Fine-grained, nodular silty to coarse-grained, planar-laminated limestone, interbedded with intraformational conglomerate in a fossiliferous groundmass in lenses, some burrows, trace fossils, scattered black chert nodules, 5 cm of green shale at 14.3 meters	43	(13.1)
Very thin- to thin-bedded, coarse-crystalline dolostone with greyish pink chert nodules and bands, interbedded with nodular silty limestone with fossiliferous lenses	8	(2.4)
Fine- to coarse-grained limestone with scattered fossils alternating irregularly laterally with dolostone. Few lenses of intraformational conglomerate with large, bladed intraclasts, abrupt and erosional contacts	6	(1.8)
Laminated to thin-bedded silty dolostone, black chert in elongated nodules, basal, very thin calcareous shaly limestone layer	4	(1.2)
Total	1225	(373.4)

Disconformity

Saint Charles Formation

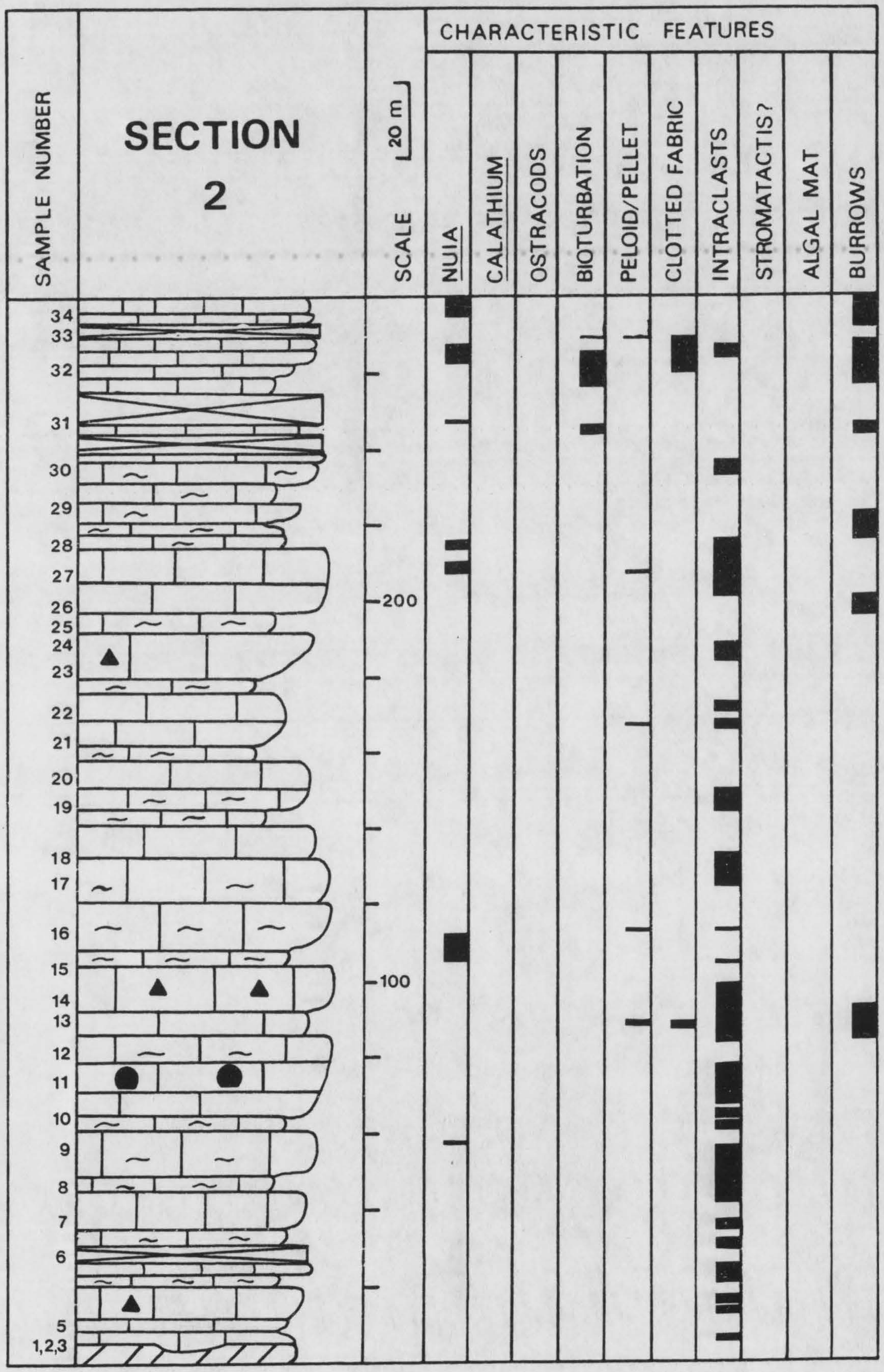
SAMPLE NUMBER
SECTION
2
SCALE
20 m
CHARACTERISTIC FEATURES
NUIA
CALATHIUM
OSTRACODS
BIOTURBATION
PELOID/PELLET
CLOTTED FABRIC
INTRACLASTS
STROMATACTIS?
ALGAL MAT
BURROWS
34
33
32
31
30
29
28
27
26
25
24
23
22
21
20
19
18
17
16
15
14
13
12
11
10
9
8
7
6
5
1,2,3
200
100

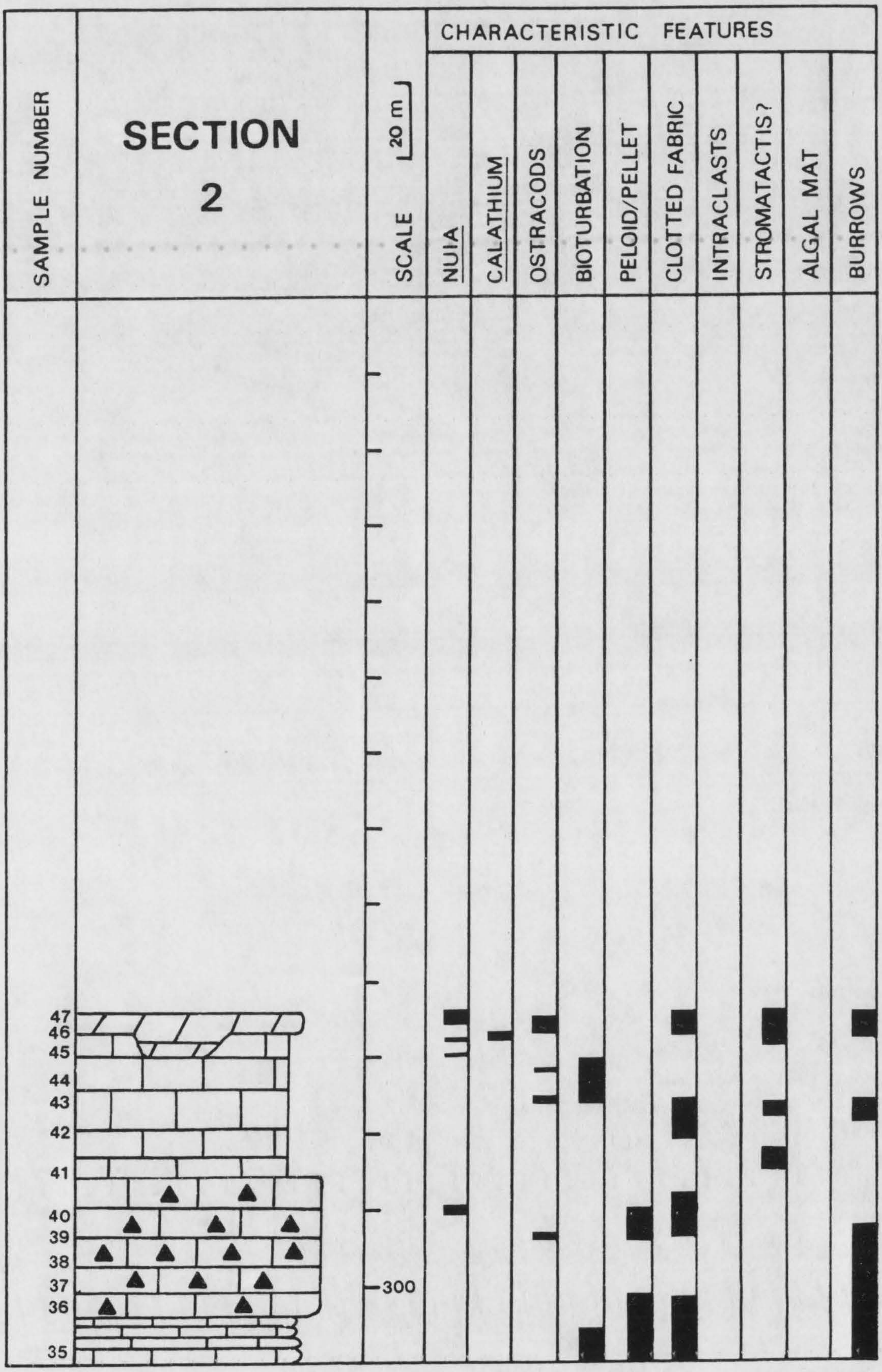

SAMPLE NUMBER
SECTION 2
SCALE
20 m
CHARACTERISTIC FEATURES
NUIA
CALATHIUM
OSTRACODS
BIOTURBATION
PELOID/PELLET
CLOTTED FABRIC
INTRACLASTS
STROMATACTIS?
ALGAL MAT
BURROWS
47
46
45
44
43
42
41
40
39
38
37
36
35
300

HIGH CREEK
SECTION 3

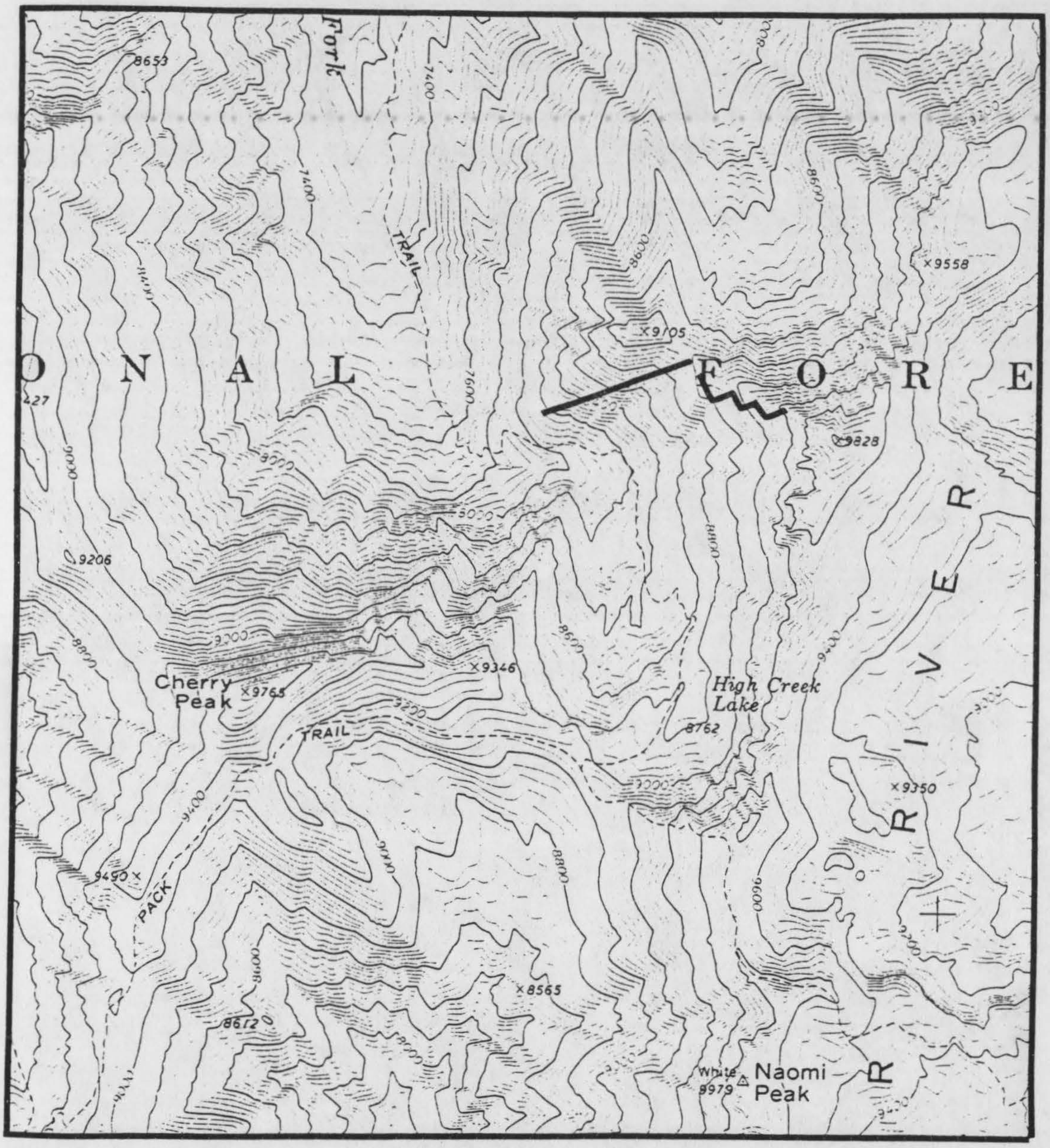

Location: Four miles up High Creek trail, composite section measured on southwest-facing slopes (Naomi Peak 7 1/2 minute quadrangle).

Swan Peak Formation

Abrupt contact

Garden City Formation

	Thickness in feet	and (meters)
Fine-grained, arenaceous limestone with fossil fragments, laterally irregular contact to dolostone . .	3	(0.9)
Thin- to thick-bedded, crystalline dolostone with fossil fragments, some burrowing and wavy silty partings, scattered black chert nodules	48	(14.6)
Fine-grained limestone with coarse-grained lenses, scattered fossils, laterally and vertically irregular contact with dolostone	3	(0.9)
Thin- to thick-bedded, crystalline dolostone with fossil fragments, wavy silty partings, some burrowing	14	(4.3)
Covered slope	16	(4.9)
Massive to thick-bedded beds of fine- to coarse-grained limestone, silt blebs and partings, scattered fossils, gastropod-rich lense at 441.6 meters	5	(1.5)
Covered slope	19	(5.8)
Thin- to thick-bedded, fine- to coarse-grained limestone with scattered fossils, silty wavy partings with a gradational decrease of silt upwards	25	(7.6)
Covered slope	23	(7.0)
Thin-bedded, mixed, fine- to coarse-grained limestone with scattered fossils, wavy silty partings and ~5% nodular black chert	10	(3.1)
Covered slope	7	(2.1)
Mixed, coarse- to fine-grained fossiliferous limestone, burrowed with lenses of nodular to coarse-grained, planar-laminated limestone, nodular and banded black chert comprises ~30% of the rock	69	(21.0)
Nodular to planar-laminated limestone and dolostone with lenses of intraformational conglomerate, scattered fossils, burrowed, nodular and banded black chert comprises ~20% of the rock	11	(3.3)

	Thickness in feet and (meters)	
Banded and anastomosing white chert which comprises ~50% of the rock with dolostone, planar-laminated, silty limestone with fossils and intraformational conglomerate in between	10	(3.1)
Fine- to coarse-grained, planar-laminated limestone with fossils and some intraformational conglomerate layers between varying amounts (30-60%) of white and black nodular to banded and anastomosting chert	74	(22.5)
Thin- to thick-bedded, fossiliferous, mixed, fine- to coarse-grained limestone with varying amounts (5-20%) of nodular and banded black chert, few dasycladacean fossils seen	66	(20.1)
Fine-grained with some coarse-grained lenses, fossiliferous, thin-bedded, silty limestone, burrowed .	30	(9.1)
Thick-bedded, fine-grained, fossiliferous limestone, wavy silty partings, burrowed, dasycladacean algae is predominate fossil	10	(3.1)
Thin-bedded limestone fossil hash with some intraclasts and lenses of coarse-grained, planar-laminated limestone, interbedded with intraformational conglomerate in a fossiliferous groundmass, silty wavy partings, burrowed, gradational to abrupt contacts, gastropod-rich at 362.7 meters	65	(19.8)
Silty, nodular to coarse-grained, planar-laminated, sometimes burrowed limestone with trace fossils, from 15 cm to 2.7 m thick, interbedded with intraformational conglomerate, rounded to occasional bladed intraclasts in a fossiliferous groundmass, interbedded with thick-bedded beds of fine-grained limestone with scattered fossils, burrowed, silty wavy partings. Occasional black chert nodules found throughout, contacts are abrupt and erosional with a few gradational. Green calcareous shale layers from 2 to 30 cm thick at 174.9, 158.5, 148.1, 146.3, 140.2, and 135.0 meters	685	(208.8)
Coarse-grained, very fossiliferous (fossil hash) limestone with some intraclasts, burrowed, interbedded with some fine-grained, silty, nodular to planar-laminated limestone and layers of intraformational conglomerate, contacts are abrupt to erosional. Mud mounds with channels eroded in them appear at		

	Thickness in feet and (meters)	
117.3 meters. Mud mounds draped by nodular to planar-laminated limestone or fossil hash at 88.4, 86.7, and 75.3 meters	228	(69.6)
Intraformational conglomerate layers and lenses are interbedded with nodular to planar-laminated limestone, some fossil hash in layers and lenses, occasional grey chert nodules, many erosional contacts, some burrowing	72	(21.9)
Intraformational conglomerate limestone layers with large bladed intraclasts set in a fossiliferous groundmass with many erosional contacts, interbedded with nodular silty limestone with some fossil hash lenses, and thin fossil hash layers	31	(9.5)
Fine-grained, silty, nodular limestone with trace fossils, interbedded with few intraformational conglomerate layers and lenses	14	(4.4)
Nodular to planar-laminated limestone layers with some trace fossils, interbedded with intraformational conglomerate lenses with large bladed intraclasts set in a fossiliferous groundmass, many erosional contacts, interbedded with fossil hash and mixed fossil hash and fine-grained limestone	49	(14.9)
Covered slope	9	(2.7)
Thin-bedded, planar-laminated limestone with coarse-grained and fossiliferous lenses, wavy silty partings .	20	(6.1)
Intraformational conglomerate with large bladed intraclasts which changes laterally irregularly to dolostone	2	(0.6)
Silty, nodular limestone with lense of fossil hash . .	7	(2.1)
Crystalline, laminated dolostone interbedded with some intraformational conglomerate, silty partings, white to grey chert nodules and stringers, basal, thin (4 cm) calcareous shaly limestone layer	8	(2.4)
Total	1633	(494.7)

Disconformity

Saint Charles Formation

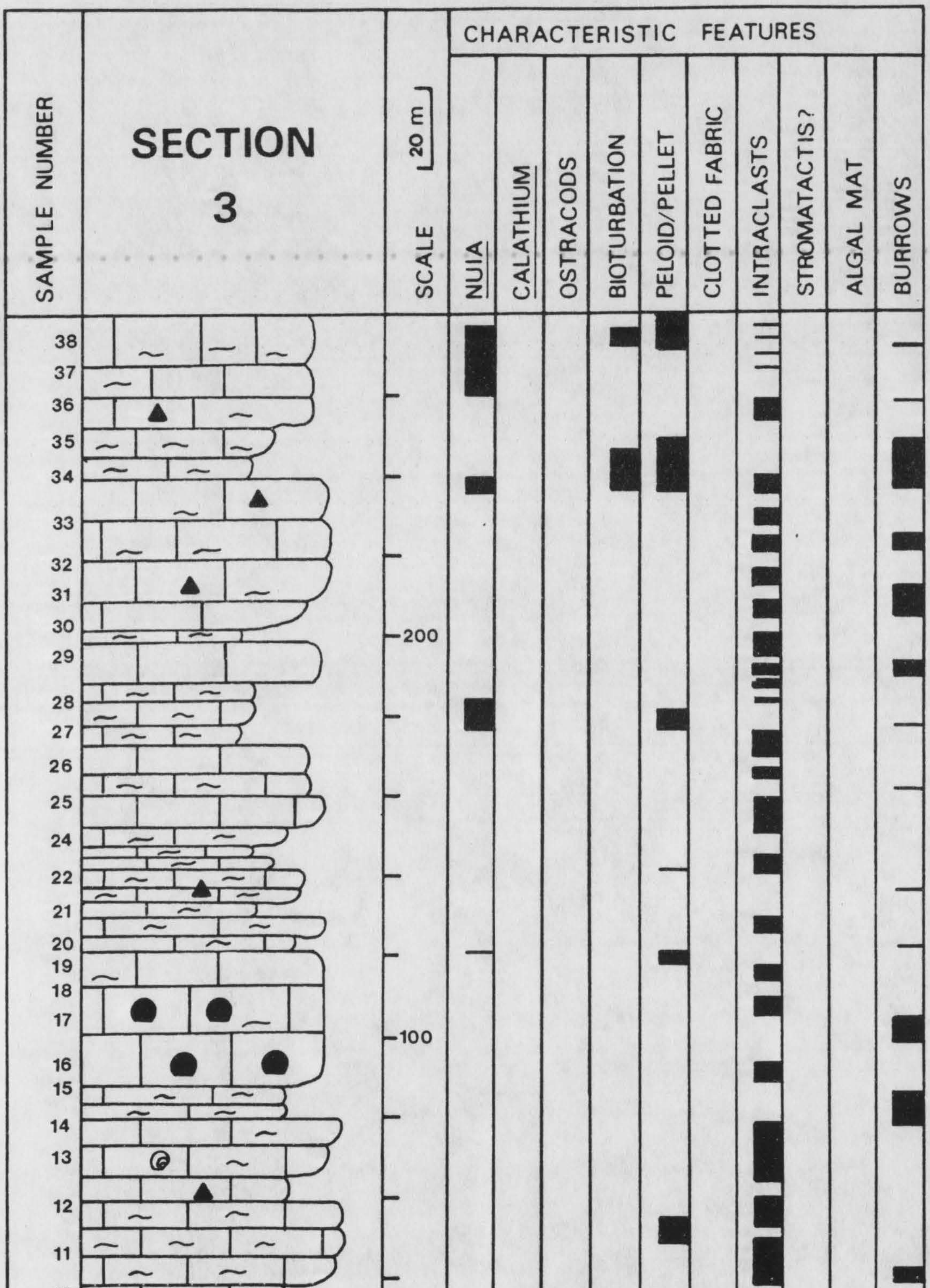
SAMPLE NUMBER
SECTION 3
SCALE
20 m
CHARACTERISTIC FEATURES
NUIA
CALATHIUM
OSTRACODS
BIOTURBATION
PELOID/PELLET
CLOTTED FABRIC
INTRACLASTS
STROMATACTIS?
ALGAL MAT
BURROWS
38
37
36
35
34
33
32
31
30
29
28
27
26
25
24
22
21
20
19
18
17
16
15
14
13
12
11
10
9
7
6
5,4
2,3,1
200
100

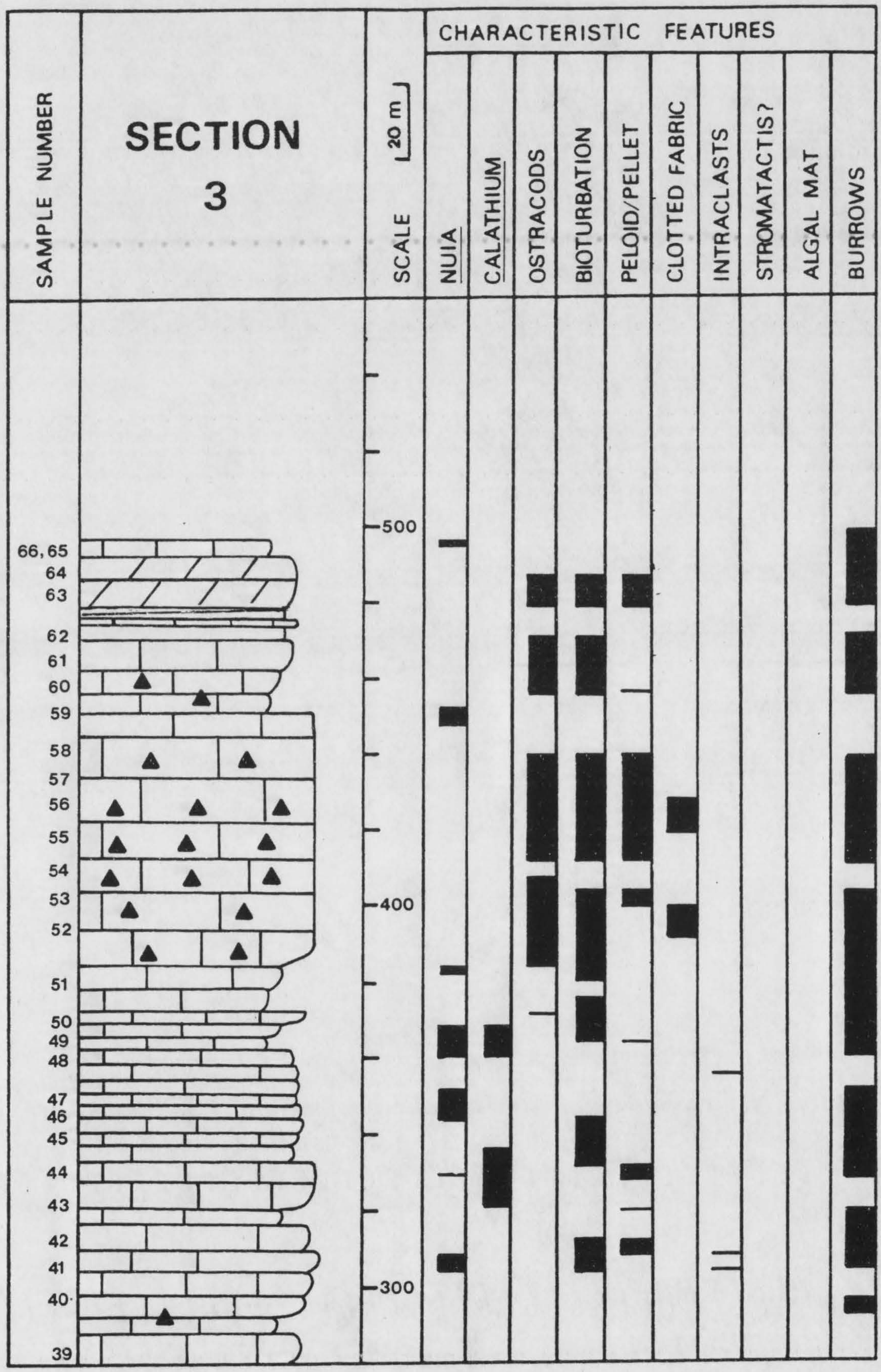
SAMPLE NUMBER
SECTION 3
SCALE
20 m
CHARACTERISTIC FEATURES
NUIA
CALATHIUM
OSTRACODS
BIOTURBATION
PELOID/PELLET
CLOTTED FABRIC
INTRACLASTS
STROMATACTIS?
ALGAL MAT
BURROWS
500
400
300
66, 65
64
63
62
61
60
59
58
57
56
55
54
53
52
51
50
49
48
47
46
45
44
43
42
41
40
39

MANTUA
SECTION 4

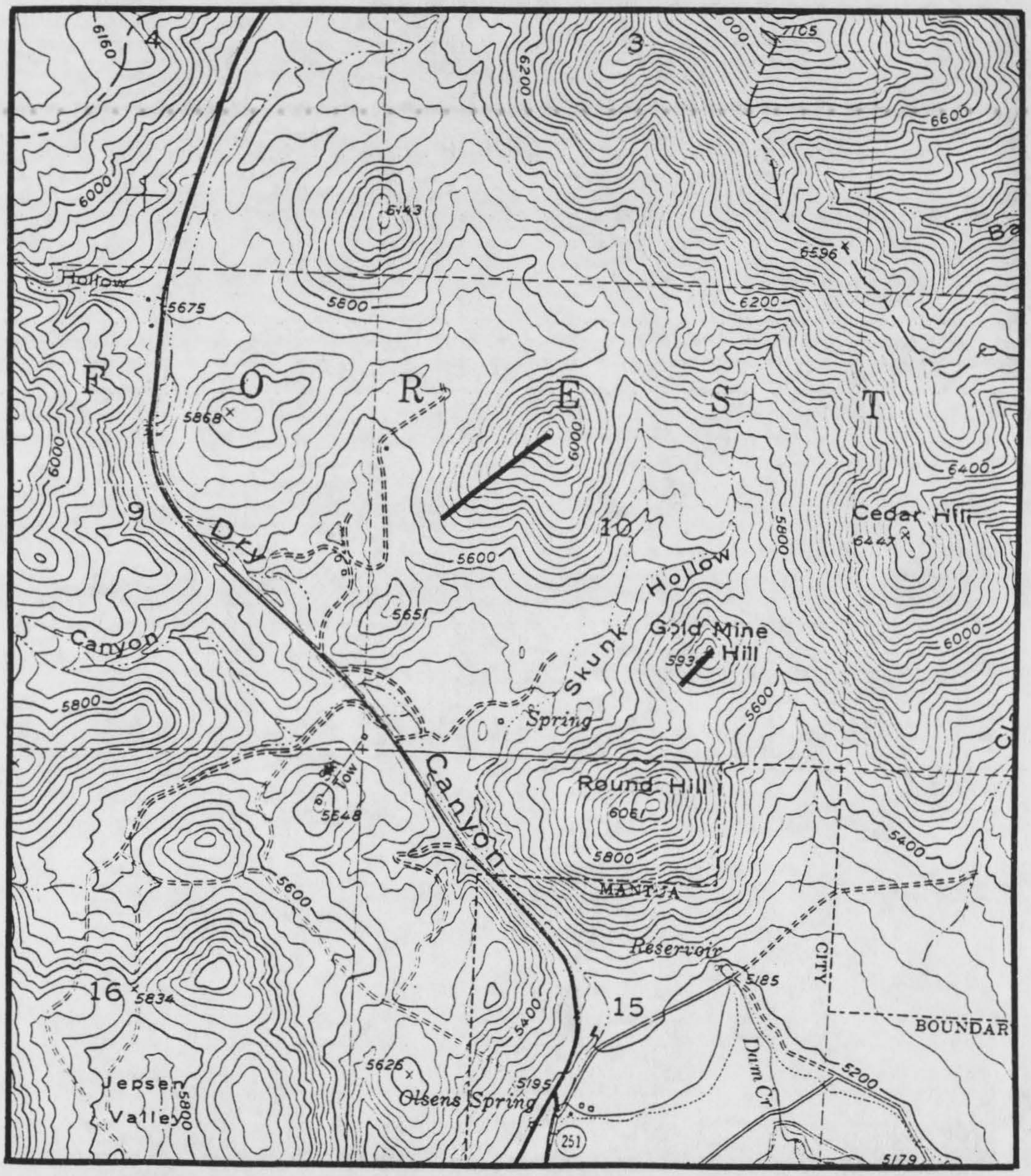

Location: Gold Mine Hill and the hill northwest of Gold mine Hill, composite section measured on southwest-facing slopes, Sec 10, T. 9 N., R. 1 W. (Mount Pisgah 7 1/2 minute quadrangle).

Swan Peak Formation

Abrupt contact

Garden City Formation

	Thickness in feet	and (meters)
Crystalline dolostone, scattered fossil fragments, mottled. silty wavy partings, coarse-grained lenses, occasional black chert nodules, gradational variation in the amount of silt, horizontal calcite veins (stromatactis ?) at 419.1 meters recurring upwards . .	141	(43.0)
Laterally irregular contact to fine-grained, fossiliferous, burrowed limestone with coarse-grained lenses, silty wavy partings, erosional contacts, ~2% nodular black chert, gastropod-rich layers, possible peloid layer at 379.5 meters	45	(13.7)
Fine- to coarse-grained, burrowed limestone with scattered fossils and silty blebs, erosional to abrupt contacts, varying amounts of banded and nodular black chert comprising ~20-30% of the rock	29	(8.8)
Fine- to coarse-grained, burrowed limestone with scattered fossils and silt blebs with banded to anastomosing black chert which comprises ~40% of the rock	26	(7.9)
Fine- to coarse-grained, fossiliferous limestone burrowed, wavy silty partings, varying amounts (5-10%) of black banded and nodular chert	50	(15.2)
Thin- to thick-bedded, fine- to coarse-grained, fossil-rich, burrowed limestone, silty blebs and wavy partings, erosional to abrupt contacts	45	(13.7)
Thin-bedded, very fossiliferous (fossil hash), burrowed limestone, wavy silty partings, lenses of planar-laminated to hummocky cross-stratified limestone. Fossil hash has some intraclasts, cross-bedding, numerous dasycladacean fossils and gastropods, contacts abrupt and erosional	125	(38.1)
Fine-grained, nodular to planar-laminated, silty limestone, burrowed, trace fossils, scattered fossil fragments, interbedded with intraformational conglomerate layers and lenses with small, round intraclasts set in a fossil groundmass, some are burrowed, abrupt, erosional to gradational		

	Thickness in feet	and (meters)
contacts, varying amounts of silt, occasional black chert nodules	135	(41.2)
Intraformational conglomerate limestone layers and lenses, rounded to some bladed intraclasts in a fossil groundmass, interbedded with nodular to planar-laminated limestone. from 15 cm to 2.7 m thick, burrowed, varying amounts of silt, some cross-bedding, rare possible mudcracks (?), abrupt to erosional contacts, calcareous shale, from 4 to 30.5 cm thick at 179.8, 120.4, and 117.0 meters	540	(164.7)
Very fossiliferous (fossil hash), burrowed limestone, interbedded with intraformational conglomerate lenses and layers, interbedded with silty, planar-, thin-bedded, coarse-grained limestone, contacts are abrupt and erosional. Mud mounds covered with fossil hash appear at 67.1, 65.5, 57.9, and 56.4 meters	85	(25.9)
Fine- to coarse-grained limestone, burrowed, scattered fossils, lenses of planar-bedded limestone, interbedded with silty, nodular limestone. Mud mounds draped by silty, planar to nodular limestone appear at 54.9 meters	20	(6.1)
Intraformational conglomerate lenses and layers with large bladed intraclasts, in some lenses intraclasts are imbricated, cross-bedding, many abrupt and erosional contacts, especially within conglomerate layers, interbedded with coarse-grained, planar-, very thin-bedded silty limestone	139	(42.4)
Covered slope	3	(0.9)
Coarse-crystalline dolostone alternating irregularly with fine-grained limestone, some intraformational conglomerate, greyish pink chert in nodules and stringers	11	(3.3)
Very thin-bedded crystalline dolostone, irregularly changing to fine-grained limestone, ~10-20% banded greyish orange chert	7	(2.1)

	Thickness in feet and (meters)
Coarse-crystalline dolostone with greyish pink banded chert, basal 8 cm layer of very silty limestone	5 (1.5)
Total	1406 (428.5)

Disconformity

Saint Charles Formation

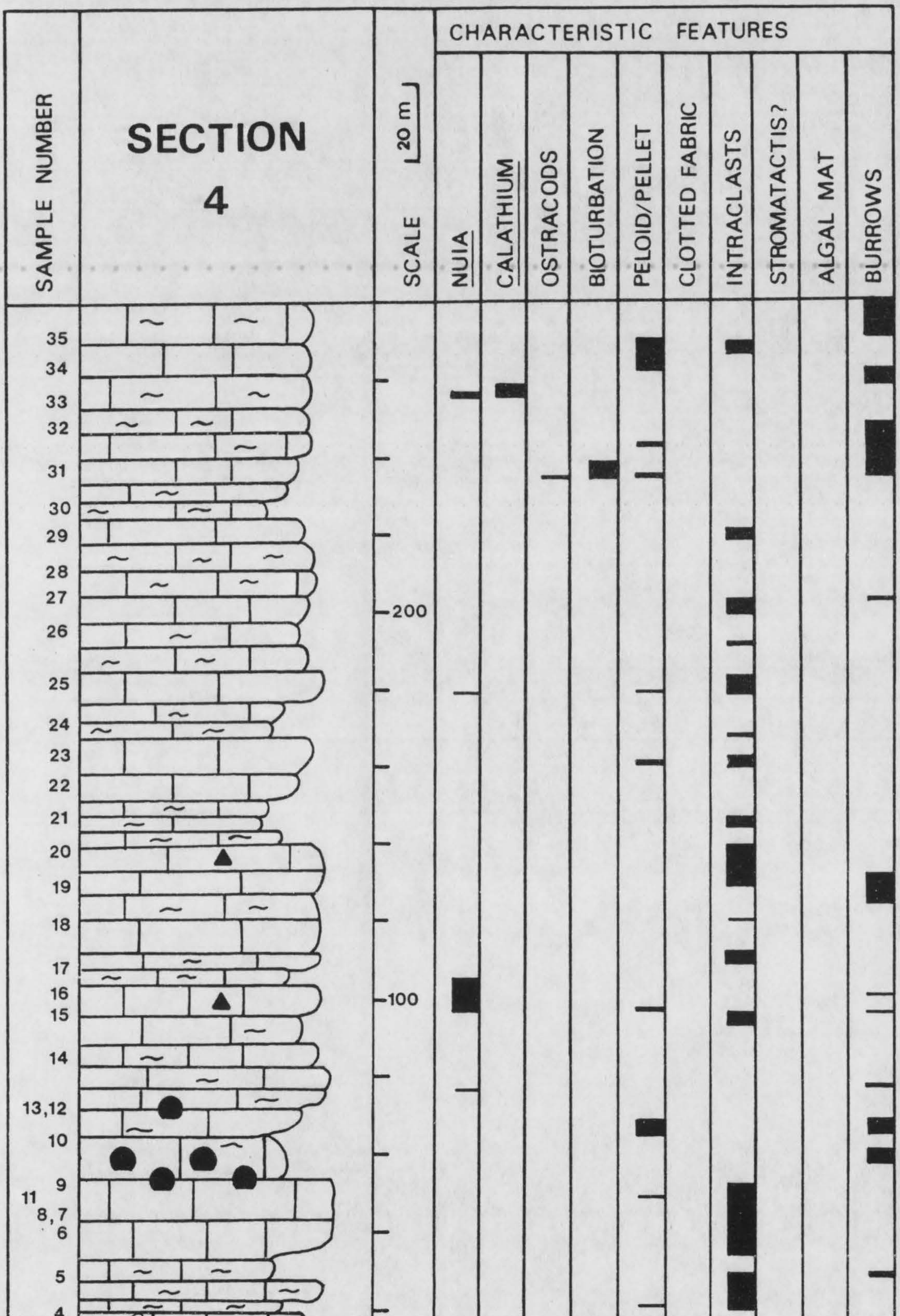
SAMPLE NUMBER
SECTION 4
SCALE
20 m
CHARACTERISTIC FEATURES
NUIA
CALATHIUM
OSTRACODS
BIOTURBATION
PELOID/PELLET
CLOTTED FABRIC
INTRACLASTS
STROMATACTIS?
ALGAL MAT
BURROWS
35
34
33
32
31
30
29
28
27
26
25
24
23
22
21
20
19
18
17
16
15
14
13,12
10
9
11
8,7
6
5
4
3
2,1
200
100

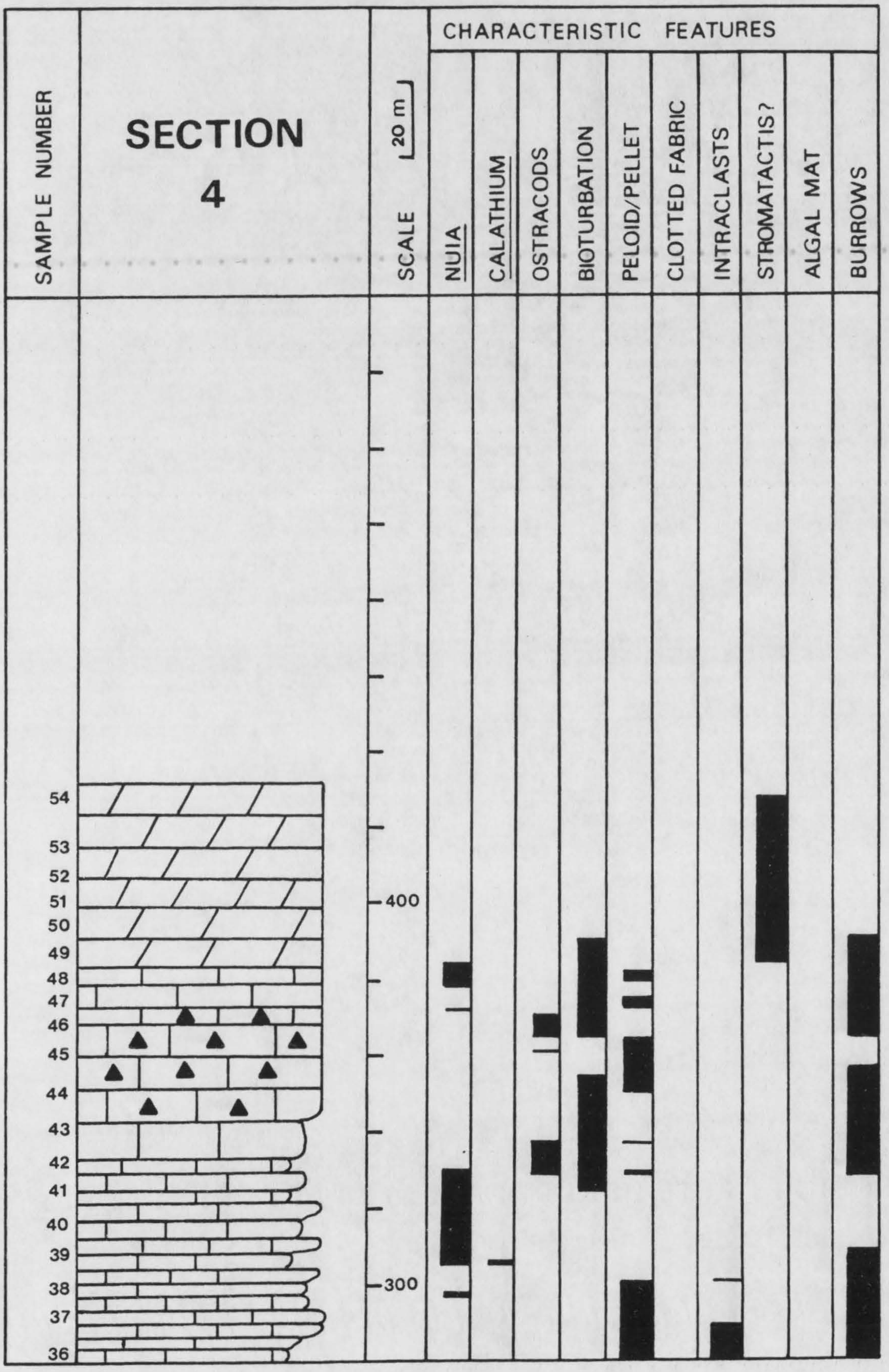
SAMPLE NUMBER
SECTION 4
SCALE
20 m
CHARACTERISTIC FEATURES
NUIA
CALATHIUM
OSTRACODS
BIOTURBATION
PELOID/PELLET
CLOTTED FABRIC
INTRACLASTS
STROMATACTIS?
ALGAL MAT
BURROWS
54
53
52
51
50
49
48
47
46
45
44
43
42
41
40
39
38
37
36
400
300

WELLSVILLE
SECTION 5

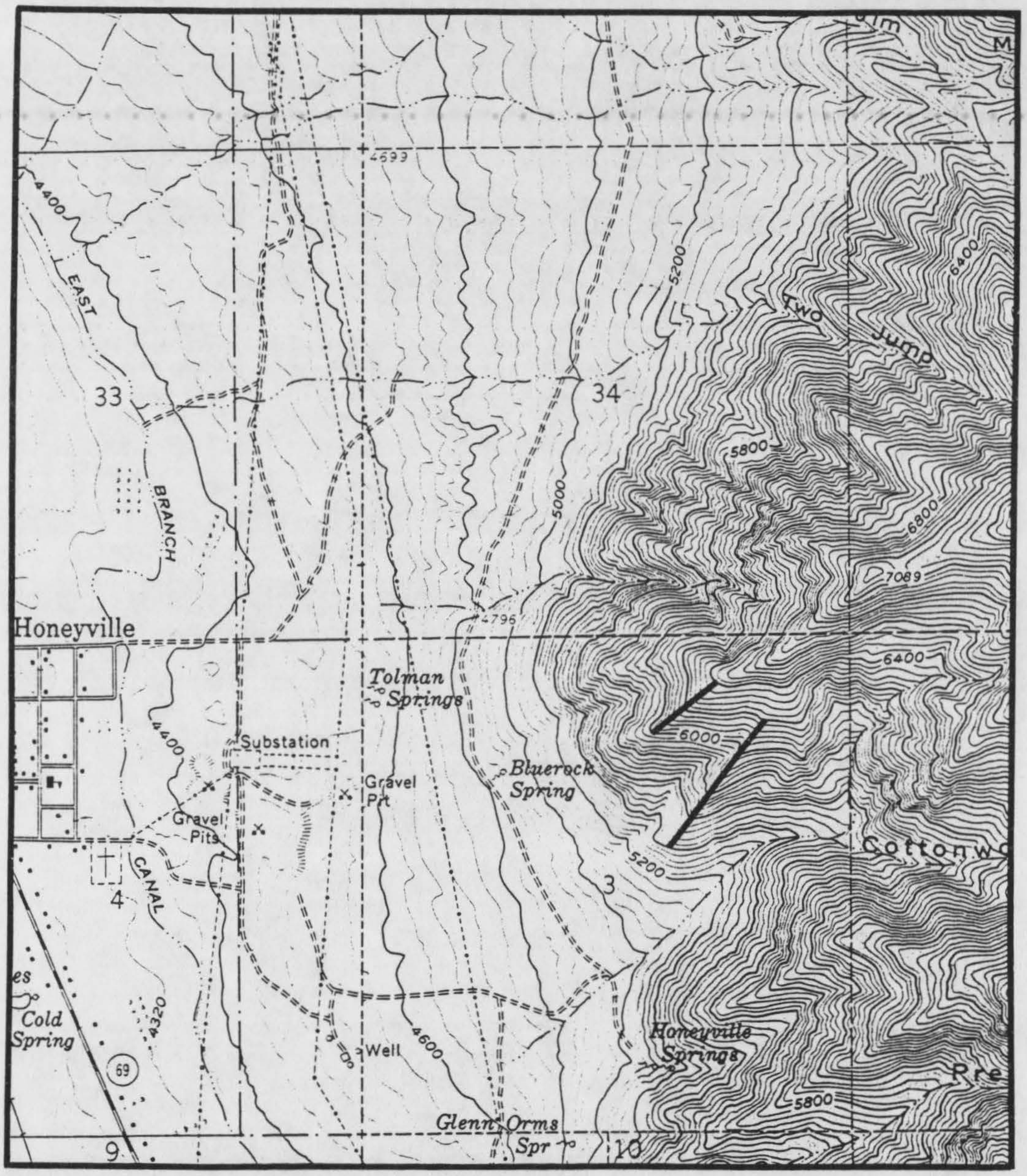

Location: Mouth of Cottonwood Canyon, east of Honeyville, Wellsville Mountain, composite section measured on southwest-facing slopes, NE 1/4, sec. 3, T. 10 N., R. 2 W. (Honeyville 7 1/2 minute quadrangle).

Swan Peak Formation

Abrupt contact

Garden City Formation

	Thickness in feet and (meters)	
Coarse- to medium-crystalline dolostone, faintly mottled and burrowed, wavy silty partings, few small intraformational conglomerate lenses, scattered grey chert nodules, recurring horizontal calcite veins (stromatactis ?)	66	(20.1)
Fine- to medium-crystalline limestone with silty wavy partings, few burrows	5	(1.5)
Coarse- to medium-crystalline dolostone, faintly mottled and burrowed, wavy silty partings, few small intraformational conglomerate lenses, scattered black chert nodules, recurring horizontal calcite veins (stromatactis ?)	46	(14.0)
Thin- to thick-bedded limestone, scattered fossils and small intraclasts, fine-grained with coarse-grained lenses, burrowed, silty wavy partings with varying amounts (1-10%) of black banded and nodular chert . . .	63	(19.2)
Fine-grained, nodular to coarse-grained planar-laminated limestone with thin very fossiliferous, burrowed layers	9	(2.7)
Banded and anastomosing black chert, makes up ~40% of the rock with mixed, fine- to medium-grained, fossiliferous limestone between chert	31	(9.4)
Mixed, medium- to coarse-grained limestone with fossiliferous lenses, silty wavy partings increasing towards the bottom, ~5% nodular to banded black chert, many erosional contacts	34	(10.4)
Coarse- to fine-grained limestone with fossiliferous lenses, some silty blebs, erosional contacts, burrowed with rare black chert nodules, interbedded with very silty, planar-laminated, burrowed limestone, with trace fossils	94	(28.7)
Thin-bedded, very fossiliferous, coarse-grained limestone with some planar-laminated, very burrowed lenses, silty wavy partings, few dasycladacean fossils .	37	(11.3)

	Thickness in feet and (meters)	
Thin-bedded, mixed, fine-grained and fossil-rich with small intraclast intraformational conglomerate limestone, silty blebs and partings, gradational to abrupt and erosional contacts, interbedded with thin lenses of coarse-grained, planar-laminated to hummocky cross-stratified limestone with some burrowing	215	(65.5)
Intraformational conglomerate limestone layers and lenses, from 15 cm to 46 cm thick, with large bladed to small, irregular shaped intraclasts in a fossil background, interbedded with 15 cm to 3 m thick, nodular to coarse- to fine-grained, planar-laminated limestone, burrowed with varying amounts of silt, interbedded with olive green limy shale, from 30 cm to 1.2 m thick. Some gradational but mostly abrupt and erosional contacts, some hummocky cross-stratification and burrowing in conglomerate and fossiliferous layers. Increasing amounts of banded and nodular black chert near top	348	(106.1)
Thin- to thick-bedded beds of fossil hash with lenses of intraformational conglomerate, some burrowing and silty partings, abrupt to gradational contacts to nodular to planar-laminated, silty limestone, interbedded with massive, fine- to coarse-grained, burrowed limestone with wavy silty partings, mud mounds covered with fossil hash at 120.7, 87.8, and 68.9 meters, there are scattered rare nodules of black chert throughout	249	(75.9)
Large intraclast, bladed, intraformational conglomerate limestone lenses and layers with numerous erosional surfaces, gradational to abrupt contacts, interbedded with massive, fine- to coarse-grained limestone, interbedded with nodular to planar-laminated, silty limestone, some burrowing, hummocky cross-stratification, graded bedding, some scattered banded to nodular grey chert	153	(46.7)
Coarse-crystalline dolostone with irregular contacts to limestone	3	(0.9)
Covered slope	5	(1.5)
Coarse-crystalline dolostone with pink chert nodules and silty partings	3	(0.9)
Large intraclast intraformational conglomerate lenses		

	Thickness in feet and (meters)	
in mixed, coarse- to fine-grained limestone with pink chert nodules	10	(3.1)
Coarse-crystalline, laminated dolostone with pink chert, irregular contacts to limestone, basal 1 cm layer of very silty limestone	2	(0.6)
Total	1373	(418.5)

Disconformity

Saint Charles Formation

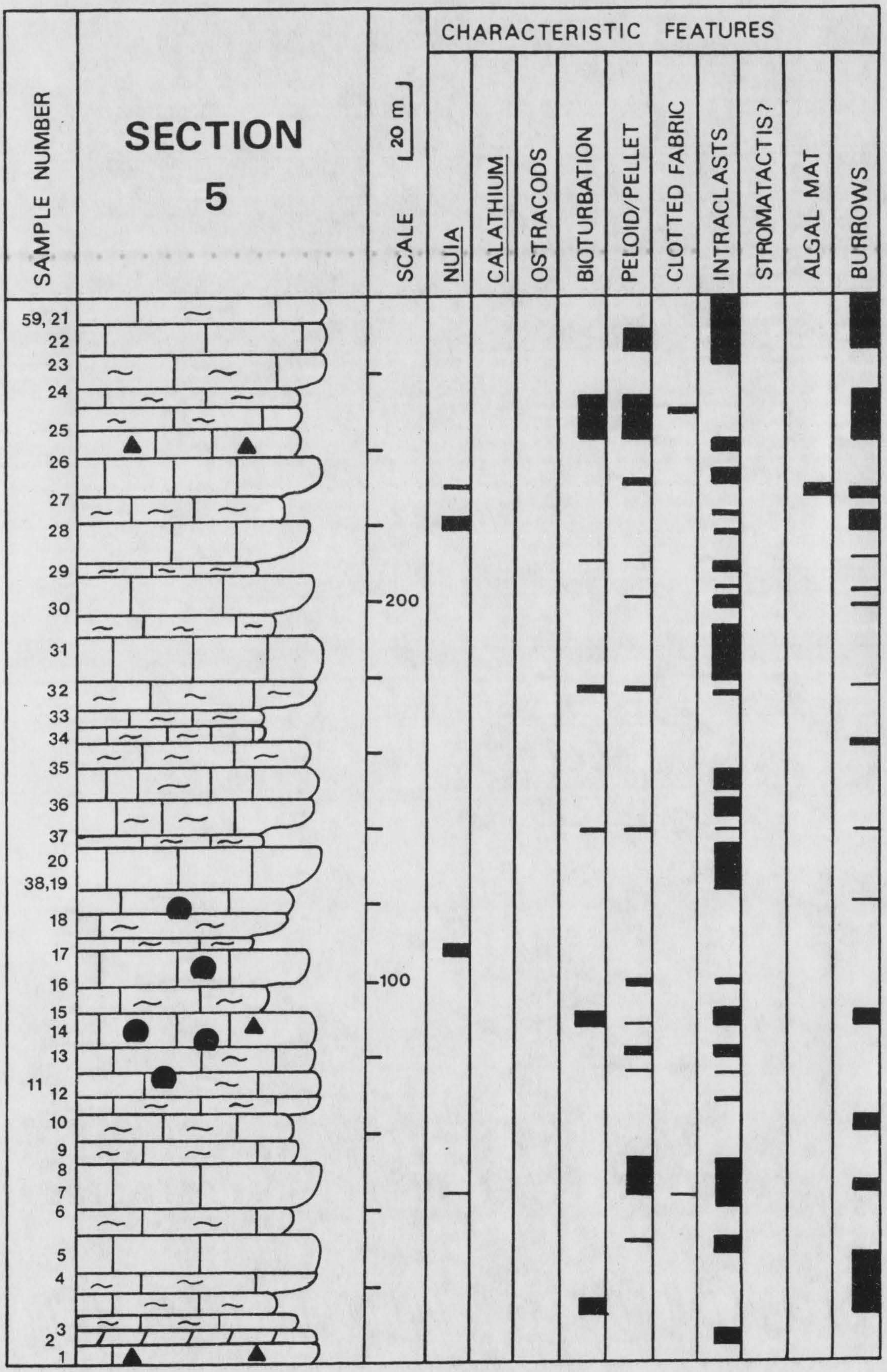
SAMPLE NUMBER
SECTION
5
SCALE
20 m
CHARACTERISTIC FEATURES
NUIA
CALATHIUM
OSTRACODS
BIOTURBATION
PELOID/PELLET
CLOTTED FABRIC
INTRACLASTS
STROMATACTIS?
ALGAL MAT
BURROWS
59, 21
22
23
24
25
26
27
28
29
30
31
32
33
34
35
36
37
20
38,19
18
17
16
15
14
13
11
12
10
9
8
7
6
5
4
2
3
1
200
100

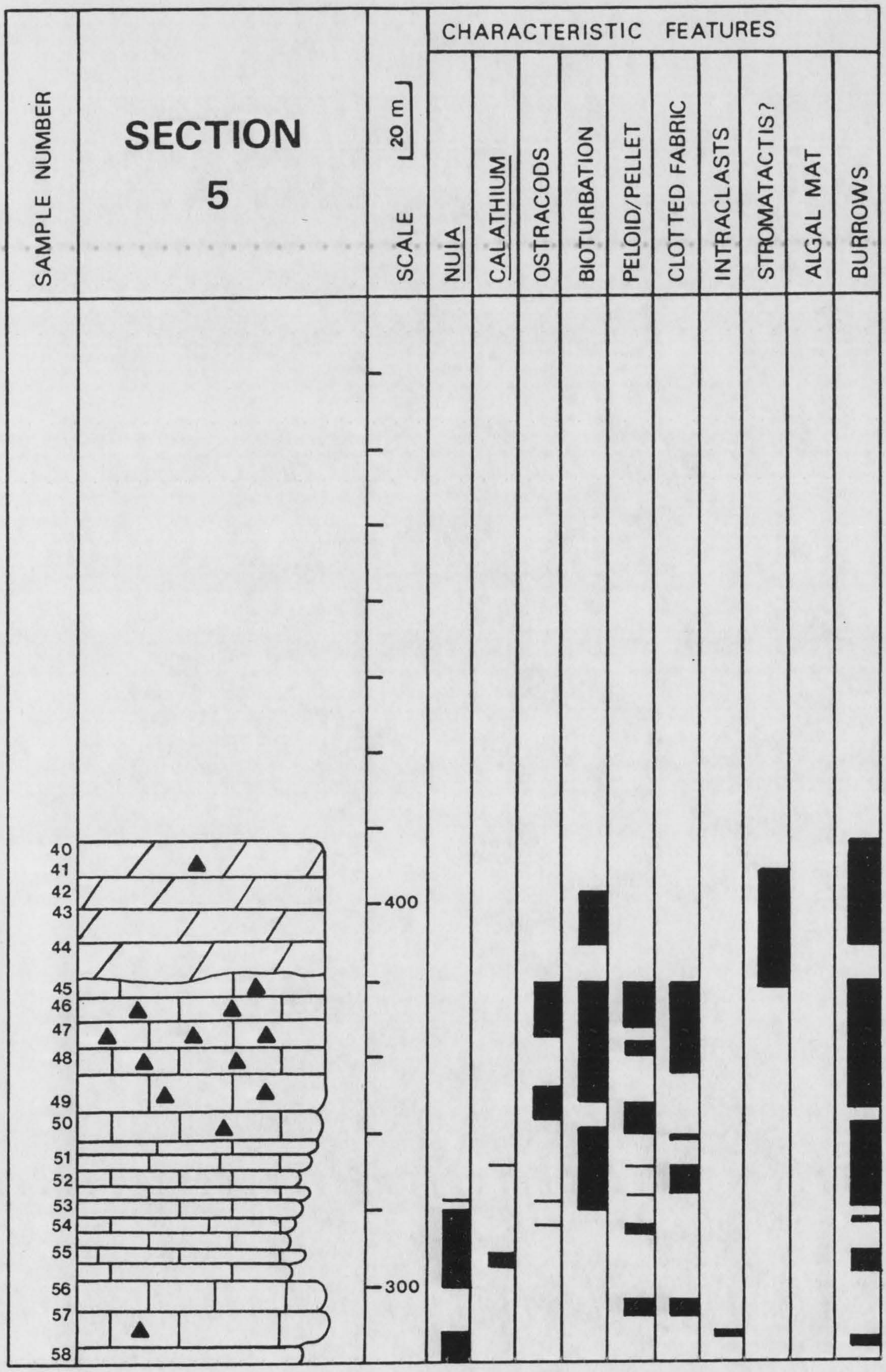
SAMPLE NUMBER
SECTION 5
SCALE
20 m
CHARACTERISTIC FEATURES
NUIA
CALATHIUM
OSTRACODS
BIOTURBATION
PELOID/PELLET
CLOTTED FABRIC
INTRACLASTS
STROMATACTIS?
ALGAL MAT
BURROWS
400
300
40
41
42
43
44
45
46
47
48
49
50
51
52
53
54
55
56
57
58

Appendix C

Point Count Data

Explanation

Thin section numbers followed by an asterisk (*) were point counted with a minimum of 300 points. All other thin sections were estimated using estimation charts from Flugel (1982). The data are listed as percentages. The term bioclast refers to unidentified fossil fragments.

ALLOCHEMS	THIN SECTION						
	HC-01*	HC-02*	HC-03*	HC-04A*	HC-04C*	HC-05*	HC-06*
Conodonts	00	00	00	01	00	00	00
Brachiopods	00	00	00	00	02	00	00
Pelmatozoans	05	00	00	04	25	00	04
Gastropods	00	00	00	00	00	00	00
Lingula	00	01	00	01	01	00	01
Bioclasts	00	01	00	01	04	11	02
Trilobites	06	00	00	06	06	00	03
Ostracods	00	00	00	00	00	00	00
Nuia	00	00	00	00	00	00	00
Molluscs	00	00	00	00	05	00	06
Sponge Spicules	00	00	00	00	00	00	00
Calathium	00	00	00	00	00	00	00
Peloids	00	00	00	00	10	00	06
Intraclasts	10	00	00	00	00	47	04
Quartz Silt	02	02	03	02	00	00	01
Chert	01	00	07	00	00	00	00
Clay/Limonite	02	03	01	00	01	01	01
Sparite	01	00	00	03	20	01	12
Micrite	00	00	00	82	15	00	59
Pyrite/Hematite	01	00	00	00	01	00	00
Dolomite	72	93	89	00	10	40	01

ALLOCHEMS	THIN SECTION						
	HC-07*	HC-09	HC-10*	HC-11*	HC-12	HC-13	HC-14
Conodonts	00	00	00	05	01	01	01
Brachiopods	02	00	00	06	00	00	00
Pelmatozoans	11	42	00	10	05	02	05
Gastropods	00	00	00	00	00	00	00
<u>Lingula</u>	01	01	01	05	01	01	02
Bioclasts	02	01	04	11	02	10	20
Trilobites	03	11	00	00	02	02	00
Ostracods	00	00	00	00	00	00	00
<u>Nuia</u>	00	00	00	00	00	00	00
Molluscs	03	02	00	01	02	05	00
Sponge Spicules	00	00	02	01	02	03	05
<u>Calathium</u>	00	00	00	00	00	00	00
Peloids	00	05	01	11	40	10	00
Intraclasts	50	05	00	00	08	00	00
Quartz Silt	01	01	07	17	06	06	06
Chert	00	00	01	00	00	00	00
Clay/Limonite	01	01	02	03	05	10	10
Sparite	23	26	05	20	18	10	09
Micrite	02	04	76	07	07	38	41
Pyrite/Hematite	01	01	01	03	01	02	01
Dolomite	00	00	00	00	00	00	00

ALLOCHEMS	THIN SECTION						
	HC-15*	HC-16	HC-17*	HC-18*	HC-19*	HC-20*	HC-21*
Conodonts	00	00	00	01	00	00	01
Brachiopods	00	01	00	00	01	00	02
Pelmatozoans	00	12	06	08	06	05	08
Gastropods	00	00	00	00	01	00	00
Lingula	00	00	01	01	00	00	00
Bioclasts	04	06	06	06	04	09	04
Trilobites	00	06	03	01	05	01	03
Ostracods	00	00	00	00	00	00	00
Nuia	00	00	00	00	01	00	14
Molluscs	00	01	02	00	02	00	01
Sponge Spicules	02	02	04	02	00	05	02
Calathium	00	00	00	00	00	00	00
Peloids	01	05	02	02	00	02	05
Intraclasts	00	11	02	00	08	00	04
Quartz silt	01	00	01	02	00	02	02
Chert	00	00	00	00	01	00	00
Clay/Limonite	03	02	02	03	01	04	05
Sparite	05	25	14	21	60	09	22
Micrite	79	28	56	52	07	62	25
Pyrite/Hematite	01	01	01	00	00	01	00
Dolomite	04	00	00	01	03	00	02

ALLOCHEMS	THIN SECTION						
	HC-22*	HC-24	HC-25*	HC-26	HC-27*	HC-28	HC-29*
Conodont	00	00	00	00	00	00	00
Brachiopods	03	00	02	00	01	01	02
Pelmatozoans	15	05	13	15	10	08	13
Gastropods	00	00	00	00	06	00	00
Lingula	00	01	00	01	01	00	01
Bioclasts	02	18	05	09	02	01	03
Triolobites	03	00	03	01	02	02	06
Ostracods	00	00	00	00	00	00	00
Nuia	01	00	00	00	01	01	01
Molluscs	04	00	02	01	02	02	02
Sponge Spicules	00	05	00	02	00	01	00
Calathium	00	00	00	00	00	00	00
Peloids	02	00	02	02	01	00	04
Intraclasts	42	00	36	00	48	60	32
Quartz Silt	01	06	02	12	00	01	01
Chert	00	00	06	00	01	00	01
Clay/Limonite	00	05	01	06	00	00	03
Sparite	27	05	24	05	19	12	17
Micrite	00	55	04	46	05	12	11
Pyrite/Hematite	00	00	00	00	01	00	00
Dolomite	00	00	00	00	00	00	03

ALLOCHEMS	THIN SECTION						
	HC-30	HC-31*	HC-32	HC-33	HC-34*	HC-35	HC-36*
Conodonts	00	01	00	00	00	00	00
Brachiopods	01	01	00	01	00	00	00
Pelmatozoans	12	04	00	11	09	07	01
Gastropods	00	00	00	00	00	00	00
Lingula	00	00	00	00	01	00	00
Bioclasts	00	01	05	00	11	00	03
Trilobites	06	02	00	05	02	02	01
Ostracods	00	00	00	00	00	00	00
Nuia	07	00	00	00	07	00	00
Molluscs	01	01	00	00	00	00	00
Sponge Spicules	00	00	01	00	00	00	03
Calathium	00	00	00	00	00	00	00
Peloids	03	03	00	03	05	25	00
Intraclasts	50	48	00	55	01	00	00
Quartz Silt	01	00	00	00	01	04	01
Chert	00	01	00	01	01	00	01
Clay/Limonite	01	01	02	00	03	03	02
Sparite	12	07	00	10	47	25	01
Micrite	02	28	92	12	11	34	82
Pyrite/Hematite	00	01	00	01	00	00	00
Dolomite	05	01	00	01	01	00	05

ALLOCHEMS	THIN SECTION						
	HC-37*	HC-38*	HC-39	HC-40*	HC-41	HC-42	HC-43A
Conodonts	00	01	00	00	00	00	00
Brachiopods	01	01	00	04	01	01	00
Pelmatozoans	09	14	00	13	14	02	02
Gastropods	00	00	00	00	01	00	00
Lingula	00	00	00	00	00	00	00
Bioclasts	00	05	04	01	00	06	06
Trilobites	03	01	01	06	04	03	00
Ostracods	00	00	00	00	00	00	00
Nuia	02	14	00	02	02	00	00
Molluscs	01	00	00	02	01	00	00
Sponge Spicules	00	00	04	00	00	01	01
Calathium	00	00	00	00	00	00	00
Peloids	02	06	00	03	03	04	02
Intraclasts	50	00	05	12	13	00	00
Quartz Silt	00	04	01	03	00	05	06
Chert	00	00	01	03	20	02	00
Clay/Limonite	00	12	05	04	00	12	11
Sparite	29	35	02	34	24	11	08
Micrite	02	03	76	11	14	50	62
Pyrite/Hematite	00	00	01	01	01	01	00
Dolomite	01	04	00	01	02	02	02

ALLOCHEMS	THIN SECTION						
	HC-44*	HC-45	HC-46*	HC-47	HC-48*	HC-49	HC-50*
Conodont	00	00	00	00	00	00	00
Brachiopods	01	00	01	01	01	00	01
Pelmatozoans	19	02	22	13	09	02	02
Gastropods	00	00	02	01	01	00	00
Lingula	00	00	00	00	00	00	00
Bioclasts	01	04	04	14	14	11	00
Trilobites	03	01	03	02	03	03	02
Ostracods	00	00	00	00	00	00	00
Nuia	03	00	11	01	22	00	00
Molluscs	01	00	01	01	01	00	01
Sponge Spicules	00	00	00	00	00	00	04
Calathium	00	00	00	00	00	70	00
Peloids	13	01	03	01	03	00	00
Intraclasts	00	00	09	30	09	00	00
Quartz Silt	04	09	00	00	02	05	04
Chert	00	00	01	01	00	01	00
Clay/Limonite	00	03	01	00	03	02	01
Sparite	51	04	27	30	17	03	19
Micrite	01	75	09	04	14	02	47
Pyrite/Hematite	02	01	00	01	01	01	01
Dolomite	01	00	06	00	00	00	18

ALLOCHEMS	THIN SECTION						
	HC-51*	HC-52*	HC-53	HC-54	HC-55*	HC-56*	HC-57B
Conodonts	00	00	00	00	00	00	00
Brachiopods	00	00	01	00	00	00	00
Pelmatozoans	01	04	04	00	00	03	02
Gastropods	00	01	00	00	00	00	00
Lingula	00	00	00	00	00	00	00
Bioclasts	06	07	07	00	00	02	04
Trilobites	01	01	03	00	00	04	00
Ostracods	00	03	05	04	02	02	00
Nuia	00	01	00	00	00	01	00
Molluscs	00	01	00	00	00	00	00
Sponge Spicules	00	07	00	10	21	04	03
Calathium	00	00	00	00	00	00	00
Peloids	00	05	10	03	03	09	01
Intraclasts	00	00	00	00	00	00	00
Quartz Silt	09	04	05	02	02	01	01
Chert	12	01	15	78	42	00	02
Clay/Limonite	00	00	00	00	00	04	08
Sparite	02	36	30	00	15	34	09
Micrite	63	25	17	00	02	14	66
Pyrite/Hematite	00	01	02	01	01	01	01
Dolomite	06	03	01	02	12	21	03

ALLOCHEMS	THIN SECTION						
	HC-58*	HC-59*	HC-60	HC-61*	HC-62	HC-63	HC-64
Conodonts	00	00	00	00	00	00	00
Brachiopods	00	00	01	02	00	00	00
Pelmatozoans	02	07	01	02	00	00	00
Gastropods	00	00	00	01	00	00	00
Lingula	00	00	00	00	00	00	00
Bioclasts	04	08	06	10	00	10	00
Trilobites	01	01	03	02	00	00	00
Ostracods	02	01	03	04	00	00	00
Nuia	00	06	00	00	00	02	00
Molluscs	00	00	01	01	00	01	00
Sponge Spicules	03	04	04	12	00	02	00
Calathium	00	00	00	00	00	00	00
Peloids	09	01	03	01	00	03	00
Intraclasts	01	01	03	00	00	00	00
Quartz Silt	02	11	02	04	02	03	04
Chert	23	01	01	01	02	02	02
Clay/Limonite	04	02	06	01	00	00	00
Sparite	21	01	05	06	00	00	03
Micrite	15	44	60	47	00	16	00
Pyrite/Hematite	01	07	01	01	01	01	01
Dolomite	12	05	00	05	95	60	90

ALLOCHEMS	THIN SECTION		
	HC-65	HC-66*	BF-23*
Conodonts	00	00	00
Brachiopods	00	02	00
Pelmatozoans	00	04	01
Gastropods	00	00	00
Lingula	00	00	00
Bioclasts	00	04	01
Trilobites	00	01	00
Ostracods	00	01	00
Nuia	00	04	01
Molluscs	00	00	00
Sponge Spicules	00	00	13
Calathium	00	00	00
Peloids	00	00	00
Intraclasts	00	00	00
Quartz Silt	25	50	04
Chert	00	00	00
Clay/Limonite	00	05	01
Sparite	00	05	18
Micrite	00	20	61
Pyrite/Hematite	02	01	00
Dolomite	73	03	00